Ollscoil na hÉireann, Corcaigh

National University of Ireland, Cork

Interrogating regulated intramembrane proteolysis of IGF-1R, and its role in cell migration

Thesis presented by

Jordan Christopher O'Donoghue, BSc

For the degree of

MSc Biochemistry by Research

University College Cork

School of Biochemistry and Cell Biology

Head of school: Professor Justin McCarthy

Supervisors: Professor Justin McCarthy, Professor Rosemary O'Connor

2023

Table of Contents

Declaration

This is to certify that the work I am submitting is my own and has not been submitted for another degree, either at University College Cork or elsewhere. All external references and sources are clearly acknowledged and identified within the contents. I have read and understood the regulations of University College Cork concerning plagiarism and intellectual property.

- ***Jordan Christopher O'Donoghue***

Abstract

The IGF-1R has long been implicated in numerous malignant characteristics of cancers including enhanced proliferation, insensitivity to apoptosis, chemoresistance, increased migratory and invasive capacity, epithelial-to-mesenchymal transition, and metabolic augmentation. IGF-1R, much like other receptor tyrosine kinases, has been characterised as a substrate for gamma-secretase-mediated regulated intramembrane proteolysis (RIP). This proteolytic pathway begins with ectodomain shedding, mediated by sheddases, which produces a soluble fragment in the extracellular space. Following ectodomain shedding, a membrane anchored C-terminal fragment (CTF) is produced which is then cleaved by gamma-secretase at the internal juxtamembrane region to produce a soluble intracellular domain (ICD). Classically, RIP was thought to be a means by which cells would terminate receptor signalling, however contemporary research indicates a more nuanced role. It is now understood that the fragments generated through RIP can retain signalling of the full-form receptors and, in some instances, may acquire novel functionality. Although the RIP of IGF-1R has been outlined, the underlying dynamics of this pathway and the consequences of such remain to be elucidated. With this in mind, we endeavoured to identify the regulatory mechanisms underlying IGF-1R RIP and subsequently aimed to identify potential functions of the fragments produced.

Firstly, we generated a GFP-tagged K1003 IGF-1R point mutant, termed a kinase dead mutant, which lacks the ability to catalyse trans-autophosphorylation of the IGF-1R kinase domains thus preventing downstream signal transduction. Trans-autophosphorylation is a critical step in the activation of receptor tyrosine kinases during which the kinase domain of one intracellular domain catalyses the phosphorylation of tyrosine residues within the other intracellular domain. With this tool, we validated the cleavage of IGF-1R and the production of its CTF via transient transfection of HEK293T cells with plasmids expressing either wild-type or K1003R kinase dead mutant forms of IGF-1R C-terminally tagged with GFP. We subsequently

identified receptor kinase activation as a potential driver of IGF-1R RIP and determined that ligand stimulation significantly catalyses the accumulation of IGF-1R CTF. This was accomplished via transient transfection of HEK293T cells with plasmids expressing the aforementioned IGF-1R forms. Following this, we elucidated clathrin-mediated endocytosis as a probable regulatory pre-requisite step for IGF-1R RIP by gamma-secretase. Furthermore, our data indicates that ectodomain shedding of IGF-1R is likely catalysed in a metalloprotease dependent fashion, consistent with other receptor tyrosine kinases. We also confirmed that the CTF can undergo nuclear translocation in a clathrin-mediated endocytosis dependent manner, consistent with the translocation of the holoreceptor. Utilising wound healing assays, conducted in Hela cells, our data indicates that gamma-secretase inhibition by DAPT (a small molecule gamma-secretase inhibitor) alone does not antagonise IGF-1-induced cell migration. Similarly, the administration of Pitstop alone does not impinge upon IGF-1 induced cell migration. Interestingly, the administration of batimistat (a broad spectrum metalloprotease inhibitor) significantly suppresses cell migration in the presence of IGF-1.

Collectively, our data provides a framework for the construction of the IGF-1R RIP cascade. Following ligand-binding it appears that IGF-1R undergoes metalloprotease-dependent ectodomain shedding leading to loss of the extracellular alpha-chains. The CTF, which remains in the plasma membrane, then undergoes clathrin-mediated endocytosis and packaging into early endosomes. Following internalisation, the CTF is cleaved by gamma-secretase to generate a soluble ICD. Our data also demonstrates that IGF-1R CTF undergoes nuclear translocation in a clathrin-mediated endocytosis dependent fashion. Lastly, data gathered from our wound healing assays indicates that IGF-1R ectodomain shedding is likely a required event for the efficient IGF-1-induced migration of cells, possibly through the proteolytic augmentation of focal adhesion complexes containing IGF-1R.

Chapter 1:
Introduction

1.1 IGF-1R structure and activation

The IGF-1R functions as a hetero-tetrameric receptor tyrosine kinase comprised of two alpha and two beta-chains joined by disulfide bonds. Numerous oncogenic mutations have been identified within the IGF-1R and, while the functions of many such mutations still require characterisation, IGF-1R overexpression has been identified as critical indicator of reduced patient survival (Wang *et al.,* 2023*)*. For instance, head and neck squamous cell carcinoma patients presenting with IGF-1R overexpression had a marked reduction in overall survival . Three ligands have been identified for IGF-1R. IGF-1 is the primary ligand, however IGF-1R can also bind IGF-2 and insulin to varying degrees (LeRoith, Holly and Forbes, 2021). Each alpha-chain is 710 amino acid residues in length and is confirmed to contain two leucine rich domains (L1/2), a cysteine-rich domain (CR), three fibronectin-like domains (FnI/II/III) and an α-C-terminal tail (α-CT) (Kavran *et al.*, 2014; Li *et al.*, 2019)(Figure 1 A). Each beta-chain contains a small extracellular protrusion (196 residues) composed of two fibronectin-like domains (FnII/III), an alpha-helical transmembrane domain (23 residues) and a large intracellular component (Girnita *et al.*, 2014; Kavran *et al.*, 2014)(Figure 1A). The intracellular portion of the beta-chain is subdivided into three regions, those being an intracellular juxtamembrane region (~40 residues), a kinase domain (~267 residues) and a C-terminal domain (~101 residues) (Girnita *et al.*, 2014; Kavran *et al.*, 2014). The kinase domains of the beta-chains contain ATP-binding motifs (residues 976-981) and a critical catalytic lysine residue at position 1003 which is crucial for ATP binding and coordination by the receptor (Hanks, Marie Quinn and Hunter, 1985; Girnita *et al.*, 2014).

Crystallographic analysis of IGF-1 binding to IGF-1R elucidated the structural basis by which ligand binding induces receptor activation. In the absence of ligand, IGF-1R alpha-chains assume an autoinhibited Λ-shaped conformation which spatially segregates the beta-chains thus preventing proximity-dependent trans-autophosphorylation (Li *et al.*, 2019)(Figure 1B). It was determined that IGF-1 binds the alpha-chain L1/α-CT domains, surrounded by the L2 and CR domains, thus disrupting autoinhibition and inducing a conformational change (Xu *et al.*, 2018; Li *et*

al., 2019). Once autoinhibition has been lifted, IGF-1R components rearrange into a Γ-shaped confirmation (Li *et al.*, 2019). This rearrangement orients the beta-chains in such a way that the kinase domains can catalyse trans-autophosphorylation thus producing various phospho-tyrosine docking sites for downstream signalling apparatus (Girnita *et al.*, 2014; Li *et al.*, 2019). Three critical tyrosine residues, Tyr1131/1135/1136, reside within the kinase domain of the beta-chain. More specifically, these residues are present in the activation loop of the kinase domain. Phosphorylation of these residues leads to stabilisation of the activation loop which is an essential step in receptor activation (Favelyukis *et al.*, 2001). Once such residues are phosphorylated, IGF-1R activates a diverse range of downstream signalling pathways, many of which are central to carcinogenesis.

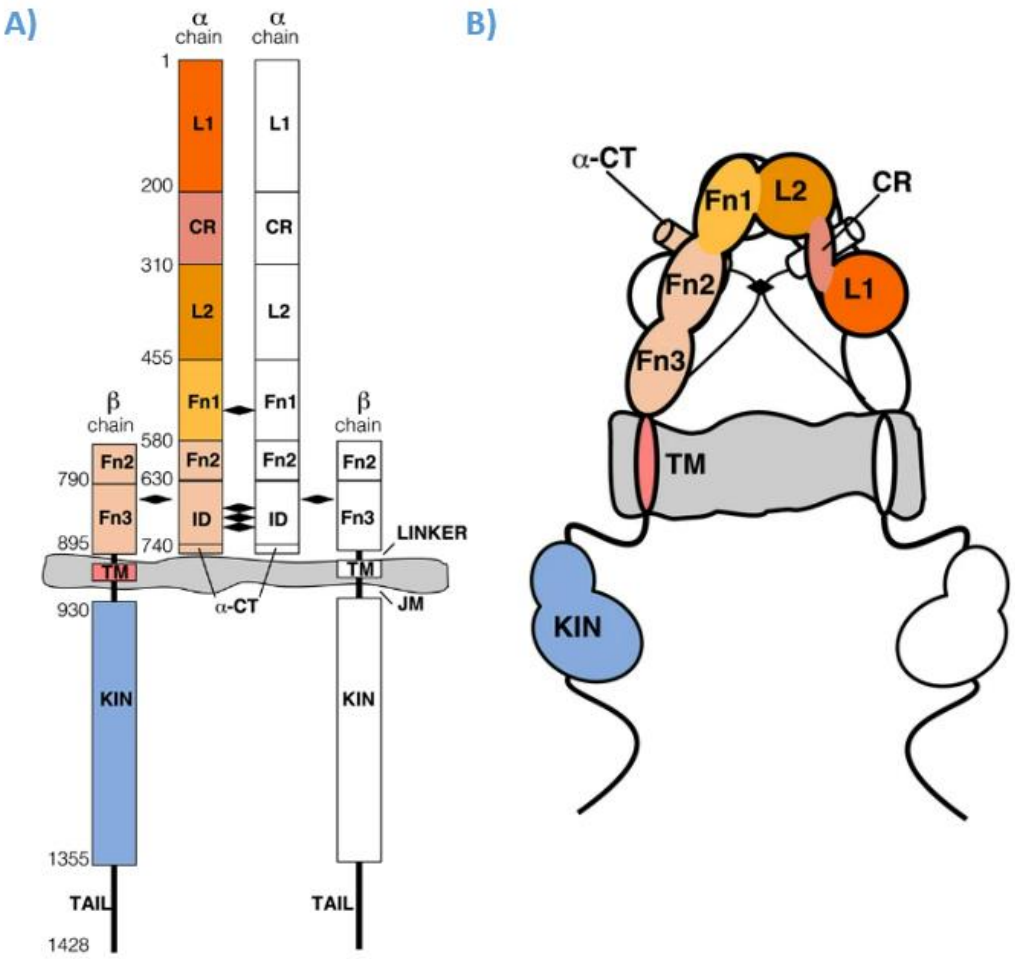

Figure 1: Diagrammatic depiction of IGF-1R structure

A) *Schematic outlining the general structural organisation of the IGF-1R. The α-chain is found in the extracellular space while the β-chain traverses the plasma membrane. The α-chain contains two leucine-rich domains (L1/2), a cysteine-rich domain (CR), two fibronectin-like domains (Fn1/2), an insert domain (ID) and an α C-terminal tail (α-CT). The β-chain consists of two fibronectin-like domains (Fn2/3), a transmembrane domain (TM), a kinase domain and a C-terminal tail.* ***B)*** *Cartoon depiction of the proposed 3D confirmation that the IGF-1R assumes as a heterotetramer once implanted in the plasma membrane. Figure taken from* (Kavran *et al.*, 2014).

1.2 IGF-1R signal transduction

The IGF-1R is considered a major driver of carcinogenesis and malignant transformation due to its broad array of signalling outputs. IGF-1R signalling underlies many of the malignant hallmarks of cancer including potentiation of epithelial-to-mesenchymal transition; enhanced proliferation; increased migration and metastatic capacity; insensitivity to apoptosis and therapeutic resistance (Kucab and Dunn, 2003; Li *et al.*, 2017; Yuan *et al.*, 2018; Hua *et al.*, 2020a; Wang, Mak and Cheung, 2022). Due to its pleiotropic signalling activities, IGF-1R has been implicated in the pathogenesis of multiple cancers with overexpression being observed across lung, breast, gastrointestinal, prostate and brain cancer, among many others (Trojan *et al.*, 2007; SUN *et al.*, 2015; Yeo *et al.*, 2015; Sun, Sun and Shen, 2017).

1.2.1 Classical signalling pathways downstream of IGF-1R

As previously mentioned, ligand-induced IGF-1R trans-autophosphorylation generates numerous phospho-tyrosine residues within the beta-chains of the receptor. These residues serve as docking sites for the induction of multiple signalling pathways through direct binding of pathway components, or via indirect activation through cytoplasmic adaptors (Girnita *et al.*, 2014; Mayer and Yu, 2018). Insulin receptor substrate (IRS) proteins bind to phospho-tyrosine residues via their phospho-tyrosine binding domains, located at their N-terminus. IRS-1 and IRS-2 are the most ubiquitously expressed IRS family members and serve as integral scaffolding proteins for the subsequent activation of various pathways (Mardilovich, Pankratz and Shaw, 2009). Crucially, IRS proteins also contain binding domains for downstream effectors in which tyrosine residues are phosphorylated by IGF-1R, namely phosphatidyl-inositol-3 kinase (PI3K) and Growth factor receptor-bound protein 2 (Grb-2) (Mardilovich, Pankratz and Shaw, 2009).

The binding of downstream effectors to IRSs/IGF-1R leads to activation of signal transduction, with the two most prominent pathways being the PI3K/Akt and Ras/Raf/MEK/ERK pathways. The Ras/Raf/MEK/ERK pathway is well characterised as a driver of cellular proliferation across numerous cancer types (Kim and Choi, 2010).

This pathway is activated downstream of IGF-1R via Shc binding to phospho-tyrosine residues (Song *et al.*, 2004)(Figure 2). Shc subsequently recruits Grb-2 and SOS to the IGF-1R to form a heterotrimeric scaffolding complex which physically interacts with Ras (Song *et al.*, 2004)(Figure 2). This physical interaction induces Ras GTPase activity, catalysing GDP dissociation thus allowing GTP binding (Simanshu, Nissley and McCormick, 2017; Bandaru, Kondo and Kuriyan, 2019). Ras-GTP is then responsible for the activation of Raf, which is a cytoplasmic serine/threonine kinase, through binding to the "conserved region 1" domain (Rukhlenko *et al.*, 2018; Terrell and Morrison, 2019). Raf activation leads to the phosphorylation of MEKs on key regulatory serine residues, catalysed by the interaction of a Raf proteins C-terminal catalytic domain with MEKs regulatory catalytic subdomain (Guo *et al.*, 2020). MEKs are unique, dual-specificity, threonine/tyrosine kinases which phosphorylate ERKs thus liberating them from cytoplasmic anchors which otherwise spatially segregate ERKs from their downstream targets. Following this, ERKs also undergo homo-dimerisation and nuclear translocation (Guo *et al.*, 2020)(Figure 2).

The terminal outcome of this pathway is enhanced cellular proliferation and cell growth, primarily due to ERK1/2 translocation to the nucleus wherein they alter the transcriptional profile of the cell (Maik-Rachline, Hacohen-Lev-Ran and Seger, 2019). Although a huge range of ERK substrates have been identified, the most common targets in the context of the nucleus are c-Myc and c-Fos (Chuang and Ng, 1994; Maik-Rachline, Hacohen-Lev-Ran and Seger, 2019) . ERK1/2 mediate phosphorylation of c-Myc on Ser62 which is a key regulatory serine that rescues c-Myc from ubiquitination by Mdm2, and subsequent proteasomal degradation (Sears *et al.*, 2000). This sustains c-Myc protein levels thus facilitating c-Myc transcriptional activity which is intimately linked to malignant transformation (Meyer Natalie and Penn, no date; Adhikary and Eilers, 2005). Active Myc catalyses the degradation of p27, a cell cycle inhibitor, via upregulating the expression Skp2. Skp2 mediates p27 ubiquitination and subsequent proteasomal degradation following p27 phosphorylation on Thr-187, which is partly induced by CDK1/2 (García-Gutiérrez *et al.*, 2019). This suppression results in the formation of the CDK1/cyclin B complex

which is a driver of mitosis within the cell cycle (Santamaría *et al.*, 2007). ERK1/2 both upregulate the expression of c-Fos and phosphorylate c-Fos on its C-terminal transactivation domain thus enhancing its activity (Monje *et al.*, 2005). Importantly, beyond its independent roles in carcinogenesis, c-Fos is also a component of the multifunctional AP-1 transcription factor complex in a heterodimer with c-Jun (Wang *et al.*, 2017; Wu, Nicoll and Ingham, 2021). AP-1 proteins have broadly been implicated in many of the pathogenic mechanisms pertinent to cancer including cell cycling and proliferation, apoptosis, lipid biosynthesis and migration/metastasis (Wu, Nicoll and Ingham, 2021). ERKs are also active in a much wider range of pathways encompassing pyrimidine biosynthesis via CAD complex activation; chromatin remodelling through Histone H3/HMG-14 phosphorylation; TSC1/2 complex regulation and spatio-temporal cyclin-D1 regulation (Chambard *et al.*, 2007).

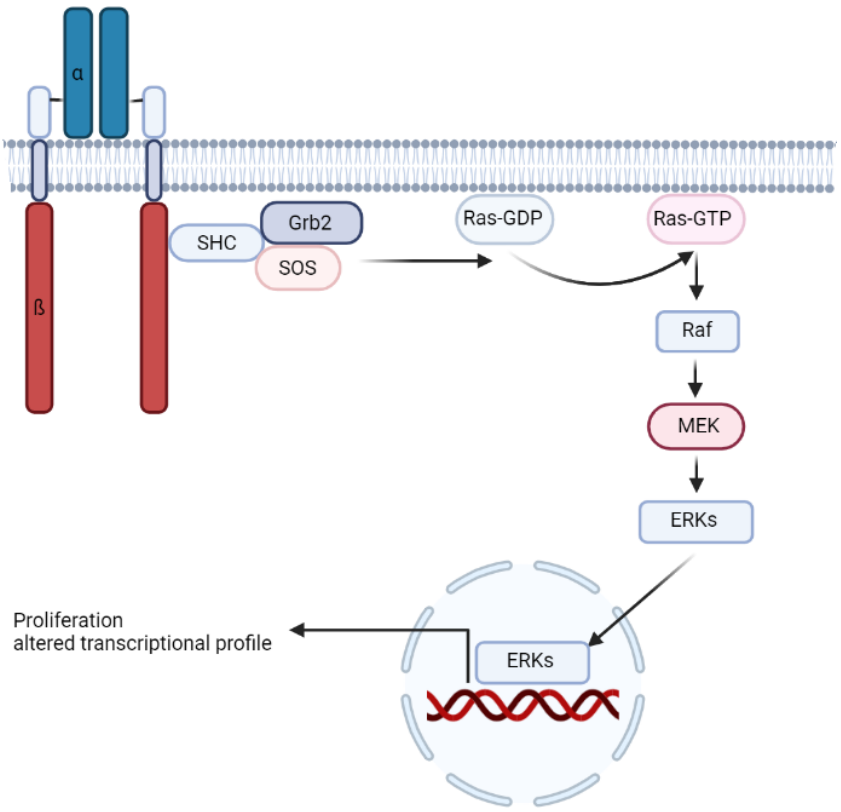

Figure 2: Ras/Raf/MEK/ERK signalling apparatus is activated downstream of IGF-1R

Diagrammatic overview of the Ras/Raf/MEK/ERK signalling cascade. This cascade is initiated via the trimeric SHC/GRb2/SOS complex binding to phospho-tyrosine residues generated on the IGF-1R following ligand activation. ERKs are the terminal effectors of the pathway which undergo nuclear translocation wherein they augment the transcriptional profile of the cell. Figure created utilising Biorender.

The second most prominent signalling pathway downstream of IGF-1R is the PI3K/Akt pathway. PI3K/Akt signalling is activated downstream of IGF-1R signalling, namely through a physical interaction between PI3K and phosphorylated IRS1/2 (Park *et al.*, 2010; Costa *et al.*, 2012)(Figure 3). Importantly, PI3K can also be activated through physical interaction with other proteins such as activated Ras therefore its activation is not constrained to specific receptor (P Rodriguez-Viciana *et al.*, 1994). Due to the activation of Akt, this pathway has far-reaching effects in the context of intracellular signalling related to cell survival and metabolic augmentation in particular.

Although PI3K/Akt signalling is classically considered as the "survival pathway" it is increasingly apparent that this pathway intersects with many other oncogenic pathways (Mundi *et al.*, 2016). PI3Ks are lipid kinases which phosphorylate 3'-OH groups of inositol rings on inositol-containing phospholipids present in the inner leaflet of the plasma membrane (Mundi *et al.*, 2016; Liu *et al.*, 2018). While PI3Ks are divided in four classes, class 1 PI3Ks are the most implicated class in cancer due to their coupling with receptor tyrosine kinases. Class 1 PI3Ks can be further subdivided into class 1a and 1b, with class 1a being the most well characterised in the context of pro-tumourigenic signalling. This class of PI3Ks contains a p85 regulatory subunit and a p110 catalytic subunit (Liu *et al.*, 2018). The p110 catalytic subunit is composed of an amino-terminal adaptor-binding domain which interfaces with the p85 regulatory subunit, a Ras-binding domain, a protein kinase C homology-2 domain which mediates PI3K binding to the inner plasma membrane, and intermediary alpha-helical domain and a carboxy-terminal catalytic domain (Walker EH *et al.*, 1999; Liu *et al.*, 2018). The regulatory p85 domain contains numerous binding domains including a Src-homology 3 domain which binds proline rich motifs is signalling partners; two Src-homology 2 (SH2) domains which bind phosphotyrosine residue on signalling adaptors; a breakpoint-clustered homology domain and an inter-SH2 domain which has autoregulatory functions (Zhao and Vogt, 2008; Liu *et al.*, 2018).

In the absence of physical interaction with signalling partners, the inter-SH2 domain binds to the p110 subunit thus locking PI3K in an autoinhibitory confirmation. Physical interaction of signalling partners with the p85 subunit, via the numerous binding domains, induces a conformation rearrangement leading to disinhibition (Liu *et al.*, 2018). Alternatively, Ras binding to the p110 Ras-binding domain can bypass the p85 regulatory subunit. This occurs following Ras activation downstream of receptor tyrosine kinase or G-protein coupled receptor signalling (P Rodriguez-Viciana *et al.*, 1994). Following activation, this PI3K sub-class mediates the phosphorylation of phosphatidyl-inositol-4,5-bisphosphate (PIP2) thus generating phosphatidyl-inositol-3,4,5-trisphopshate (PIP3) (Mundi *et al.*, 2016)(Figure 3).

Akt is the primary effector downstream of PI3K activation. Akt is a serine/threonine kinase which has been widely implicated in multiple carcinogenic pathways due to the wide menagerie of proteins subject to Akt-mediated phosphorylation (Vivanco and Sawyers, 2002; Mundi *et al.*, 2016). Akt contains three principal domains those being an amino-terminal pleckstrin-homology (PH) domain, a central kinase domain and a carboxy-terminal regulatory region with a hydrophobic sub-domain (Mundi *et al.*, 2016; Truebestein *et al.*, 2021). PIP3, generated by the action of PI3K, serves as a binding site for Akt leading to Akt localisation to the plasma membrane via Akt's PH domain (Figure 3). Following localisation to the plasma membrane, Akt undergoes a dual phosphorylation on Thr308 (catalysed by PDK1) and Ser473 (mediated by mTORC2), both of which are essential for proper activation of Akt (D. Sarbassov and et al, 2005; Truebestein *et al.*, 2021). Akt is believed to assume an autoinhibitory conformation in the absence of phosphorylation, induced by the binding of the PH domain with the kinase domain, however the dual phosphorylation is thought to disrupt this structure thus alleviating the inhibition (Truebestein *et al.*, 2021).

The most eminent effect of Akt is enhanced cell survival and insensitivity to apoptosis, which is accomplished through various means. Akt phosphorylates the BH3-only protein BAD on Ser136 which generates a 14-3-3 binding site. Through this,

14-3-3 can sequester BAD therefore preventing its binding to Bcl-2/Bcl-xL thus suppressing apoptosis (Datta *et al.*, 2000; Manning and Cantley, 2007). Akt further enhances apoptotic resistance by suppressing the expression of various BH3-only proteins. One way in which this occurs is the Akt-mediated phosphorylation of FOXO transcription factors in the nucleus (Manning and Cantley, 2007). Intra-nuclear localisation of FOXO proteins induces the expression of key BH3-only proteins such as BIM, along with components of apoptotic cascades such as Fas ligand (Manning and Cantley, 2007). Lastly, in the context of cell survival, Akt can promote the degradation of p53 thus preventing its activity as a pro-apoptotic transcription factor in response to cellular stress and oncogenic signalling (Shen and White, 2001). Akt catalyses the dual phosphorylation of MDM2, and E3 ubiquitin-ligase, on two regulatory serine residues (Ser166/Ser186) which promotes the nuclear translocation of MDM2 (Mayo and Donner, no date). Once within the nucleus, MDM2 ubiquitinates p53 leading to p53 nuclear exclusion and subsequent proteasomal degradation (Zhou *et al.*, 2001). As a result of p53 degradation, the expression of cell cycle suppressors (namely p21) and pro-apoptotic BH3-only proteins, specifically Puma and Noxa, are inhibited (Manning and Cantley, 2007).

Beyond its well defined role in cell survival, Akt is relevant to other aspects of tumorigenesis including; increased anabolic signalling through mTORC1 disinhibition leading to enhanced cell growth and translation; cell cycle progression and promotion of cell proliferation through GSK3β phosphorylation and synergistic signalling with the Ras/Raf/MEK/ERK pathway; metabolic reprogramming through GSK3 and glucose transporter-4 control; increased migration and invasion through ERK1/2 cross-talk and potentiation of angiogenesis through HIF-1α and VEGF regulation. All such activities of Akt are comprehensively reviewed within (Vivanco and Sawyers, 2002; Manning and Cantley, 2007; Mundi *et al.*, 2016).

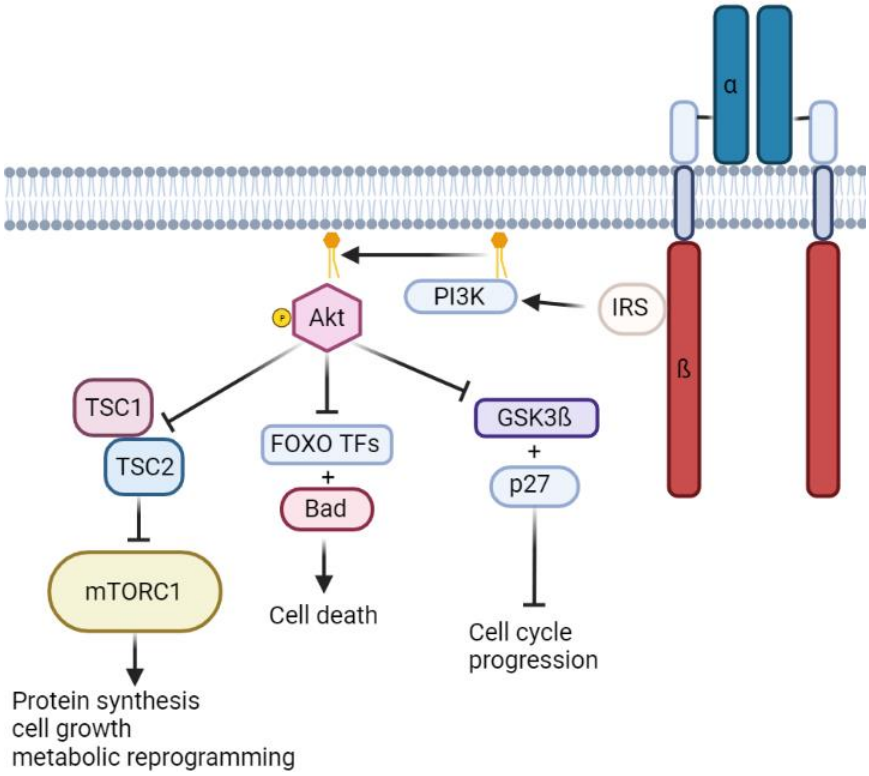

Figure 3: PI3K/Akt pathway affects an array of downstream effectors following IGF-1R activation.

IGF-1R Phospho-tyrosine residues serve as binding sites for insulin-receptor substrate (IRS) proteins which serve as adaptor proteins for the activation of phosphatidyl-inositol 3 kinase (PI3K). PI3K activates Akt in a phosphatidyl-inositol-3-dependent manner which subsequently phosphorylates numerous downstream effectors. Forkhead transcription factors (FOXO TFs), tuberous sclerosis complex 1/2 (TSC1/2), mammalian target of rapamycin complex 1 (mTORC1) and glycogen synthase kinase 3-β (GSK3β) are some of the notable downstream targets. Figure generated utilising Biorender.

1.2.2 IGF-1R and adhesion signalling

Beyond the typical signal transduction activities of IGF-1R, outlined previously, the receptor's role in cell migration, invasion and metastasis, is partly regulated by IGF-1R adhesion signalling (Cox *et al.*, 2015). IGF-1R has been characterised as a prominent component of focal adhesion complexes alongside adaptor proteins such as FAK, Src, RACK1, Shc, PDLIM2 and integrin protein family members (Cox *et al.*, 2015).

Integrins are α-β heterodimeric cell surface proteins which recognise and bind to the extracellular matrix thus leading to intracellular signal transduction. Integrins span the plasma membrane and thus exert their intracellular effects through the cytoskeleton (Hynes, 2002). Importantly, integrins also co-localise with various receptor tyrosine kinases including FGFR, EGFR, Met, ErbB2 and indeed IGF-1R (Takada, Takada and Fujita, 2017). It is believed that integrin binding to such receptors can augment their activity in various instances. The α6β4 integrin receptor binds to the extracellular matrix laminin family of proteins and has been widely implicated in the metastasis and poor prognosis of numerous cancers (Mercurio and Rabinovitz, 2001; Lu *et al.*, 2008). Interestingly, α6β4 integrin has been shown to bind IGF-1R in MCF-7 cells. This interaction seems to drive proliferation of such cells thus correlating with a more aggressive phenotype (Fujita *et al.*, 2012). Furthermore, IGF-1R was found to associate with αvβ3 integrin and ligand-occupancy of this integrin appears to enhance IGF-1R signalling to drive DNA synthesis and cell migration (Takada, Takada and Fujita, 2017). Cooperative IGF-1R-integrin signalling remains poorly characterised however it does appear as though the interaction of these receptors coincides with a more malignant cancer phenotype.

Src is a non-receptor tyrosine kinase comprised of 536 amino acid residues in humans. The notable components of Src include an N-terminal myristolated glycine residue, a "unique domain", an SH3 domain, an SH2 domain, an SH2-kinase linker region, a tyrosine-kinase domain and a short regulatory C-terminal region (Roskoski,

2015). Src is primarily regulated by two key tyrosine residues those being Tyr416 (located in the kinase domain) and Tyr527 (situated in the C-terminal region). Approximately 95% of Src rests inactivate in the cell due to phosphorylation on Tyr527. When this residue is phosphorylated Src is maintained in an auto-inhibitory structure through the intramolecular interaction of the C-terminal region with the SH2 domain (Bjorge, Jakymiw and Fujita, 2000; Roskoski, 2015). Dephosphorylation of this residue alleviates the auto-inhibition of Src. Similarly, phosphorylation of Tyr416 (present in the activation loop of the kinase domain) appears to induce Src activation. This residue is also considered a candidate residue for intermolecular phosphorylation which may be a means by which IGF-1R induces Src activation (Bjorge, Jakymiw and Fujita, 2000). Evidence from non-small cell lung carcinoma suggests that IGF-1R and Src may reciprocally phosphorylate one another to induce a feedback loop which enhances the activity of both kinases (Min *et al.*, 2015). Src has also been implicated in numerous other cancers including breast cancers and various sarcomas (Chen *et al.*, 2015; Luo *et al.*, 2022). The activities of Src across these cancers converges on insensitivity to apoptosis, increased metastatic potential and potentiation of epithelial-to-mesenchymal transition. Such activities culminate in a more aggressive metastatic phenotype, in part driven by adhesion signalling (Chen *et al.*, 2015; Chuang *et al.*, 2022; Luo *et al.*, 2022).

Another major downstream effector partly activated by IGF-1R/adhesion signalling is focal adhesion kinase (FAK). FAK is a non-receptor tyrosine kinase composed of 1052 amino acid residues and contains 3 principal domains those being an N-terminal FERM domain (residues 35-362), a kinase domain (residues 411-686) and a C-terminal FAT domain (functions as a protein-protein interacting domain) (Martínez, Navajas and Lietha, 2020). FAK exists in the cytosol as an inactive monomer with an autoinhibited conformation maintained by the intramolecular interaction of the FERM domain with a region of the kinase domain (Martínez, Navajas and Lietha, 2020). Tyr397 is a critical regulatory residue located in the inter-FERM/kinase region of FAK. When this tyrosine is un-phosphorylated, FAK assumes its autoinhibited conformation (Brami-Cherrier *et al.*, 2014). Other critical regulatory residues include

Tyr576/577 (located in the kinase domain) and Tyr925 (found in the FAT domain) (Martínez, Navajas and Lietha, 2020). FAK activation occurs through FAK autophosphorylation on Tyr397, found to be induced by FAK oligomerisation mediated through FAK/integrin interactions (Goñi *et al.*, 2014). This phosphorylation event unveils a binding site for Src family kinase (SFKs) via their SH2 domains. SFK binding to FAK subsequently catalyses the phosphorylation of various tyrosine residues including Tyr576/577/925 (based on the specific family member) (Lietha *et al.*, 2007). Tyr576/577 lie within the kinase activation loop of FAK hence, the phosphorylation of these residues by SFKs induces full activation of FAK kinase activity (Lietha *et al.*, 2007). Crucially, the phosphorylation of Tyr576 also shelters the kinase domain from the binding of the FERM domain thus sustaining FAKs open dis-inhibited conformation (Lietha *et al.*, 2007).

FAK activity has been identified as a driver of various malignant characteristics of cancer. FAK has been implicated in cell survival and proliferation through cooperative signalling with the PI3K/Akt pathway and nuclear translocation of FAK promoting MDM2-dependent degradation of p53 (Lim *et al.*, no date; Sonoda *et al.*, 2000; Chuang *et al.*, 2022). FAK signalling is also seen to drive cellular proliferation via cyclin upregulation and FAK-activated YAP/TAZ-mediated cellular proliferation in the context of IGF-1 signalling (Zhao, Pestell and Guan, 2001; Rigiracciolo *et al.*, 2020). Furthermore, FAK also modulates cytoskeletal organisation, cell migration, angiogenesis and mechanotransduction, all of which are reviewed by (Chuang *et al.*, 2022). IGF-1R-RACK1 complexes are seen to form at sites of cell adhesion in coordination with β1-integrin. These complexes serve as a platform for the integration of adhesion signalling and IGF-1R activation through ligand binding (Kiely *et al.*, 2005; Zhang *et al.*, 2006). FES-related tyrosine kinase (FER) is another downstream signalling component which is thought to drive cell-adhesion dependent IGF-1R-mediated cell survival, proliferation and migration (Stanicka *et al.*, 2018). FER is found to co-localise with IGF-1R independent of receptor interactions with adhesion complexes however, FER may enhance IGF-1R association with integrin-adhesion complexes which may then augment receptor signalling (Stanicka

et al., 2018). Herein, FER overexpression was seen to enhance IGF-1R expression and phosphorylation at Tyr950 and Tyr1131. Furthermore, FER enhanced Src and FAK activation thus indirectly promoting the phosphorylation of various tyrosine residues of the IGF-1R kinase domain (Stanicka *et al.*, 2018). Cumulatively, the reciprocal phosphorylation of IGF-1R and FER by one another prompted the activation of multiple signalling nodes and pathways including FAK, PI3K/Akt and MAPK/ERK pathways all of which are drivers of oncogenesis (Stanicka *et al.*, 2018).

Evidently, IGF-1R is involved in a diverse range of signalling nodes that are integrated with adhesion signalling receptors and molecules. Collectively, these activities amount to a more migratory and proliferative molecular phenotype which is relatively insensitive to cell death programmes. Integrating this information with the typical signalling of IGF-1R, via pathways previously described, it becomes clear that IGF-1R is a major cornerstone in various pathophysiological pathways which underlie and drive many of the hallmarks of cancers.

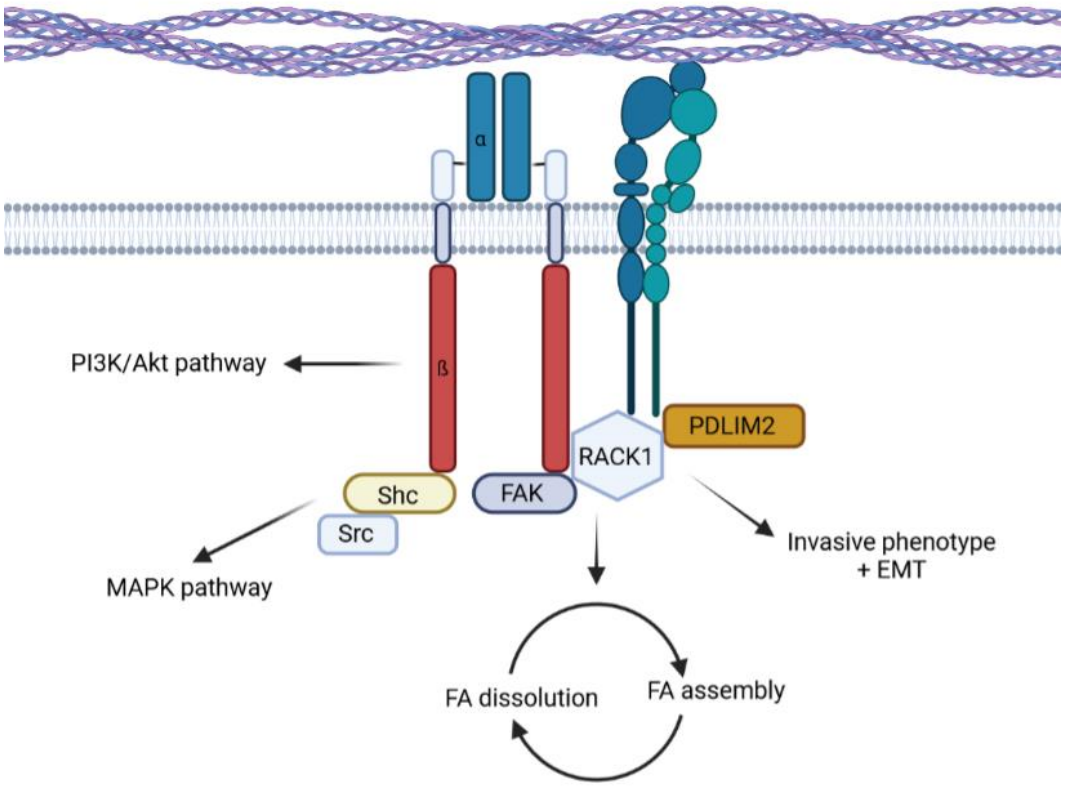

Figure 4: Overview of IGF-1R adhesion complex composition and signalling outputs

IGF-1R co-localises with integrins (namely β1-integrin) at sites of cell adhesion wherein integrins bind components of the extracellular matrix. FAK/RACK1 interplay mediates focal adhesion turnover, which is permissive to cell migration. FAK is also involved in signalling which drives metastasis and EMT. Adhesion signalling potentiates the activation of the MAPK/ERK and PI3K/Akt pathways, in part, through reciprocal activation of FES-related tyrosine kinase. Cooperative IGF-1R/adhesion signalling is believed to contribute to the malignancy of various cancers. Figure created utilising Biorender. Adapted from Cox et al. 2015.

1.3 IGF-1R internalisation and endocytic trafficking

Various mechanisms are employed by cells as a means of internalising proteins localised to the plasma membrane. Clathrin-mediated endocytosis (CME) and Caveolin-mediated endocytosis (CavME) are the most prominent modes for the internalisation of activated receptors at the cell surface, classically considered a means of signalling cessation (Goh and Sorkin, 2013). Thought both pathways are pertinent to receptor internalisation, they are mechanistically distinct in several ways (Elkin, Lakoduk and Schmid, 2016). CME involves the formation of clathrin-coated pits (CCPs) at the plasma membrane into which cargo is clustered for internalisation. The clathrin shell of CCPs is principally composed of clathrin triskelia, each of which is comprised of three clathrin heavy chains with associated clathrin light chains (Mettlen *et al.*, 2018). The nucleation and assembly of the clathrin shell is catalysed by the heterotetrameric adaptor protein 2 (AP2) complexes. AP2 serves a dual role as a cargo-recognition protein and scaffold which links the clathrin coat to the lipid bilayer. Alongside AP2, various other proteins (collectively called "clathrin associated sorting proteins) assemble to facilitate cargo coordination and clathrin oligomerisation (Elkin, Lakoduk and Schmid, 2016; Mettlen *et al.*, 2018). Fission of CCPs from the plasma membrane is catalysed by dynamin GTPase which is recruit to mature CPPs through SH3-containing adaptor proteins which bind dynamin's proline-rich domain (Schmid and Frolov, 2011). Once dynamin is correctly oriented in a collar-like structure around the "neck" of mature CPPs, GTP hydrolysis is initiated thus leading to CCP release from the plasma membrane (Schmid and Frolov, 2011). Free CCPs then undergo clathrin-shedding therefore allowing subsequent fusion with early endosomes for cargo release (Mettlen *et al.*, 2018).

As previously stated, the second predominant mode of internalisation is CavME. The primary protein responsible for CavME is caveolin, of which there are three isoforms (caveolin-1/2/3). Caveolin-1/2 are neigh-ubiquitously active at plasma membranes across cell types whereas caveolin-3 is primarily expressed in muscle cells (Kumari, Mg and Mayor, 2010). Caveolin proteins are small integral membrane proteins which are situated in the inner leaflet of the plasma membrane. Membrane anchoring of

caveolin proteins is mediated by their cytosolic amino-terminal domain which binds to cholesterol thus stabilising their membrane localisation (Parton and Del Pozo, 2013). This region is thought to possess an alpha-helical hairpin-like structure which may contribute to membrane curvature. Importantly, this region is also involved in protein-protein interactions and therefore is also important in the functionality of caveolin proteins (Parton and Del Pozo, 2013). In terms of CavME initiation, caveolin proteins associate with cavin protein family members to induce membrane curvature (Nassar and Parat, 2015). The formation of caveolae is also heavily influenced by membrane composition and is determined to require enrichment in both sphingolipids and cholesterol (Elkin, Lakoduk and Schmid, 2016). Membrane regions rich in these lipids coincidentally mediate receptor clustering and thus it is believed that receptor clustering into so-called "lipid rafts" rich in cholesterol may be a pre-requisite step in CavME (Kumari, Mg and Mayor, 2010; Parton and Del Pozo, 2013). The intermediate steps of CavME are not as well characterised as with CME however, the liberation of mature invaginated caveolae is catalysed by dynamin GTPase in a similar manner to that of CME (Henley *et al.*, 1998).

IGF-1R internalisation occurs following ligand-induced activation via both CME and CavME, with CME considered the predominant mode of internalisation, consistent with the internalisation of other receptor tyrosine kinases. Internalisation via CME is the most rapid form of receptor turnover from the plasma membrane following ligand-induced activation. Once CME is saturated, CavME may then mediate receptor internalisation as an auxiliary mode (Goh and Sorkin, 2013; Davis *et al.*, 2018a; Rieger and O'Connor, 2021). Internalisation through CME first requires the binding of proteins containing ubiquitin-interacting motifs. Next, the receptor undergoes poly-ubiquitination thus forming a scaffold for the coordination of receptors into clathrin-coated pits (Rieger and O'Connor, 2021). The ubiquitination of IGF-1R is thought to occur on Lys1138/Lys1141 which are situated in the kinase domain of the receptor beta-chain. This involves the formation of Lys-48 and Lys-29-linked polyubiquitin chains. The importance of these residues was validated using a site directed mutagenesis approach wherein alteration of these lysine residues to arginine

suppressed IGF-1R internalisation (Mao *et al.*, 2011). Importantly, IGF-1R also contains a key NPxY motif which interacts with the phosphotyrosine-binding motifs of several adaptor proteins. These adaptor proteins then bind to and recruit the adaptor protein 2 (AP2) heterotetrameric complex which catalyses CME as previously described above (Goh and Sorkin, 2013).

Classically, receptor internalisation was considered a pre-requisite step for termination of receptor signalling and subsequent receptor degradation via the lysosome (Rieger and O'Connor, 2021). Advances in cell biology have now elucidated a diverse set of intracellular fates for internalised receptors. Receptors which have undergone ubiquitination and internalisation are sorted by a complex termed the ESCRT (Endosomal Sorting Complexes Required for Transport) complex. Following ESCRT recognition, receptors are packaged into endocytic vesicles which contain a diverse distribution of membrane associated proteins, including Rab-proteins, which modulate the destinations and fates of vesicles (Katzmann, Babst and Emr, 2001; Cullen and Steinberg, 2018). Internalised IGF-1R may undergo trafficking back to the membrane to continue signalling, undergo Tyr1250/1251 phosphorylation-dependent localisation to the Golgi apparatus, or undergo CME-dependent nuclear translocation (Packham *et al.*, 2015a; Aleksic *et al.*, 2018; Rieger *et al.*, 2020; Rieger and O'Connor, 2021). As a result of its divergent trafficking, IGF-1R at distinct subcellular compartments may gain access to new sets of substrates in order to elicit non-canonical effects. Indeed, IGF-1R localisation to the nucleus and Golgi apparatus coincides with an altered transcriptional landscape (in the case of the nucleus) and a more malignant, aggressive and migratory phenotype (in the case of both organelles) (Lin *et al.*, 2017; Aleksic *et al.*, 2018; Poreba and Durzynska, 2020; Rieger *et al.*, 2020; Martin *et al.*, 2022a).

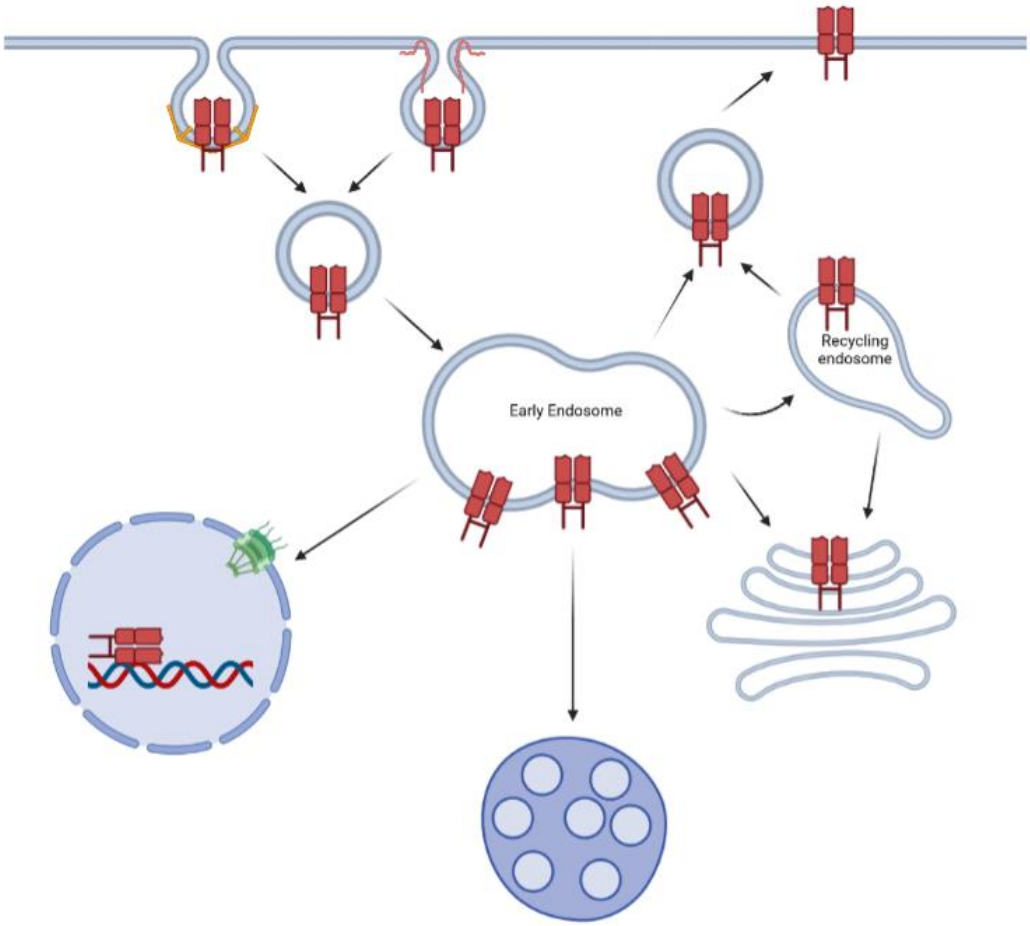

Figure 5: Intracellular fates of internalised receptor tyrosine kinases

Following internalisation via either clathrin or caveolin-mediated endocytosis, receptor tyrosine kinases face a diverse range of fates. Internalised receptors firstly aggregate at early endosomes from which smaller vesicles bud enriched with different Rab protein family members. Signals present in the relevant cargo and the assortment of Rab proteins associated with the vesicular membrane determine the fate of the cargo in question. From early endosomes cargo can undergo recycling to the cell surface through the rapid recycling pathway. Cargo can also undergo translocation to subcellular locations including the golgi apparatus or the nucleus. Lastly, cargo may be shuttled to the lysosome for degradation. Figure created utilising Biorender.

1.4 Nuclear IGF-1R

IGF-1R nuclear translocation was initially characterised in 2010 in tumour cells (Aleksic *et al.*, 2010a). Since then, nIGF-1R has been characterised in a range of non-malignant and cancerous cells by various research groups (Sarfstein *et al.*, 2012; Solomon-Zemler, Sarfstein and Werner, 2017; Martin *et al.*, 2022a). It was found that both the alpha and beta-chains localise to the nucleus in a clathrin-mediated endocytosis dependent fashion, however caveolin-1 depletion did not impact translocation (Aleksic *et al.*, 2010a). IGF-1R nuclear translocation has also been reported to be contingent on SUMOylation of the receptor C-terminal tail (Sehat *et al.*, 2010). Side directed mutagenesis revealed that lysine 1025/1100/1120 are required for trafficking to the nucleus however it was determined that mutation of these sites did not impinge upon receptor endocytosis nor its activation of the Ras/Raf/MEK/ERK and PI3K/Akt pathways (Sehat *et al.*, 2010). Sehat and colleagues proposed a mechanism through which the IGF-1R enters the nucleus which seems to be dependent on the SUMOylation they previously identified. Initially, IGF-1R undergoes clathrin-mediated endocytosis into EEA1+ vesicles. Next, the receptor undergoes endosomal escape after which it binds the dynactin-p150Glued subunit. Lastly, IGF-1R sequentially interacts with importin-β and RanBP2 which mediate transport through the nuclear pore complex in a SUMOylation-dependent manner (Sehat *et al.*, 2010; Packham *et al.*, 2015b). Interestingly, IGF-1R appears to enter the nucleus as hetero-dimers consisting of one alpha and one beta-chain, instead of its hetero-tetrameric holoreceptor form (Packham *et al.*, 2015b). It has also been determined that IGF-1R inhibition suppresses nuclear translocation, consistent with the phosphorylation status of the beta-chain (Aleksic *et al.*, 2010a). A potential clinical significance of nuclear IGF-1R (nIGF-1R) has been elucidated in multiple studies. Multivariate analysis revealed that renal clear-cell carcinoma patients with a high incidence of pervasive IGF-1R nuclear translocation had shorter survival times (Aleksic et al., 2010). Research also indicates that IGF-1R nuclear translocation correlated with higher pathological grade in patient prostate cancer samples (Aleksic *et al.*, 2018).

1.4.1 Transcriptional activity of nuclear IGF-1R

ChIP-seq analysis in 2D *in vitro* cancer cell lines revealed that nIGF-1R co-localises with RNA polymerase II, specifically at gene promoters for JUN and FAM21 (Aleksic *et al.*, 2018). It was also determined that IGF-1R can, in fact, promote the recruitment of RNA polymerase II to these promoters and thus acts as a transcriptional co-regulator (Aleksic *et al.*, 2018). The recruitment of RNA polymerase II requires IGF-1R binding to chromatin which appears to involve both the receptor alpha and beta-chains (Mills *et al.*, 2021). FAM21 is a component of the WASH complex and thus is involved in endosomal trafficking as well as actin polymerisation/cytoskeletal remodelling (Gomez and Billadeau, 2009; Zech T, 2011). JUN (c-Jun) is an oncogenic transcription factor that also functions as a component of heterodimeric AP-1 complexes. AP-1 complexes have been intimately linked to a vast array of malignant drivers as previously outlined in section 1.2.1 (Wu, Nicoll and Ingham, 2021). Together, these target genes indicate a pro-migratory functionality for nIGF-1R which coincides with the emergence of a more acutely malignant phenotype. Indeed, FAM21 and c-Jun depletion reduced the migratory capacity of cells thus indicating a pro-migratory role of nIGF-1R (Aleksic *et al.*, 2018). Transcriptional regulation of cell cycle associated genes appears to be another function of nIGF-1R. The expression levels of cyclin D1, cyclin A, CDK2 and p27 were analysed in IGF-1R-/- knockout cell lines. Cells were transfected with either Wild-type IGF-1R or a mutant IGF-1R in which Lys1025/1100/1120 were altered to arginine, thus abolishing SUMOylation (Sehat *et al.*, 2010; Lin *et al.*, 2017). Wild-type IGF-1R underwent nuclear translocation and significantly increased the expression of cyclin D1/cyclin A/CDK2 while suppressing the expression of p27 (Lin *et al.*, 2017). Altered gene expression coincided with enhanced cell cycle progression and therefore cell proliferation. The mutant IGF-1R showed minimal activity in the context of transcriptional regulation along with cell cycling (Lin *et al.*, 2017).

Nuclear IGF-1R has also been identified as a transcriptional coregulator through LEF-1 binding thus culminating in the control of LEF-1/TCF target genes. Genes encoding

Wnt signal transduction components are common target genes for LEF-1. Through upregulation of such components, nIGF-1R may potentiate cell migration, metastasis and cancer stem cell maintenance (Zhan, Rindtorff and Boutros, 2017; Poreba and Durzynska, 2020). Interestingly, the IGF-1R gene is also under the control of LEF-1 and thus nuclear translocation of the IGF-1R may induce an auto-regulatory positive feedback loop (Poreba and Durzynska, 2020). SNAI2 is described as a target of nIGF-1R transcriptional activity through indirect means. nIGF-1R was shown to phosphorylate histone H3 thus facilitating SMARC4 binding to chromatin. This augmentation of chromatin remodelling is thought to underlie enhanced SNAI2 expression, which has been identified as a driver of an aggressive and migratory phenotype (Packham *et al.*, 2015a; Alves *et al.*, 2018). Collectively, it appears as though the transcriptional activities of nIGF-1R converge on cell migration, metastasis and the emergence of an aggressive phenotype.

1.4.2 Nuclear IGF-1R potentiates DNA damage resistance and genomic instability

Beyond its multifaceted role in transcriptional regulation nIGF-1R is also observed as an enhancer of DNA damage tolerance in cells and therefore a potential driver of genomic instability (Poreba and Durzynska, 2020). The predominant target of nIGF-1R in this context is proliferating cell nuclear antigen (PCNA). PCNA is described as an integral component of the DNA damage tolerance (DTT)-pathway. The DDT-pathways allows DNA replication to occur in the presence of DNA damage through two predominant mechanisms those being trans-lesion synthesis and template switching (Andersen, Xu and Xiao, 2008; Bi, 2015). The promotion of such mechanisms is catalysed by phosphorylation-dependent post-translational modification of PCNA, namely the sequential mono and poly-ubiquitination of PCNA by DDT-dependent E3 ubiquitin ligases (Andersen, Xu and Xiao, 2008; Leung *et al.*, 2019). The ubiquitination of PCNA promotes the binding of other proteins which contribute to the DDT-pathway and thus the ubiquitination of PCNA is a mediary step in overcoming DNA damage (Leung *et al.*, 2019; Poreba and Durzynska, 2020). PCNA has been identified as a substrate for nuclear IGF-1R-mediated phosphorylation

which subsequently catalyses the covalent modification of PCNA as previously described, though this process has been identified in an embryonic context thus the translatability of this finding remains to be seen (Waraky *et al.*, 2017). Crucially, PCNA is categorised as a pathological driver and an indicator of poor prognosis in various cancers. PCNA expression is seen to correlate with pathological grade, TNM stage and the proportion of metastases (Smith *et al.*, 2015; Ye *et al.*, 2020). Through the modulation of this specific nuclear substrates, nIGF-1R may contribute to the mutational burden of cancers and thus potentially increase oncogene activation and the disruption of tumour suppressive/onco-protective proteins.

1.5 The gamma-secretase complex

Proteolytic cleavage has been identified as a regulatory mechanism for numerous cell surface receptors, with NOTCH being among the most notable. Cleavage at the cell membrane, typically by gamma-secretase, was classically considered to be a means of signalling cessation. It is now understood that receptor cleavage plays a more nuanced role in receptor signalling (Chen *et al.,* 2015; Carpenter *et al.,* 2013). Importantly, both the insulin receptor and IGF-1R have both been characterised as gamma-secretase substrates, however the function of IGF-1R cleavage remains to be seen (McElroy *et al.,* 2007; Kasuga *et al.,* 2007). The gamma-secretase complex (GSC) is a transmembrane heterotetrametric multiprotein complex that possesses aspartyl protease activity (Gertsik, Chiu and Li, 2015). The individual proteins which comprise the complex are presenilin, nicastrin, anterior pharynx defective 1 (APH-1) and presenilin enhancer 2 (PEN-2) (Bergmans and De Strooper, 2010; Zhang *et al.*, 2014; Gertsik, Chiu and Li, 2015). Mature GSCs are found to contain each component in a 1:1:1:1 stoichiometry, and full functionality of the complex necessitates one of each component (Strooper, 2003; Sato *et al.*, 2007; Zhang *et al.*, 2014). The GSC cleaves type 1 integral membrane proteins during a proteolytic cascade termed regulated intramembrane proteolysis (Lichtenthaler, Haass and Steiner, 2011). Nicastrin is a single-pass transmembrane glycoprotein which regulates substrate recognition by the gamma-secretase complex following substrate ectodomain shedding (Gertsik, Chiu and Li, 2015). Once the ectodomain of a gamma-secretase substrate is shed a

small stub of the substrate projects into the extracellular space which is subsequently recognised by nicastrin thus allowing substrate coordination into the GSC active site (Shah *et al.*, 2005). It has been proposed that the amino acid sequence of Nicastrin's substrate recognition domain may augment substrate processing (Pamrén *et al.*, 2011).

APH-1 is ~29kDa with seven transmembrane domains having been identified. APH-1 contains a critical GXXXG motif within the 4th transmembrane domain which is involved in GSC assembly (Gertsik, Chiu and Li, 2015). Humans possess two APH-1 genes encoding for APH-1a/APH-1b, however the APH-1a transcript can undergo alternative splicing to produce a short (APH-1aS) or a long (APH-1aL) isoform (Shirotani *et al.*, 2004). The incorporation of different APH-1 isoforms into GSCs appears to modulate differential cleavage of the same substrate as is the case with the production of different amyloid-β peptides in a study conducted in 2009 (Serneels *et al.*, 2019). Microscopic analysis herein indicates that different APH-1 isoforms may alter the confirmation of the presenilin component of GSCs and thus spatially augment substrate processing (Serneels *et al.*, 2019). Both presenilin-1 (PS1) and presenilin-2 (PS2) are expressed by humans as proteins of ~50kDa with nine transmembrane domains each (with PS1 being more abundant) (De Strooper and Annaert, 2010; Gertsik, Chiu and Li, 2015). Presenilins are synthesised as a full-length protein which is very unstable and thus is either rapidly degraded or incorporated into a GSC. Presenilin incorporation into a GSC induces an intramolecular endoproteolytic event in a cytosolic loop region between transmembrane domain six and seven within presenilin to generate a presenilin N-terminal fragment (PS-NTF) and presenilin C-terminal fragment (PS-CTF) (Ratovitski *et al.*, 1997; De Strooper and Annaert, 2010; Gertsik, Chiu and Li, 2015). PS-NTF contains a key catalytic aspartate at position 257 within transmembrane domain six while PS-CTF contains the sister residue at position 385 in transmembrane domain seven (Michael S. Wolfe*, 1999). These residues were identified as the critical mediators of PS1/2 aspartyl protease activity through site directed mutagenesis. Conversion of these residues to alanine abolished the catalytic activity of PS1/2 and therefore the activity of GSCs as well

(Gertsik, Chiu and Li, 2015). The final component of GSCs is presenilin enhancer-2 (PEN-2) which is a protein of ~10kDa with two transmembrane domains (Gertsik, Chiu and Li, 2015). PEN-2 is integral to the catalysis of PS1/2 endoproteolysis confirmed through RNA interference of PEN-2. In the instance where PEN-2 was knocked-down, there was a marked reduction of PS1-NTF/CTF while it appeared as though the PS1-FL holoprotein was stabilised alongside nicastrin and APH-1 (Takasugi *et al.*, 2003). Further research determined that PEN-2 has auxiliary roles beyond its modulation of presenilin posttranslational modification. A study utilised a mutant form of PS1 which is catalytically active however it does not undergo endoproteolysis to interrogate alternative roles for PEN-2. This PS1 mutant was expressed in mouse embryonic fibroblasts which lacked any PEN-2 production (PEN-2 -/-). The mutant PS1 was able to bond with nicastrin and APH-1 to form a trimeric complex however this complex lacked proteolytic activity (Bammens *et al.*, 2011). Another research group produced data which suggests that PEN-2 expression levels may influence the ratio of GSCs which contain PS1 vs PS2 and thus may modulate the processing of cellular gamma-secretase substrates (Placanica *et al.*, 2009). Evidently, PEN-2 fulfils a multifaceted role in the regulation of GSCs beyond its archaic role in presenilin cleavage.

1.5.1 Gamma-secretase complex assembly

The contemporary model for the assembly of mature GSCs is a multi-step process involving the formation of numerous intermediate complexes. Initially, APH-1 interacts with immature nicastrin within the endoplasmic reticulum wherein nicastrin undergoes N-linked glycosylation (LaVoie *et al.*, 2003). Next, the full-length presenilin (either PS1 or PS1) holoprotein is incorporated into the complex through binding with APH-1 (Lee *et al.*, 2004). APH-1 is critical for the formation of this intermediate heterotrimeric complex, mediated through a GXXXG (G denotes a glycine residue, X represents any amino acid) motif present in the fourth transmembrane domain of APH-1 (Lee *et al.*, 2004). This motif mediates helix-helix interactions within the plasma membrane interior, specifically the packing of nicastrin and presenilin (Lee *et al.*, 2004). The importance of this motif is underlined

by the fact that site directed mutagenesis of the critical Gly122 leads to suppression of Notch cleavage due to a deficiency in mature, catalytically active GSCs (Lee *et al.*, 2004). Lastly, PEN-2 is incorporated into the complex which subsequently orchestrates the intramolecular endoproteolysis of PS-FL into the catalytically active PS-NTF/CTF as previously described (Zhang *et al.*, 2014; Gertsik, Chiu and Li, 2015). Crucially, the final step of complex assembly, that being presenilin activation, necessitates the correct assembly of all prior complex components (Gertsik, Chiu and Li, 2015).

1.5.2 Regulated intramembrane proteolysis and proteolytic processing of IGF-1R

Regulated intramembrane proteolysis (RIP) is a proteolytic cascade which typically involves two key steps. The first step is the catalysis of type 1 integral membrane protein ectodomain shedding by sheddases. Ectodomain shedding is usually catalysed by members of the ADAM (a disintegrin and metalloprotease) protein family, although other protein families such as matrix metalloproteases have also been identified as sheddases (Steiner, Fluhrer and Haass, 2008; Carpenter and Liao, 2013a). The removal of the ectodomain (extracellular portion) from the target protein produces a small extracellular projection >30 residues in length which is subsequently recognised by nicastrin (Brown *et al.*, 2000). Next, once the substrate has been properly oriented within the GSC it is then cleaved by gamma-secretase's aspartyl protease activity to produce a soluble intracellular domain (ICD) (Steiner, Fluhrer and Haass, 2008). The cleavage of receptor tyrosine kinases through RIP appears to be a common event across protein families, with many of the ICDs undergoing nuclear translocation (Carpenter and Liao, 2013a). IGF-1R has been characterised as a substrate for gamma-secretase mediated RIP leading to the generation of a ~52kDa ICD (McElroy, Powell and McCarthy, 2007). Though the precise sheddase(s) responsible for IGF-1R ectodomain shedding remain(s) to be identified, the most likely mediator is ADAM17 (Hoa *et al.*, 2012). Though the IGF-1R holoreceptor can undergo nuclear translocation wherein it acts as a transcriptional

regulator as previously described, the localisation of the IGF-1R ICD remains to be fully elucidated.

It is possible that cancers may pervert RIP as a means of driving carcinogenesis since many receptor ICDs retain signalling of the holoreceptor but may also attain non-canonical localisation and activity (Carpenter and Liao, 2013a). Sheddase activity, especially ADAM family members, is enhanced by numerous signalling cascades which are frequently hyper-activated in cancers such as Ras/Raf/MEK/ERK and Protein kinase K/mTORC1 pathways (Miller, Sullivan and Lauffenburger, 2017). It has also been proposed that enhanced ectodomain shedding, and hence increased ICD production, may be an adaptive response to therapeutics (Miller, Sullivan and Lauffenburger, 2017). Most therapeutics intercede at the level of ligand-binding in an effort to suppress receptor signalling; however, ICDs which retain signalling potential lack vulnerability to such therapeutics. Hence, RIP of receptor tyrosine kinases may be a pernicious driver of carcinogenesis which has historically been overlooked.

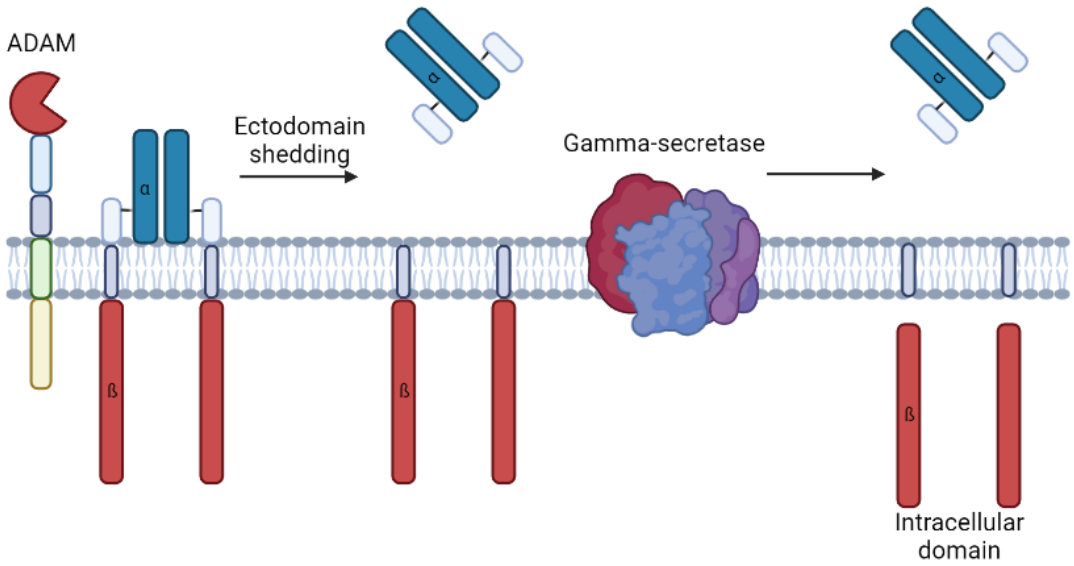

Figure 6: Predominant proteolytic steps of regulated intramembrane proteolysis

Regulated intramembrane proteolysis begins with ectodomain shedding of type 1 integral membrane proteins catalysed by sheddases, namely metalloproteases. Ectodomain shedding forms a soluble ectodomain and a membrane anchored C-terminal fragment which subsequently undergoes proteolysis by gamma-secretase complexes in the plane of the membrane. Gamma-secretase action cleaves C-terminal fragments within the intracellular juxtamembrane region thus liberating a soluble intracellular domain. Figure created utilising Biorender.

1.6 Aims and objectives

Current research demonstrates that regulated intramembrane proteolysis (RIP) has an important role in cell regulation of cell-surface to intracellular and nuclear signalling. For example, the translocation of RIP-generated ICDs to subcellular locations such as the nucleus wherein they can act as transcriptional regulators and maintain signalling activity (Carpenter and Liao, 2013; Chen and Hung, 2015). It has been proposed that RIP of receptor tyrosine kinases may contribute to chemoresistance as well as metastasis, proliferation and epithelial-to-mesenchymal transition (EMT), however the precise function of this pathway remains to be elucidated, particularly in the context of cancers (Lal and Caplan, 2011; Phillips, 2014; Miller *et al.*, 2016; Miller, Sullivan and Lauffenburger, 2017). Various cancers enhance the expression of sheddases (namely ADAM family proteins and matrix metalloprotease family members) therefore increasing potential flux through the RIP cascade (Mochizuki and Okada, 2007; Miller, Sullivan and Lauffenburger, 2017). Contemporary IGF-1R targeted therapies provide little to no clinical benefit to patients and many therapies fail to pass clinical trials. Therapies available for targeting IGF-1R include monoclonal antibodies, small molecular tyrosine kinase inhibitors and hormone-based therapies (Chen and Sharon, 2013). These drugs are often used in combination and, unfortunately, contemporaneous administration of these therapies alongside agents targeting partner pathways including EGFR, mTOR and oestrogen receptor has proven ineffective to a large degree (Chen and Sharon, 2013). Perhaps one of the means through which IGF-1R evades inhibition via therapeutics is through the production of an active CTF/ICD lacking an easily targetable region such as the alpha-chain ligand binding domain (in the case of neutralising and inhibitor antibodies) (Figure 7).

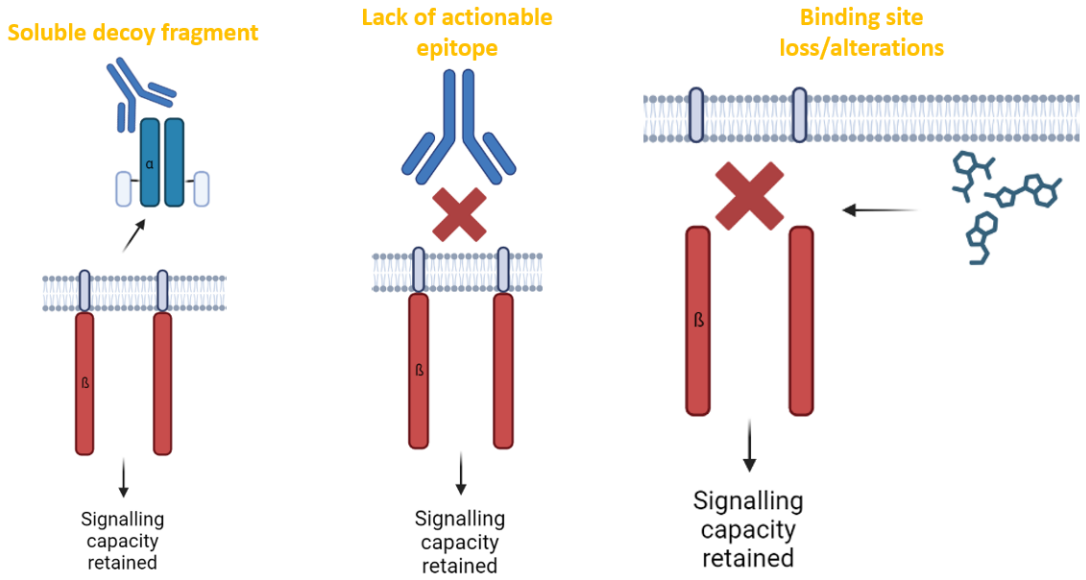

Figure 7: Potential consequences of receptor regulated intramembrane proteolysis

Due to the structural alterations of receptors throughout the process of regulated intramembrane proteolysis, the action of various therapeutic agents may be impeded. Biological agents, generally monoclonal antibodies, prevent ligand binding. The soluble ectodomains of receptors may function as decoy receptors which bind antibodies in the extracellular space prior to them reaching the desired target. Similarly, loss of receptor ectodomains deprive antibody therapeutics of an actionable epitope to exert the effects. Lastly, structural alterations of receptors may lead to the augmentation of, or complete loss of, the specific binding site for small molecule chemotherapeutics thus greatly hindering their therapeutic potential. Figure created utilising Biorender.

A major facet of how IGF-1R contributes to the malignant progression of various cancers is through its role in cell migration and metastasis. IGF-1R activation is intimately linked with the activation of ERK1/2, Akt and the AP-1 transcription factor complexes (Abd *et al.*, no date; Qiao, Sheng and Pardee, 2008; Wang *et al.*, 2017; Guo *et al.*, 2020; Wu, Nicoll and Ingham, 2021). EMT is also associated with metastatic progression and chemoresistance. IGF-1R has been frequently cited as a driver of EMT (Li *et al.*, 2017; Mittal, 2017). Further compounding this, specific IGF-1R adhesion complexes comprised of integrins and major adhesion signalling proteins such as Src and FAK have been widely reported in numerous cancers. Many IGF-1R signalling partners in such complexes are inextricably linked with cell migration and metastasis (Chen *et al.*, 2015; Svalina *et al.*, 2016; Chuang *et al.*, 2022; Obr *et al.*, 2022). Lastly, the activity of various families of proteases, namely matrix metalloproteases (MMPs) are seen to underlie the early stages of the metastatic cascade, namely degradation and remodelling of the ECM and tumour cell extravasation into circulation (‘Kleiner et al, 1999; Reunanen N, 2013). Crucially, increased MMP expression (primarily the expression of MMP-2/9) has been attributed to IGF-1R activity in numerous cancers (Samani *et al.*, 2007). Considering IGF-1Rs integration with numerous signalling pathways, its association with other key proteins such as integrins and the degree of redundancy and crosstalk between IGF-1R downstream signal transduction and other receptor tyrosine kinases, therapeutically targeting IGF-1R remains a considerable clinical challenge moving forward.

IGF-1R was characterised as a gamma-secretase substrate in 2007 but little work has been conducted on the proteolysis of the IGF-1R, and its possible functions in cancer, since this discovery. Herein, we aimed to interrogate the regulation of IGF-1R proteolysis through the RIP cascade, determine potential pathway components and relevant regulatory steps. We also endeavoured to define potential consequences of IGF-1R proteolysis in the context of cell migration using a cancer cell model due to findings in the literature converging on receptor fragmentation and IGF-1R

subcellular translocation as a driver of metastasis and a potentiator of a more malignant phenotype.

Chapter 2: Materials and Methods

2.0 Study design

Initially, work conducted by McElroy *et al.* 2007 was partly replicated with further densitometry analysis performed. This was performed in parallel with the site directed mutagenesis of IGF-1R to generate a GFP tagged kinase dead mutant. Following confirmation of IGF-1R inactivation via the K1003R point mutation, CTF accumulation in response to ligand stimulation was investigated. Having confirmed significant accumulation of IGF-1R CTF in response to ligand stimulation, we next interrogated the effects of ectodomain shedding on CTF generation utilising batimistat, a broad-spectrum metalloprotease inhibitor. Once we confirmed that inhibition of ectodomain shedding suppressed CTF accumulation, we next sough to investigate the effect of receptor internalisation on CTF accumulation following ligand stimulation. A panel of pharmacological agents targeting various components of the endocytic pathway were utilised which revealed a dependence on clathrin-mediated endocytosis for CTF generation following ligand stimulation. Next, we interrogated the effects of ligand stimulation on IGF-1R CTF nuclear translocation and whether inhibition of clathrin mediated endocytosis attenuated this translocation.

Lastly, we sought to investigate what influence IGF-1R proteolysis and trafficking may have on HeLa cell migration based on our western blot analysis. Initially we administered an IGF-1R kinase inhibitor (BMS-754807) to confirm that suppression of cell migration was feasible while using our optimal concentration of IGF-1 (50nM) over 20 hours. Next, we administered DAPT and Pitstop alone before attempting to combine them however a combination treatment was not viable due to profound cytotoxicity. Lastly, we administered batimistat alone and discovered that ectodomain shedding of IGF-1R seems to be important for cell migration.

2.1 Polymerase chain reaction and site directed mutagenesis

The IGF-1R K1003R-GFP kinase dead mutant (KDM) was generated using the KOD hot start DNA polymerase PCR kit (Sigma Aldrich). Custom overlapping primers were designed to introduce a point mutation in the nucleic acid sequence encoding for K1003 in the wild-type receptor. Custom primers were synthesised by IDT. Primer sequences are listed below.

Forward: 5′ CTGAAACCAGAGTGGCCATTAGAACAGTGAACGAGGCCGCAAGCA 3′

Reverse: 5′ TGCTTGCGGCCTCGTTCACTGTTCTAATGGCCACTCTGGTTTCAG 3′

Primers spanned the region containing K1003 within the IGF-1R kinase domain. Primers were designed to incorporate a single point mutation in the K1003 codon resulting in a K1003R point mutation. PCR reactions were created according to the manufacturer's instructions (outlined below) however the PCR reactions were also supplemented with 5% DMSO to aid in backbone melting and the dissolution of DNA secondary structures which could reduce PCR efficiency. PCR reactions were performed over a temperature gradient ranging from 73 - 81°C. This was done in order to optimise primer annealing and thus further optimise the PCR. The PCR was set to progress for 25 cycles to allow for sufficient generation of our desired amplicon. Cycle programme was created based on manufacturers protocol: 7 minutes was calculated to be the required extension time based on manufacturers recommendations of 25 seconds per Kb. PCR negative control followed the same formulation and cycle parameters however no template DNA was added. PCR products were resolved using a 0.5% agarose gel with 5 µL of safeView dye (NBS Biologicals) according to standard protocol in 1X Tris-borate buffer (89 mM borate, 89 mM Tris, 2 mM EDTA pH 8.3) supplemented with 5µL SafeView to aid with DNA fragment visualisation. The agarose gel was subsequently imaged using a Gel Dock EZ Imager (BioRad).

Table 1: PCR reaction composition

Components	Volume (µL)	Final Concentration
10X KOD Buffer	5	1X
25 mM MgSO4	3	1.5 mM
dNTPs (2 M each)	5	0.2 mM (each)
PCR Grade Water	32	-
Sense (5') Primer (10 µM)	1.5	0.3 µM
Anti-sense (3') Primer (10 µM)	1.5	0.3 µM
Template DNA	1	10 ng
KOD DNA Polymerase	1	0.02 units/µL
Total	50 µL	

PCR reaction composition and relevant concentrations of corresponding components. PCR negative control followed the same formulation however template DNA was omitted. An additional 1µL of PCR grade water was supplemented in its place.

2.2 DpnI restriction digest

DpnI restriction digest was employed in order to isolate the PCR amplicon from the parental *E.coli* DNA. *E.coli* DNA naturally has methyl adducts which are removed through the process of PCR. DpnI specifically cleaves DNA at methylated sites hence DpnI only cleaved the residual parental *E.coli* DNA which had not undergone PCR amplification. To a 200µL Eppendorf, 1µL of PCR product, 2µL of Cutsmart restriction enzyme buffer (New England Biolabs), 0.5µL of DpnI and 17.5µL of sterile (autoclaved) deionised water were added. In parallel, an enzyme control solution was also prepared which contained all the relevant components as above however, 1µg of parental plasmid DNA was added in place of PCR product (deionised water volume was adjusted accordingly to a maximum of 20µL). The solutions were incubated at 37°C for 2 hours. Following incubation, 3.5µL of 6X agarose gel loading dye (0.25% bromphenol blue, 0.25% xylene cyanol, 30% glycerol) was added to both solutions. 12µL of these solutions was loaded into a 1% agarose gel prepared using 1X TAE (40 mM Tris-acetate, 1 mM EDTA) containing 5µL of SafeView Dye (NBS Biologicals). The agarose gel was resolved at 100V for 60 minutes using 1X TAE buffer supplemented with 5µL SafeView Dye to aid with DNA fragment visualisation. 1Kb hyper ladder (Bioline) was resolved alongside the samples as a means of determining fragment

size. Once resolution was completed the gel was visualised using the BioRad Gel Dock EZ imager nucleic acid programme.

2.3 Preparation of chemically competent DH5α *E.coli* bacteria

A DH5α *E.coli* (New England Biolabs) aliquot was thawed on ice and subsequently streaked onto an LB plate. This plate was incubated overnight at 37°C to promote colony outgrowth into easily isolatable single colonies. A single colony was isolated from the plate and subsequently inoculated in 5mL of LB media over at 37°C with shaking. Following incubation, 3mL of the 5mL culture was removed and inoculated into 200mL of LB broth. The 200mL culture was incubated, for approximately 2 – 3 hours, until an optical density (at 595nm) of 0.6 – 1 was obtained. Once this threshold was reached, cells were harvested via centrifugation at 3000g for 15 minutes at 4°C. Supernatant was discarded and the remaining cell pellet was resuspended in ~70mL of cooled 0.1M $MgSO_4$ solution. Cells were once again centrifuged, as above, after which the remaining pellet was resuspended in a solution ice-cold 0.1M $CaCl_2$ with 15% (v/v) glycerol. 50µL aliquots of bacterial cell solution were placed in 1mL Eppendorf's which were subsequently stored at -80°C.

2.4 Bacterial transformation and plasmid extraction

Following amplification of the desired amplicons, PCR product was transformed into chemically competent DH5α *E.coli* cells. First, a 50µL aliquots of cells were thawed on ice for approximately 20 minutes. Next, 0.5 - 1µg of DNA was added to the bacterial solution which was then gently mixed to disperse the DNA. This bacterial solution was then incubated on ice for 30 minutes prior to a heat shock treatment at 42°C for 45 – 60 seconds. Once the cells had been heat shocked, 1mL of Super Optimal Broth was added to the Eppendorf. Bacterial cells were then incubated at 37°C with vigorous rocking for 1 hour. Following such incubation, between 5 – 20µL of bacterial cell solution was plated on pre-warmed LB agar plates supplemented with kanamycin (30µg/mL). Bacterial plates were subsequently placed in an incubator overnight at 37°C.

In order to isolate small amounts of plasmid DNA for analysis, individual cultures were isolated from the bacterial plates and placed in 5mL cultures of LB media supplemented with 5µL of kanamycin. Kanamycin was utilised to eliminate any non-transformed bacteria. Bacteria which had undergone successful transformation would survive due to the presence of the kanamycin resistance gene in the plasmid backbone. Bacterial cultures were then placed in an incubator overnight at 37°C with vigorous shaking. QIAprep Spin Miniprep kit (Qiagen) was used for plasmid extraction using the protocol outlined in the manufacturer's instructions. Once the protocol was complete, the yield and purity of the isolated plasmid DNA was validated via a Nanodrop spectrophotometer standard nucleic acid analysis protocol. For large scale plasmid extraction, 1mL of 5mL bacterial cultures was placed into 50mL of autoclaved LB broth supplemented with 50µL of kanamycin. 50mL cultures were then incubated overnight at 37°C with vigorous shaking. In order to isolate large amounts of plasmid DNA, the GenElute HP Plasmid Midiprep Kit (Sigma Aldrich) was employed as per manufacturers protocol.

2.5 Plasmid sequencing

Plasmid sequencing was proceeded by small scale plasmid isolation as outlined previously. In order to validate the incorporation of the correct mutation in the IGF-1R gene, 80 - 100µg of plasmid DNA was mixed with 6µL of EGFP-N primer (BD Biosciences) and 6µL of custom designed internal primers (procured from IDT).

Custom primer sequences:

Forward: 5′ TTCCATGATGACCAGTGTTGGCTG 3′

Reverse: 5′ CAGCCAACACTGGTCATCATGGAA 3′

This combination of primers facilitated correct sequencing of 1000bp either side of the mutation site thus facilitating high fidelity overlapping sequencing to occur. This

resulted in increased confidence in the sequencing data. Plasmid DNA solution was sent for Sanger sequencing by Eurofins Genomics.

2.5 Mammalian cell culture

2.5.1 General cell maintenance

Three human derived cell lines were utilised throughout this project, all of which were routinely tested for the presence of mycoplasma infection. Human Embryonic Kidney 293T cells (HEK293T)(ATCC), MCF-7 cells (human epithelial breast adenocarcinoma cells)(ATCC) and HeLa cells (human epithelial cervical adenocarcinoma cells)(ATCC) were all maintained using high glucose Dulbecco's Modified Eagles Medium (DMEM) supplemented with 10% foetal bovine serum, 1% penicillin/streptomycin cocktail, 1% glutamine and 1% non-essential amino acid mixture. Cells were stored in a humidified incubator at 37°C with 5% CO_2. Cells were passaged on a 3-day basis at a ratio of 1:4 (cell suspension: fresh media) utilising Trypsin-EDTA in order to detach cells from the dish. Stock cultures were kept in 10cm plastic dishes.

2.5.2 Pharmacological/ligand-stimulation assay protocol

For assays involving ligand stimulation combined with pharmacological agents, and subsequent lysate generation, HEK293T and HeLa cells were seeded into 6-well dishes at a density of 500,000 cells per well (determined via use of a haemocytometer). In the case of HeLa or MCF-7 cells, no transfections were performed due to their intrinsic expression of IGF-1R. HEK293T cells were transfected with either the wild-type IGF-1R with a C-terminal GFP-tag or the IGF-1R K1003-GFP mutant 24-30 hours after cell seeding. Transfection was accomplished using a calcium phosphate precipitation protocol, as described by Jordan *et al – 1996*, with 4µg of plasmid DNA transfected per well. Cells were incubated for ~16 hours with DNA precipitate after which expended media was replaced with fresh DMEM.

Relevant pharmacological agents were administered to HeLa/MCF-7 cells ~24-30 hours following seeding. Contrastingly, HEK293T cells were treated with relevant agents ~48 hours following seeding. If ligand stimulation was to be performed, cells were serum starved for 4 hours utilising high glucose supplemented DMEM lacking 10% foetal bovine serum. During this period, relevant pharmacological agents were administered for 2 hours. Lastly, IGF-1 was administered, at outlined concentrations in order to induce IGF-1R activation, for 10 minutes after which cells were lysed.

Table 2: Pharmacological agents/ligands utilised

Pharmacological agent/ligand	Concentration	Target
PMA	200nM	Protein kinase C
DAPT	1µM	Gamma-secretase
Pitstop	15µM	Clathrin heavy chain
Dynole	50µM	Dynamin
Methyl-β-cyclodextrin	5mM	Caveolin
BMS-754087	10nM/100nM (where indicated)	IGF-1R
Batimistat	20µM	Metalloproteases
IGF-1	10nM/50nM (where indicated)	IGF-1R

2.5.3 Cell lysis and lysate preparation

Cells were lysed using a RIPA lysis buffer (10mM Tris-HCL pH 8, 1mM EDTA, 0.5mM EGTA, 1% Triton X-100, 0.1% Sodium deoxycholate, 0.1% SDS, 140mM NaCl) supplemented with a cOMPLETE protease inhibitor cocktail (Sigma – 11697498001) and sodium orthovanadate (phosphatase inhibitor)(Sigma – 13721-39-6). To each well, 200µL of RIPA lysis buffer was added in which the cells were incubated for 30 minutes on ice with gentle rocking. Following incubation, cells were scraped into 1.5mL Eppendorf's and centrifuged at 13,200rpm at 4°C for 15 minutes to separate the cellular debris from the liquid supernatant. After centrifugation, 200µL of supernatant was isolated and placed in a fresh Eppendorf. If necessary, highly viscous lysates were sonicated at level 2 for three 5 second intervals.

A Bicinchoninic acid assay (BCA) kit (Pierce BCA protein assay kit – 23225) was used to normalise lysate concentrations. Bovine serum albumin standards provided within the kit were serial diluted to yield standard solutions ranging in concentration from

0 - 1500µg. 20µL of such standard solutions were placed into defined well on plastic 96-well plates. Similarly, 2µL of cell lysate supernatant was placed within defined sample wells. In parallel, a BCA stain solution was prepared, using “reagent part A” and “reagent part B” provided within the kit, at a ratio of 1:50 (part A: part B). To each standard and sample well, 200µL of BCA stain solution was added using a multichannel pipette. Plates were then incubated for 30 minutes at 37°C to facilitate colour development. After incubation, absorbance readings of the target wells were obtained at 562nm using a Tecan spectrophotometer. Absorbance values obtained from the standard wells were utilised to construct a standard curve in excel against which sample absorbances were compared to determine their protein concentration. Lysate concentrations were normalised by diluting a calculated volume of supernatant in deionised water. To this solution, 15µL of Laemmli buffer (5% SDS, 50% glycerol, 0.1% bromophenol blue, 250mM Tris-HCL pH 6.8, 5% 2-mercaptoethanol) (all chemicals obtained from Sigma) was added. The lysate preparations were then boiled for 5 minutes at 95°C prior to storage at -20°C.

2.5.4 Wound healing assay protocol

HeLa cells were seeded in 24-well dishes at a density of 500,000 cells per well (cell count was calculated via haemocytometry). Cells were allowed to adhere for ~24 hours prior to serum starvation for 4 hours using high glucose supplemented DMEM lacking 10% foetal bovine serum. Following an initial serum starvation, DMEM was removed at which point the circular wounds were inflicted. This was accomplished by attaching a p200 pipette tip to the laminar flow hood aspirator. The p200 tip was impressed into the cell plane with the vacuum active. 3 wounds were inflicted per well. Following wounding, wells were washed with 1mL of PBS to remove loosened cells. Serum free DMEM was then re-administered along with relevant pharmacological agents and IGF-1. Time point 0 hours wound images were then obtained via the EVOS imaging microscope. Cells were placed into the incubator for 20 hours after which time point 20 hours wound images were acquired via the EVOS.

Cell migration rate was calculated using ImageJ software combined with Microsoft excel. First, the EVOS wound images were imported into ImageJ. The image was then converted into an 8-bit format and the image contrast and brightness were adjusted to the required levels. In order to calculate the size of the wound, the ImageJ polygon selection tool was used to outline the border of the wound at both 0 hours and 20 hours. The "measure" function present in ImageJ was then used which provided a pixel count of the outlined area at each time point. From this, the percentage wound closure was calculated by first finding the average wound size across the 3 wounds at 0 hours and 20 hours followed by the calculation ((mean area T0 - mean area T20/mean area T0)*100).

2.6 Cellular fractionation

Cellular fractionation was performed utilising the Rapid Easy and Efficient Protocol (REAP) protocol (Suzuki *et al.*, 2010a), with some modifications made for use in a 6-well dish format. Cells were washed with cold 1X PBS as a quencher. 1ml of cold PBS is then applied, into which the cells are scraped from the dish. This cell solution is centrifuged at 500 rcf for 3 minutes at 4°C. After centrifugation the supernatant is carefully discarded and the cell pellet is resuspended in 250µL of ice-cold fractionation buffer (8mL 1X PBS, 0.1% Triton X-100, 1% protease inhibitor cocktail). 84µL is withdrawn from this solution and set aside, this will serve as the "whole cell lysate" fraction. The remaining solution is centrifuged at 16,000 rcf for 10 seconds at 4°C and 111µL of the supernatant is then collected. This 111µL aliquot is centrifuged again under the same conditions after which 56µL is isolated which constitutes the "cytosolic" fraction. The cell pellet which remains in the original Eppendorf is rinsed twice with 250µL of fractionation buffer. The remaining dried pellet is then considered the "nuclear" fraction.

Once all the fractions have been collected, they are subsequently dissolved in an appropriate volume of Laemmli buffer. For our purposes, 24µL of 5X Laemmli buffer was added to the "whole cell lysate", 14µL of 5X was added to the "cytosolic" fraction

and 50µL of 1X Laemmli buffer was used to dissolve the nuclear cell pellet. Following addition of the Laemmli buffer, all fractions should be sonicated at level 2 for 3 sets of 5 seconds in order to shear DNA present. After the samples have been sonicated, they are subsequently boiled at 95°C for 5 minutes. When loading the lysates into an SDS-PAGE gel the lysates should be loaded in a ratio of 1:2:1 (whole cell: cytosolic: nuclear) to account for differential protein enrichment in each fraction.

2.7 SDS-PAGE and western blotting and antibodies utilised

Cellular lysates were resolved on SDS-PAGE gels comprised of 10% resolving gels (dH20, 30% acrylamide mix, 1.5M Tris pH 8.8, 10% SDS, 10% ammonium persulfate, TEMED) and 5% stacking gels (dH20, 30% acrylamide mix, 1M Tris pH 6.8, 10% SDS, 10% ammonium persulfate, TEMED) (all chemicals obtained through Sigma). Both 10-well and 15-well gels were utilised for lysates isolated through fractionation or generic cell lysis following ligand/pharmacological agent administration. PAGE gels were resolved utilising BioRad SDS-PAGE rigs according to standard protocol with 1X SDS-PAGE running buffer. Cell lysates were resolved alongside SDS-PAGE pre-stained protein ladder plus (Thermo Fisher Scientific. Following adequate lysate resolution, proteins were transferred to nitrocellulose membrane using a generic BioRad protocol with 1X transfer buffer containing 20% methanol. Following transfer, membranes were either blocked as a whole or blocked following segmentation with 5% fat free milk or 5% bovine serum albumin in 0.1% PBS-T for 1 hour. After blocking primary antibodies were applied overnight at 4°C with gentle rocking. Between antibody applications, membranes were washed 2 times with PBS-T for 5 minutes followed by 1 was with PBS for 5 minutes. Loading controls were applied for 1 hour at room temperature with gentle rocking. Secondary antibodies were similarly applied for 1 hour at room temperature with gentle rocking. Membranes were visualised using the Li-COR Odyssey imaging system and subsequently analysed using Image Studio Light software.

Primary antibodies used:

Rabbit anti-IGF-1R β-chain (Cell Signalling Technology 3027), Rabbit anti-phospho-Akt (Ser473) (D9E) XP (Cell Signalling Technology 4060), Rabbit anti-total Akt (Cell Signalling Technology 9272), Rabbit anti-total ERK1/2 (Cell Signalling Technology 9102), Rabbit anti-phospho ERK1/2 (Thr202/Tyr204) (Cell Signalling Technology 9101) and Rabbit anti-Histone H3 (Cell Signalling Technology 4499). All primary antibodies were utilised at a concentration of 1:1000 in 5% bovine serum albumin in 0.1% PBS-T except for Histone H3 which was diluted 1:2000 in 5% fat free milk in 0.1% PSB-T.

Loading controls used:

Mouse mono-clonal anti-β-actin (Sigma Aldrich A6441) and Mouse mono-clonal anti-α-tubulin (Sigma Aldrich T6199). Loading controls were utilised at a concentration of 1:10,000 in 5% fat free milk in 0.1% PBS-T.

Table 3: Primary antibody targets and dilutions

Antibody target	Dilution	Supplier
IGF-1R β-chain	1:1000	Cell signalling technology
Phospho-Akt (Ser473)	1:1000	Cell signalling technology
Total Akt	1:1000	Cell signalling technology
Phospho-ERK1/2	1:1000	Cell signalling technology
Total ERK	1:1000	Cell signalling technology
Histone H3	1:2000	Cell signalling technology
Actin	1:10,000	Sigma Aldrich
Tubulin	1:5000	Sigma Aldrich

Secondary antibodies used:

IRDye 800CW goat anti-mouse IgG 926-32210 (Li-COR) and IRDye 800CW goat anti-rabbit IgG 926-32211 (Li-COR). Secondary antibodies were diluted 1:10,000 in 5% fat free milk in 0.1% PBS.

2.8 Crystal violet cell detachment assay

Culture media was aspirated from the cells which were subsequently washed twice with 500µL of cold 1X PBS. After washing, 200µL of 0.5% crystal violet solution (20% methanol) (obtained from Sigma – 548-62-9) was placed on the cells. Cells were incubated with crystal violet solution for 20 minutes at room temperature while rocking (20 oscillations per minute). Following incubation, cells were rinsed four times with 500µL of deionised water to remove any unbound crystal violet.

Cells were allowed to air-dry at room temperature for 2 hours after which the 24-well plates were imaged using the LiCOR Odyssey. After imaging, 1mL of methanol was added to solubilise the bound crystal violet. Once methanol was added, cells were incubated at room temperature for 20 minutes while rocking at 20 oscillations per minute. Once the crystal violet has been solubilised, 200µL of the solution was removed from each well and placed in a 96-well plate in duplicate. Absorbance of the samples were obtained at 592nm. In order to calculate the percentage of cell detachment (a measure of cell death) the following formula was utilised: = (Mean OD of sample/Mean OD of blank)*100 = % detachment

2.9 Western blot densitometry and statistical analysis

Densitometry analysis of western blot images was performed using the Image Studio Light inbuilt densitometry functionality. Values obtained from such was exported to excel for analysis. IGF-1R beta-chain and IGF-1R C-terminal fragment values were normalised to the actin values for the relevant lane. Following value normalisation, an average lane value was obtained for each lysate set for both IGF-1R beta-chain

and C-terminal fragment. The normalised values were then divided by the average lane value. Once the values were obtained the fold change in C-terminal fragment generation was then calculated by first dividing the C-terminal fragment values by the IGF-1R beta-chain values. After this was completed across the sets, an average value of the control lanes throughout the lysate sets, was calculated. Lastly, the C-terminal fragment: Beta-chain values for all lanes from all sets was divided by the control lane average value. This analysis produced a numerical value which represented the fold change in C-terminal fragment production across each lane in all relevant lysate sets.

Once these values were generated in excel, the values were then exported to Graph Pad Prism (version 9) for statistical analysis. ANOVA was conducted on the exported values, with the multiple-comparison test being conducted under the Tukey protocol. Within the test the desired P-value was set to <0.05 (95% confidence interval). During testing for statistical significance, the mean of each column was compared versus the mean of every other column. Error bars represent the standard error of the mean (SEM).

2.10 Wound healing assay statistical analysis

Following calculation of percentage wound closure, as outlined in 2.5.4, statistical analysis was performed. Initially, in excel, the percentage wound closure values were sorted into rows for each set and columns for each condition (Table 4). Next, the average wound closure observed across all conditions was calculated for each set. The percentage wound closure of each condition in each set was then divided by the relevant sets' average percentage wound closure. This provided a decimal value of wound closure. The values divided by the relevant sets' average wound closure were then averaged per each condition across sets (Table 5). Lastly, the decimal value for each condition for each set was divided by the average decimal value for serum free wound closure across sets. The final decimal values were then imported into Graph Pad Prism (version 9) for statistical analysis.

ANOVA was conducted on the exported values, with the multiple-comparison test being conducted under the Tukey protocol. Within the test the desired P-value was set to <0.05 (95% confidence interval). During testing for statistical significance, the mean of each column was compared versus the mean of every other column. Error bars represent the standard error of the mean (SEM).

Table 4: Example data processing in excel

	Serum Free	BMS-754	IGF-1	Combo	Avg. wound closure within set
Set 1	22.67%	21.32%	51.02%	35.01%	32.505%
Set 2	26.28%	20.12%	54.84%	37.04%	34.57%
Set 3	23.87%	20.615%	52.75%	26.06%	30.8237%

Table 5: Example data processing in excel

	Serum Free	BMS-754	IGF-1	Combo
	0.69743116	0.655899092	1.569604676	1.077065067
	0.7601967	0.582007521	1.586346543	1.071449233
	0.77440285	0.668802466	1.711342715	0.845451965
Average across sets per condition	0.74401024	0.635569693	1.622431311	0.997988755
	0.93739458	0.881572668	2.109654667	1.447648175
	1.0217557	0.782257406	2.132156867	1.440100116
	1.04084973	0.898915672	2.300160161	1.136344527

Chapter 3:
Results

3.1 Site-directed mutagenesis and mutant validation

As previously mentioned, custom primers were synthesised with a nucleic acid sequence designed to cause a single point mutation (K1003R) in the PCR amplicon. This key lysine residue is situated in the kinase domain of the β-chain within the region responsible for ATP coordination by the receptor (Kooijman, 2006; Li, Pourpak and Morris, 2009). This ATP coordination facilitates the liberation of phosphate groups from ATP which are subsequently used for the trans-autophosphorylation of the receptor on tyrosine residues. This step is essential for the binding of downstream adaptor proteins and signalling apparatus (Hua *et al.*, 2020b). The sequences of the designated primers are listed below.

Forward: 5′CTGAAACCAGAGTGGCCATTAGAACAGTGAACGAGGCCGCAAGCA 3′

Reverse: 5′TGCTTGCGGCCTCGTTCACTGTTCTAATGGCCACTCTGGTTTCAG 3′

The point mutation introduced (underlined) encodes arginine in place of lysine thus disrupting ATP binding. This has been reported to abrogate ATP coordination by the receptor thus inhibiting the receptor's ability to undergo autophosphorylation. PCR solutions were supplemented with 5% DMSO to optimise template melting. PCR was conducted for 30 cycles according to the specifications outlined in table 1. To facilitate more efficient primer annealing, PCR was also performed over a temperature gradient ranging from 73 °C to 81 °C. The desired amplicons were amplified successfully at all temperatures across the defined temperature (Figure 1B top) gradient and at the median temperature of 77 °C (Figure 1B bottom).

Table 1: PCR cycle parameters

PCR Step	Condition	
	Temperature (°C)	Time
Polymerase Activation	95	2 minutes
DNA Denaturation	95	20 seconds
Annealing	77.3	10 seconds
Extension	70	7 minutes (25 s/Kb)

Incorporation of the correct mutation was validated using sanger sequencing. The validated amplicons were subsequently Dpn1 digested prior to transformation into DH5α *E.coli* cells in order to amplify and isolate plasmid DNA for mammalian cell transfection.

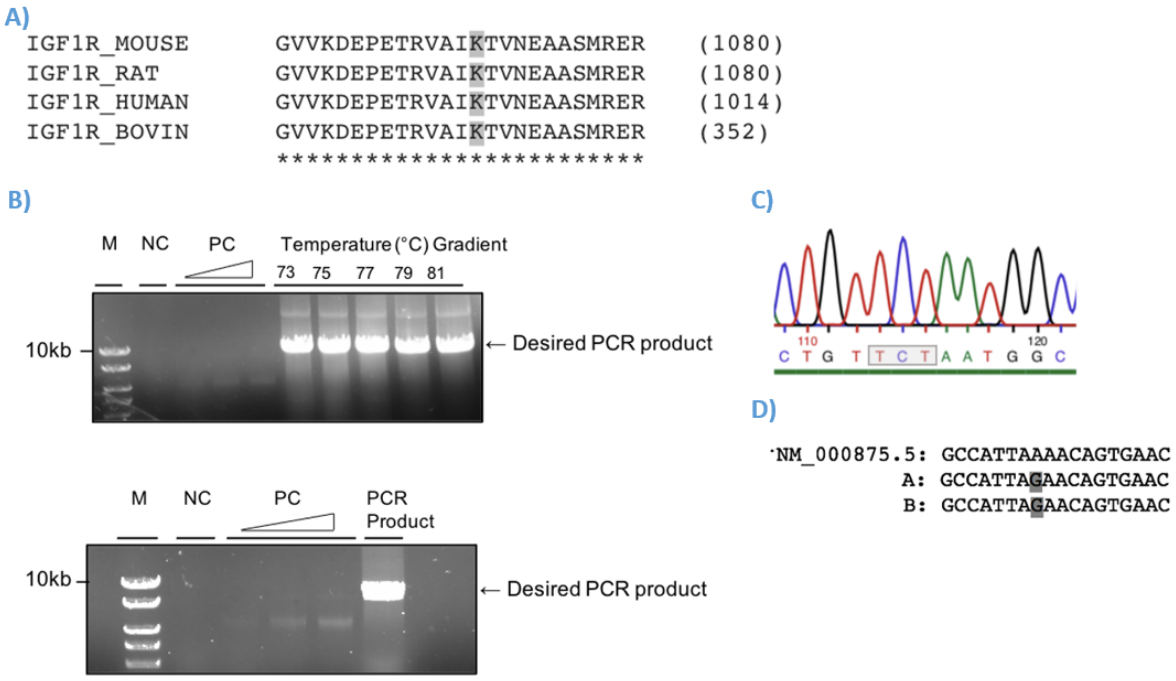

Figure 1: Successful amplification of a IGF-1R K1003R-GFP kinase dead mutant construct

A) *Clustal multiple sequence alignment of various species expressing the IGF-1R. The key lysine (K1003) present within the ATP binding domain (highlighted) is conserved across each species analysed.* ***B Top)*** *PCR products that were amplified over a temperature gradient from 73 °C to 81 °C, as indicated.* ***B Bottom)*** *PCR product produced at the optimised temperature of 77 °C with the addition of 5% DMSO. NC; negative control containing all PCR reagents excluding the 10 ng of pEGFP-IGF-1R template DNA. PC; Positive control loaded in increasing concertation of 2ng, 10ng and 20ng of pEGFP-IGF-1R template DNA. M; 1 kb DNA molecular weight marker.* ***C)*** *Sequencing chromatogram spanning the area of interest, with the triplet codon encoding arginine at position 1003 highlighted. The green line present at the bottom indicates the sequence is of high fidelity.* ***D)*** *Sequence comparison of the sequencing results versus the wild-type sequence with the mutated G highlighted.*

Following transient transfection of both the wild-type and KDM plasmids into HEK293T cells, the expression of the KDM was compared to that of the wild-type receptor. Both the wild-type and kinase dead mutant IGF-1R-GFP constructs were well expressed in HEK293T cells. We also validated that the K1003R mutant was, in fact, kinase dead via a 4-hour serum starvation followed by stimulation with IGF-1 (10nM) of transiently transfected HEK293T cells. Cells expressing either the wild-type or kinase dead mutant constructs were lysed, and lysates were resolved via SDS-PAGE (Figure 2). Western blotting was performed to identify phospho-ERK, total ERK, Tubulin and IGF-1R β-chain levels. Evidently, ERK was phosphorylated following ligand stimulation only in cells expressing the wild-type receptor whereas ERK phosphorylation was minimal in cells expressing the KDM (Figure 2). Minute amounts of ERK phosphorylation were still observed in these lysates owing to the native expression of IGF-1R in HEK293T cells. Total ERK, tubulin and IGF-1R β-chain levels were consistent across the lysates. From this we determined that the mutation incorporated was successful in abolishing receptor tyrosine kinase activity of the mutant and that HEK293T cells were a suitable cell system for the overexpression of both receptor constructs.

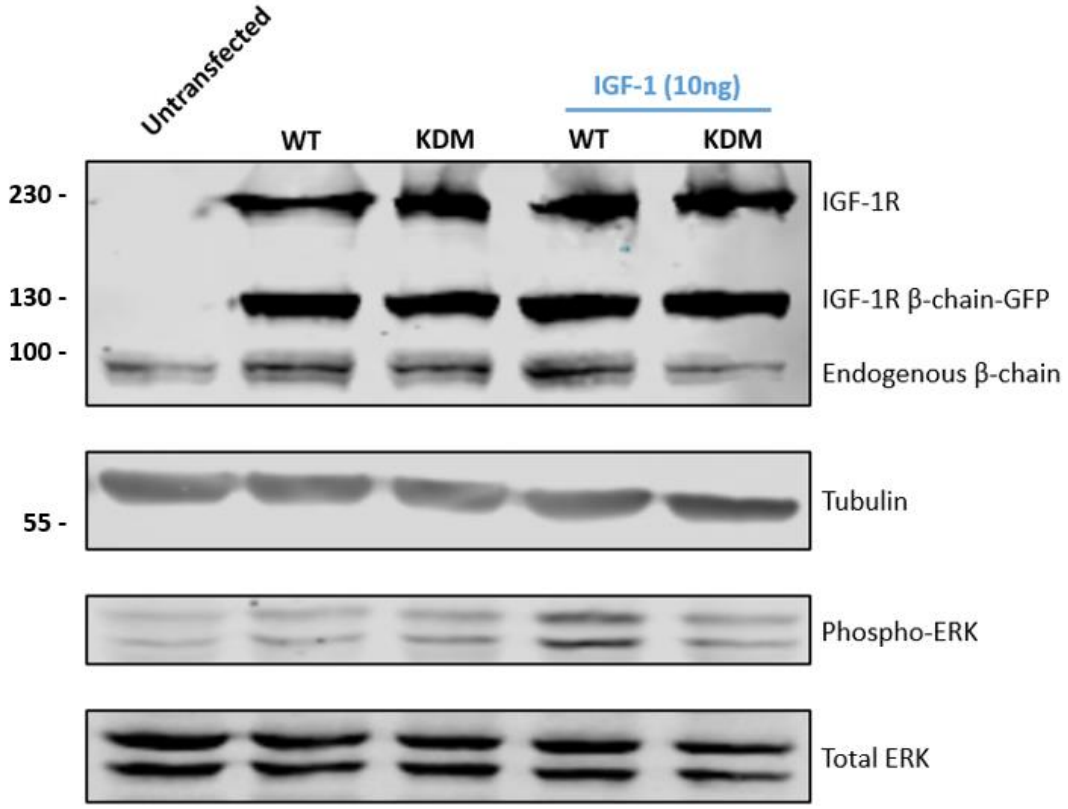

Figure 2: Validation of IGF-1R K1003R-GFP kinase dead mutant via ERK phosphorylation

HEK293T cells were untransfected or transfected with a plasmid expressing either the wild-type (WT) or IGF-1R K1003-GFP kinase dead mutant (KDM) with a C-terminal GFP tag where indicated. Cells were serum starved for 4 hours prior to administration of IGF-1 (10nM) where indicated. Cells were lysed and the supernatant was resolved on a 10% SDS-PAGE gel and subsequently subjected to western blotting. Blots were probed for IGF-1R β-chain, phospho-ERK and tubulin initially and then visualised using a combination of mouse and rabbit secondary antibodies. Membrane stripping was then performed on the phospho-ERK blot which was then re-probed for total ERK and visualised once again. Total ERK was then detected using a rabbit secondary antibody. (n=1).

3.2 Validation of IGF-1R C-terminal fragment generation by pharmacological agents

Having successfully generated and validated expression and kinase activity of our wild-type and IGF-1R K1003R-GFP constructs, we next sought to interrogate the pharmacological generation of IGF-1R CTF as previously described by McElroy et al (McElroy, Powell and McCarthy, 2007). To accomplish this, we utilised phorbol 12-myristate 13-acetate (PMA) and N-[N-(3, 5-difluorophenacetyl)-l-alanyl]-s-phenylglycine t-butyl ester (DAPT) to modulate IGF-1R proteolysis. PMA is a phorbol ester which serves as a potent activator of protein kinase C (PKC) (Tahara *et al.*, 2009; Jiang and Fleet, 2012). PKC activation leads to enhanced activity of sheddases which catalyse the ectodomain shedding of the extracellular IGF-1R component (Hayashida *et al.*, 2010a; Reiss and Bhakdi, 2017). This generates the membrane-anchored CTF which is subsequently processed by gamma-secretase to generate the soluble IGF-1R ICD. DAPT is a gamma-secretase inhibitor and thus prevents breakdown of the IGF-1R CTF by gamma-secretase proteolytic activity (Feng *et al.*, 2019). HEK293T cells were transiently transfected with vectors expressing either the wild-type (WT) or IGF-1R K1003R mutant constructs. 36 hours post transfection, cell cultures were supplemented with PMA (200nM for 2 hours) and DAPT (1µM for 16 hours) as indicated (Figure 3A). Western blot analysis was performed on HEK293T lysates to visualise IGF-1R β-chain-GFP, IGF-1R CTF-GFP and β-actin. Following visualisation, densitometry analysis was performed to analyse the accumulation of the IGF-1R CTF-GFP relative to the amount of β-chain-GFP present (Figure 3B and 3C). It was revealed that there was a significant accumulation (approximately 2.5 fold change in the case of the WT, and approximately 4 fold change in the case of the KDM) of the IGF-1R CTF-GFP in the presence of PMA and DAPT however only a minor accumulation of such was observed with PMA treatment alone across three independent replicates. This was observed for both the WT and IGF-1R K1003R-GFP lysates (Figure 3B and 3C). This indicates that the IGF-1R can undergo proteolysis in the absence of ligand-stimulation as described in the literature previously. This also confirmed that the IGF-1R K1003R-GFP construct is amenable to regulated intramembrane proteolysis and demonstrated that the point mutation introduced does not affect the structural integrity nor expression of the receptor.

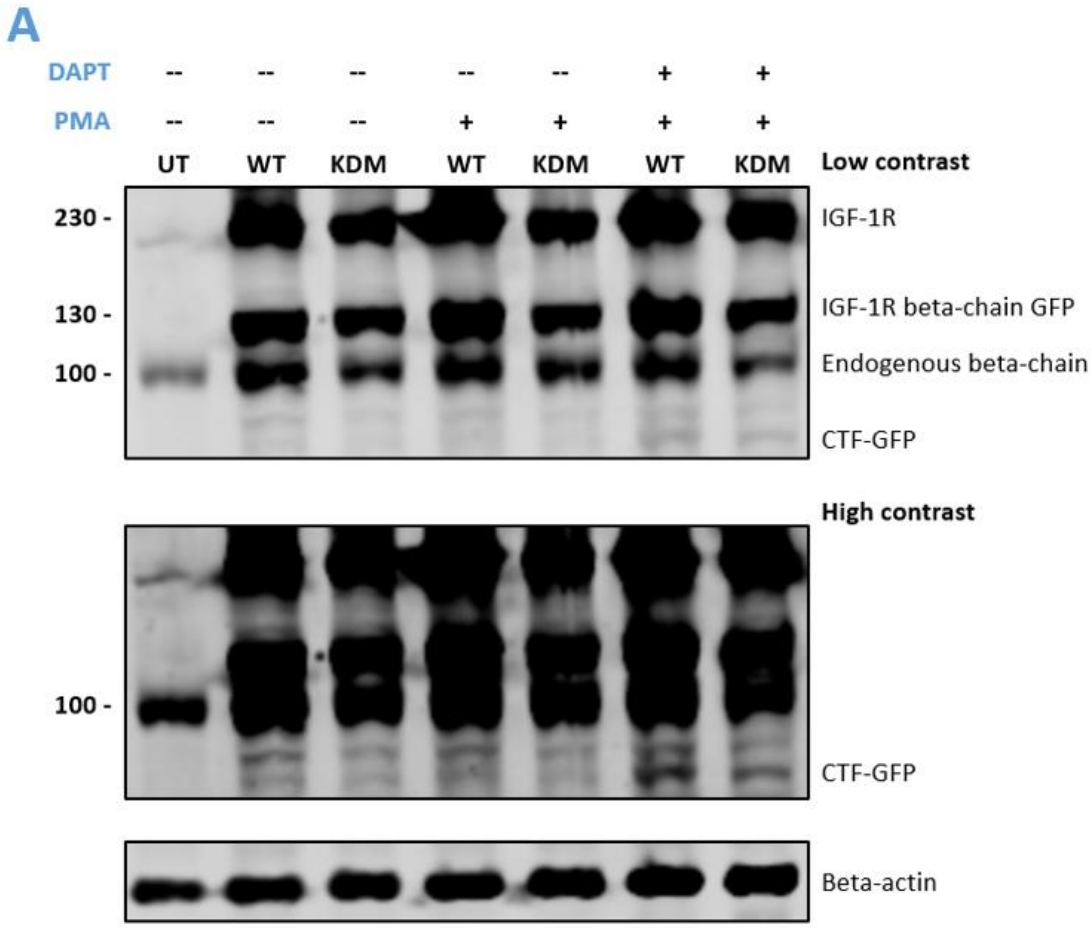
A
DAPT -- -- -- -- -- + +
PMA -- -- -- + + + +
UT WT KDM WT KDM WT KDM
Low contrast
230 -
130 -
100 -
IGF-1R
IGF-1R beta-chain GFP
Endogenous beta-chain
CTF-GFP
High contrast
100 -
CTF-GFP
Beta-actin

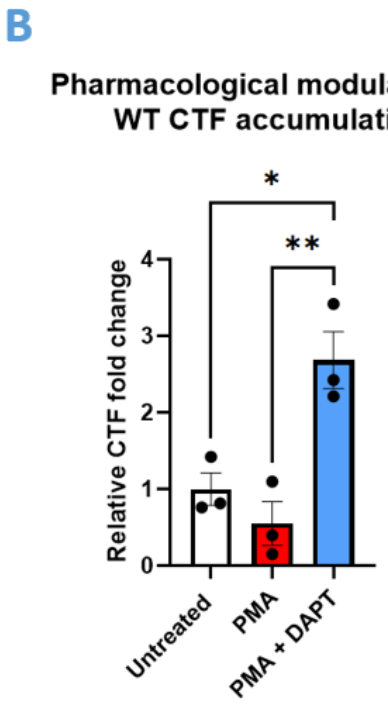
B
Pharmacological modulation of WT CTF accumulation
Relative CTF fold change
0
1
2
3
4
*
**
Untreated
PMA
PMA + DAPT

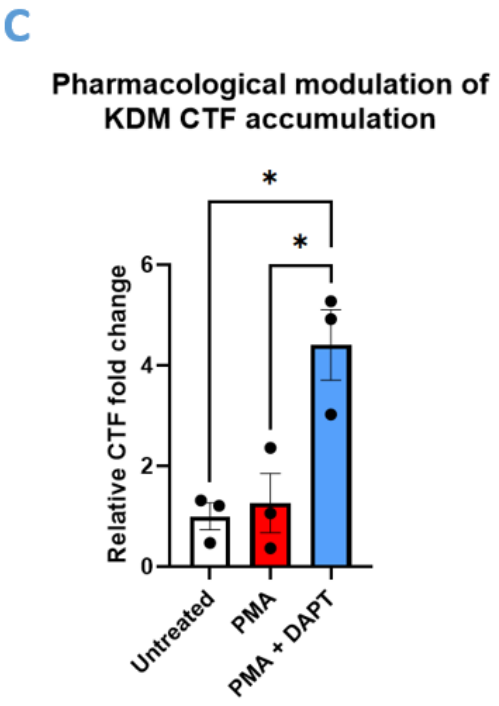
C
Pharmacological modulation of KDM CTF accumulation
Relative CTF fold change
0
2
4
6
*
*
Untreated
PMA
PMA + DAPT

Figure 3: IGF-1R regulated intramembrane proteolysis can occur in a kinase independent fashion

A) *HEK293T cells were transiently transfected with vectors expressing either wild-type (WT) or K1003R kinase dead (KD) IGF-1R C-terminally tagged with GFP. Cells were treated with 200nM PMA (2 hours) and 1µM DAPT (20 hours) prior to cell lysis. Cell lysates were resolved via SDS-PAGE and IGF-1R fragments were detected utilising an anti-β-chain primary antibody. Beta-actin served as a loading control. Primary antibodies were detected using LICOR secondary rabbit and mouse antibodies. Blots were visualised using the LICOR odyssey system.* ***B)*** *Densitometry analysis of WT-IGF-1R accumulation in the presence of pharmacological agents. *: p <0.05: ** p<0.01.* ***C)*** *Densitometry analysis of KDM-IGF-1R CTF-GFP accumulation in the presence of pharmacological agents. *: p <0.05. Data indicative of replicated experiments (n=3).*

3.3 Ligand activation of IGF-1R induces a significant accumulation of IGF-1R CTF

Having validated PMA-induced porteolysis of IGF-1R and IGF-1R CTF generation as previously outlined by McElroy et al, we next sought to determine if with its physiological ligand IGF-1 also enhanced regulated intramembrane proteoysis of IGF-1R. To accomplish this, HEK293T cells transiently transfected with wild-type (WT) or IGF-1R K1003R-GFP mutant constructs. 36 hours post transfection, cell cultures were serum starved for 4 hours and then treated with IGF-1 (10nM for 10 minutes) and DAPT (1µM for 16 hours), where indicated (Figure 4A and 4C). Western blot analysis was performed on HEK293T lysates to visualise IGF-1R β-chain-GFP, IGF-1R CTF-GFP and β-actin (Figure 4A and 4C). Densitometry analysis revealed a significant ligand-induced accumulation of the IGF-1R CTF in the presence of DAPT while very little IGF-1R CTF was detected with just ligand treatment alone (Figure 4A and 4B). In the presence of IGF-1 and DAPT, there was approximately a 3.5 fold change in CTF accumulation acorss 3 independent replicates. Contrastingly, in cells expressing the IGF-1R K1003R-GFP mutant there was minimal IGF-1R CTF accumulation across three independent replciates (Figure 4C). Accumulation observed is likely due to the native basal turnover of the receptor which occurs across cell types. This increase was not statistically significant (Figure 4D) when compared to the untreated cells nor cells treated exclusively with IGF-1. Together, this data indicates that regulated intramembrane proteolysis of IGF-1R is enhanced by IGF-1 ligand stimulation.

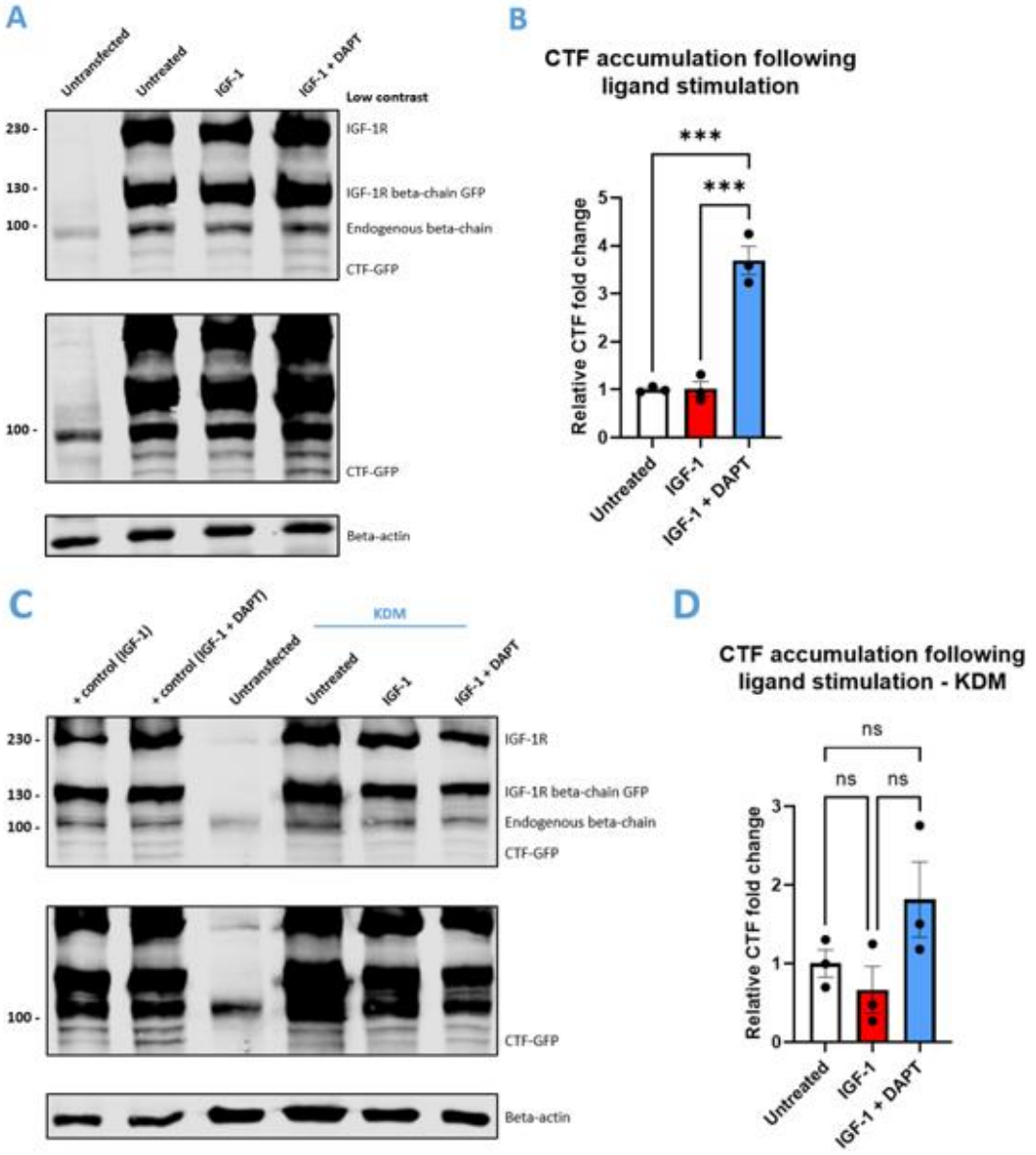
A
Untransfected
Untreated
IGF-1
IGF-1 + DAPT
Low contrast
230 -
130 -
100 -
IGF-1R
IGF-1R beta-chain GFP
Endogenous beta-chain
CTF-GFP
100 -
CTF-GFP
Beta-actin
B
CTF accumulation following ligand stimulation
***
***
Relative CTF fold change
0
1
2
3
4
5
Untreated
IGF-1
IGF-1 + DAPT
C
KDM
+ control (IGF-1)
+ control (IGF-1 + DAPT)
Untransfected
Untreated
IGF-1
IGF-1 + DAPT
230 -
130 -
100 -
IGF-1R
IGF-1R beta-chain GFP
Endogenous beta-chain
CTF-GFP
100 -
CTF-GFP
Beta-actin
D
CTF accumulation following ligand stimulation - KDM
ns
ns
ns
Relative CTF fold change
0
1
2
3
Untreated
IGF-1
IGF-1 + DAPT

Figure 4: Receptor tyrosine kinase activation catalyses regulated intramembrane proteolysis

A) *HEK293T cells were transiently transfected with a vector expressing wild-type IGF-1R-GFP. Cells were serum starved for 4 hrs prior to stimulation with 10ng/mL IGF-1 (10 minutes). Cells were also treated with 1μM DAPT (20 hours) where indicated. Following ligand stimulation, cells were lysed. IGF-1R fragments were detected utilising an anti-β-chain primary antibody. Beta-actin served as a loading control Primary antibodies were detected using secondary rabbit and mouse antibodies. Blots were visualised using the LICOR odyssey system.* ***B)*** *Densitometry analysis of WT IGF-1R-GFP CTF accumulation following ligand stimulation. ***: p<0.001* ***C)*** *Procedure as with A) however, previously validated WT CTF-GFP lysates were run alongside the kinase dead mutant (IGF-1R K1003R-GFP) lysates for clarity.* ***D)*** *Densitometry analysis of IGF-1R K1003R CTF-GFP accumulation following ligand stimulation. No significance was observed. Data indicative of replicated experiments (n=3).*

3.4 Metalloprotease-dependent ectodomain shedding is required for IGF-1R CTF generation

It is well documented that ectodomain shedding of receptor tyrosine kinases is necessary for receptor processing through regulated intramembrane proteolysis (Lal and Caplan, 2011). While both serine proteases and metalloproteases have both been implicated in ectodomain shedding, metalloproteases tend to be the dominant sheddases (Hayashida *et al.*, 2010b). With this is mind, we wanted to determine the protease subtype (serine or metallo) responsible for shedding of the IGF-1R ectodomain via the administration of batimistat (a broad spectrum metalloprotease inhibitor). HEK293T cells transiently expressing wild-type IGF-1R GFP were treated with Batimistat (20µM for 2 hours) in conjunction wth IGF-1 (10nM for 10 minutes +/- DAPT (1µM for 16 hours), as indicated (Figure 5A). Following lysate resolution on 10% SDS-PAGE gels and subsequent western blotting for IGF-1R β-chain-GFP, IGF-1R CTF-GFP and β-actin, densitometry analysis revealed a significant decrease in CTF generation in cells treated with batimistat. Cells treated with IGF-1 and batimistat displayed a similar amount of CTF generation versus cells treated with IGF-1 alone as expected. Importantly, the addition of DAPT failed to result in further CTF accumulation in cells also subject to batimistat treatment. From this data, we have determined that metalloproteases are likely the sheddases responsible for the bulk of IGF-1R ectodomain shedding. This is evident from the significant suppression of CTF accumulation in the presence of IGF-1 with batimistat and DAPT.

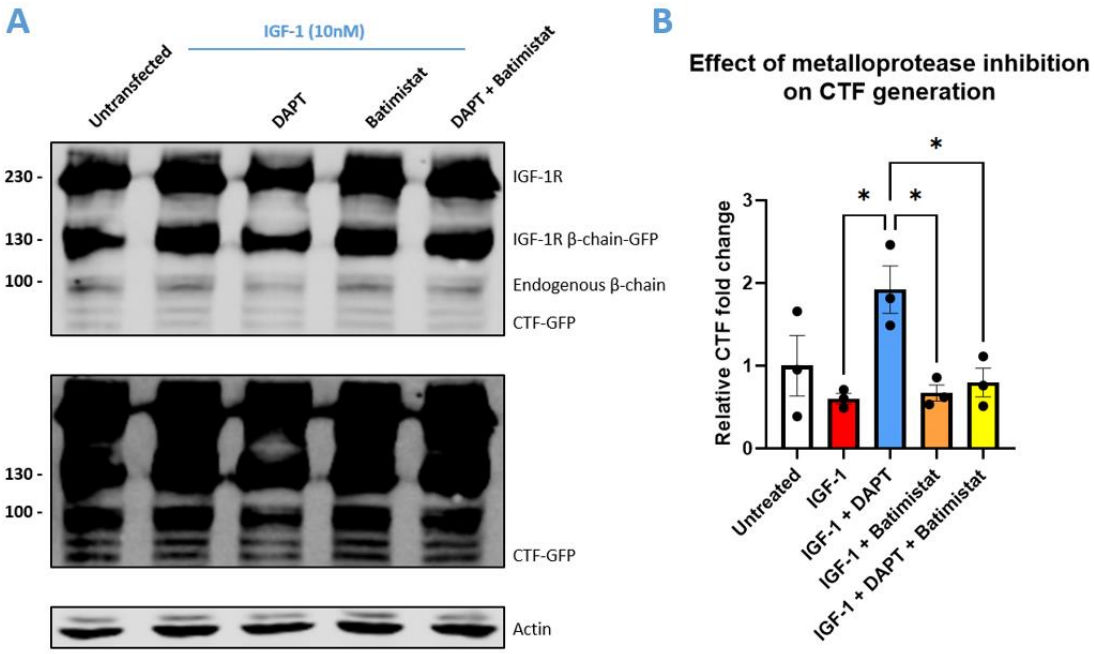

Figure 5: Metalloprotease inhibition with batimistat suppresses IGF-1R CTF accumulation

A) *HEK293T cells were transfected with a vector expression wild-type IGF-1R-GFP. Cells were treated with DAPT (1µM for 16 hours), IGF-1 (10nM for 10 minutes) and batimistat (20µM for 2 hours) where indicated. Prior to the administration of IGF-1 and batimistat, cells were serum starved for 4 hours. IGF-1R fragments were detected utilising an anti-β-chain primary antibody. B-actin served as a loading control. Primary antibodies were detected using secondary rabbit and mouse antibodies. Blots were visualised using the LI-COR Odyssey system.* ***B)*** *Densitometry analysis of WT-IGF-1R CTF-GFP accumulation following treatment with pharmacological agents. *: $p<0.05$. Data indicative of replicated experiments (n=3).*

3.5 Clathrin-mediated endocytosis may be a pre-requistite step for IGF-1R proteolysis

Following confirmation of regulated intramembrane proteolysis of IGF-1R following IGF-1 stimulation, we next wanted to interrogate the potential role of receptor endocytosis during regulated intramembrane proteolysis. The IGF-1R is believed to undergo endocytosis following ligand stimulation, mediated through both clathrin and caveolin-mediated endocytosis (Martins *et al.*, 2011; Davis *et al.*, 2018b). The activity of sheddases and gamma-secretase complexes seem to be spatially regulated and this coincides with the differential distribution of family members/complex forms. In order to investigate this, HEK293T cells were seeded, transfected and treated as previously outlined. Following 4 hours of serum starvation, cell cultures were treated with IGF-1 (10nM for 10 minutes), DAPT (1µM for 16 hours) or clathrin-mediated (pitstop 15µM for 2 hours/dynasore 35µM for 2 hours) and caveolin-mediated (methyl-β-cyclodextrin 5mM for 2 hours) endocytosis inhibitors, as indicated (Figure 6A). Pitstop suppresses clathrin-mediated endocytosis through inhibiton of clathrin heavy-chain oligomerisation (Willox, Sahraoui and Royle, 2014). Dynasore also inhibits such endocytosis however it functions as a GTPase inhibitor and thus prevents the severing of mature clathrin-coated invaginations from the plasma membrane by dynamin (Kirchhausen, Macia and Pelish, 2008). Methyl-β-cyclodextrin functions as a cholesterol stripping agent (Mahammad and Parmryd, 2008). This is thought to inhibit caveolin-mediated endoyctosis through prevention of receptor organisation into lipid rafts which is a pre-requisite step to caveolin-mediated endocytosis (Kiss and Botos, 2009; Kumari, Mg and Mayor, 2010). Western blot analysis was used to visualise receptor components and β-actin (Figure 6A) and densitometry analysis was conducted (Figure 6B). Statistical analysis of the densitometry data revealed that gamma-secretase mediated IGF-1R proteolysis seems to be contingent on clathrin-mediated endocytosis. In the presence of pitstop/dynasore IGF-1R CTF accumulation following gamma-secretase inhibition was suppressed (Figure 6B). Contranstingly, IGF-1R CTF accumulation (and thus gamma-secrtease processing of IGF-1R) appears to be insensitive to caveolin-mediated endocytosis inhibiton as no marked decrease in IGF-1R CTF generation was detected in the presence of methyl-β-cyclodextrin (Figure 6B). Taken together, this

data indicates that clathrin-mediated endocytosis may be a pre-requisite step for IGF-1R processing by gamma-secretase.

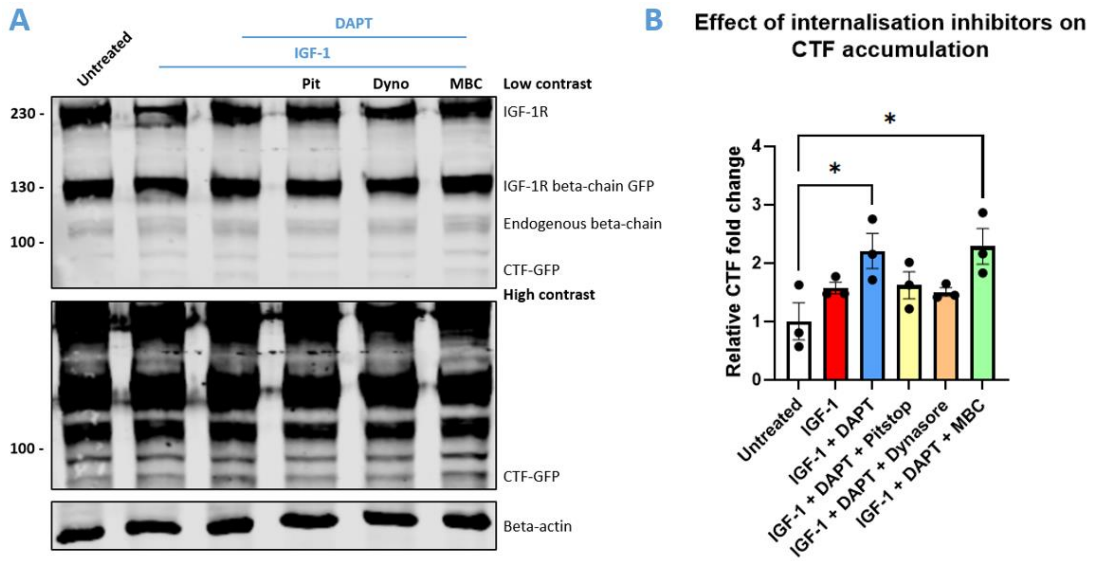

Figure 6: Inhibition of clathrin-mediated endocytosis suppresses CTF accumulation

A) *HEK293T cells were transiently transfected with a vector expressing wild-type IGF-1R-GFP. Cells were treated with 1 µM DAPT (16 hours) where indicated. Cells were serum starved for 4 hours prior to stimulation with 10 nM IGF-1 (10 minutes). During the 4 hour serum starvation, cells were also treated with 15 µM Pitstop 2, 35 µM Dynasore and 5mM methyl-ß-cyclodextrin for 2 hours (after 2 hours had elapsed). IGF-1R fragments were detected utilising an anti-ß-chain primary antibody. B-actin served as a loading control. Primary antibodies were detected using secondary rabbit and mouse antibodies. Blots were visualised using the LI-COR Odyssey system.* ***B)*** *Densitometry analysis of WT-IGF-1R CTF-GFP accumulation following treatment with various pharmacological agents. *: p<0.05. Data indicative of replicated experiments (n=3).*

3.6 - IGF-1R CTF undergoes nuclear translocation in a clathrin dependent manner

Numerous receptor tyrosine kinases have been found to undergo nuclear translocation upon ligand binding, including IGF-1R (Aleksic *et al.*, 2010b; Carpenter and Liao, 2013b). Many such receptors are capable of shuttling to the nucleus as their full-forms or as fragments following gamma secretase-mediated regulated intramembrane proteolysis (Carpenter and Liao, 2013). Interestingly, reports have indicated that the IGF-1R, unlike other receptor tyrosine kinases, retains its hetero-tetrameric structure once at the nucleus (Aleksic *et al.*, 2010b). Furthermore, nuclear translocation of receptors seems to correlate with poor patient prognosis and a more malignant phenotype (Aleksic *et al.*, 2010b; Song, Rosen and Corfas, 2013; Martin *et al.*, 2022b; Molina *et al.*, 2022). Taking this into consideration, HEK293T cells were transiently transfected with a vector expressing WT-IGF-1R-GFP (Figure 7 and 8). Cells were serum starved and treated with IGF-1 and pharmacological agents as previously described. Cells were lysed according to REAP protocol with modifications made to optimise its use for a 6-well dish format (Suzuki *et al.*, 2010b). REAP yielded whole cell lysates, cytosolic fractions and nuclear fractions for each cell culture. These lysates were loaded in a ratio of 1:2:1 (whole cell: cytosolic: nuclear) to account for expected protein levels and differential enrichment in the various fractions. IGF-1R CTF accumulation was observed in cells treated with DAPT consistent with previous data (Figure 7). Interestingly, IGF-1R CTF accumulation was also observed even in the presence of TAPI (broad spectrum metalloprotease inhibitor) (Rasmussen and Mccann, 1997). IGF-1R CTF was visualised across all 3 fractions in the samples thus indicating that IGF-1R CTF undergoes nuclear translocation. These data also indicates that IGF-1R CTF subcellular translocation appears to occur in a metalloprotease independent fashion.

To further investigate the dynamics of IGF-1R nuclear translocation, the same fractionation protocol was performed, however, cells were treated with Pitstop in place of batimistat in this assay (Figure 8). This aimed to determine whether clathrin-mediated endocytosis was required for nuclear translocation of the CTF as is the case

with the full-form receptor. We wanted to further investigate clathrin-mediated endocytosis based on the data of our internalisation assays which identified clathrin-mediated endocytosis as a potential mediary step in IGF-1R regulated intramembrane proteolysis. Western blot analysis revealed that IGF-1R CTF accumulation was observed in the cells treated with ligand and DAPT however this accumulation was suppressed in the whole cell lysates with the addition of Pitstop (Figure 8). IGF-1R CTF appeared to accumulate in the nuclear fraction in the presence of DAPT and IGF-1, however, this accumulation was decreased by the addition of Pitstop in concordance with the whole cell lysates. In this assay, Histone H3 was utilised as a nuclear marker. Due to the intrinsic variability with lysates generated using the REAP protocol, the levels of Histone H3 appear to be inconsistent across the sample types. Regardless this data, together with data acquired from our internalisation assays, indicates a potential multi-functional role for clathrin-mediated endocytosis in the processing of the receptor by regulated intramembrane proteolysis and subsequent shuttling of the relevant CTF to the nucleus.

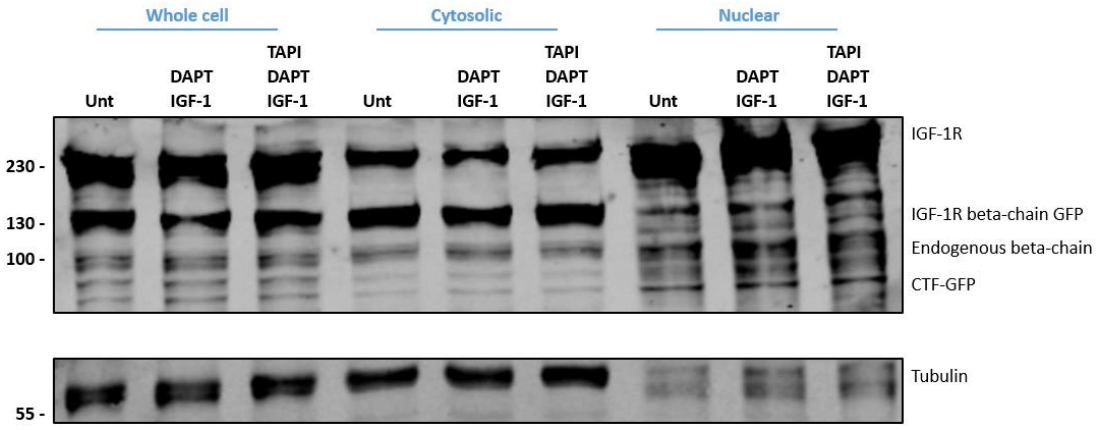

Figure 7: IGF-1R CTF can undergo nuclear translocation

HEK293T cells were transiently transfected with a vector expressing wild-type IGF-1R-GFP. Cells were either left untreated (UNT) or treated with 10nM IGF-1 (10 minutes) following serum starvation for 4 hours. Where indicated, cells were also treated with 1µM DAPT (20 hours) and 20µM TAPI (2 hours). Cells were processed into whole cell, cytosolic and nuclear fractions according to the REAP protocol (Suzuki et al, 2010). These fractions were loaded on the SDS-PAGE gel in a ratio of 1:2:1. IGF-1R fragments were detected utilising an anti-β-chain primary antibody. Tubulin was used as a loading control and as a means of determining nuclear fraction purity. Primary antibodies were detected using secondary rabbit and mouse antibodies. Blots were visualised using the LICOR Odyssey system. Data indicative of replicated experiments (n=3).

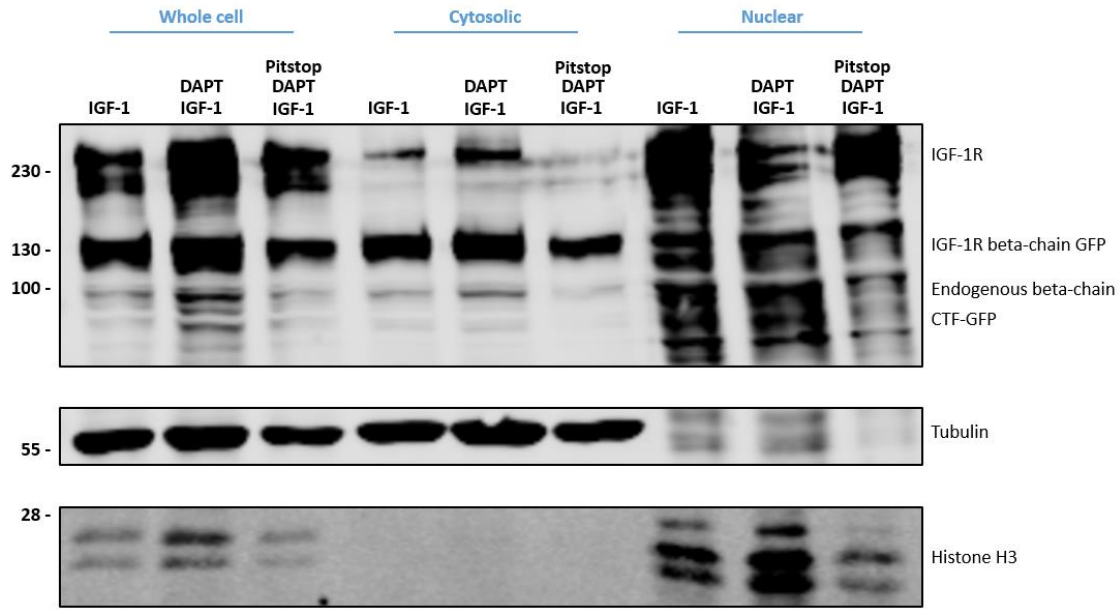

Figure 8: Nuclear translocation of IGF-1R CTF is clathrin-mediated endocytosis sensitive *HEK293T cells were transiently transfected with a vector expressing wild-type IGF-1R-GFP. Cells were either left untreated (UNT) or treated with 10nM IGF-1 (10 minutes) following serum starvation for 4 hours. Where indicated, cells were also treated with 1µM DAPT (20 hours) and 15µM Pitstop (2 hours). Cells were processed into whole cell, cytosolic and nuclear fractions according to the REAP protocol (Suzuki et al, 2010). These fractions were loaded on the SDS-PAGE gel in a ratio of 1:2:1. IGF-1R fragments were detected utilising an anti-β-chain primary antibody. Tubulin was used as a loading control and as a means of determining nuclear fraction purity. Histone H3 was utilised as a nuclear loading control. Primary antibodies were detected using secondary rabbit and mouse antibodies. Blots were visualised using the LICOR Odyssey system. Data indicative of replicated experiments (n=3).*

3.7 Effects of pharmacological agents on cell migration

Due to the functions of nuclear IGF-1R targets converging upon cell migration and metastasis, we next investigated the effects of our pharmacological agents on HeLa cell migration in the form of a puncture wound healing assay. Initially, an IGF-1 dose response was performed to identify the optimal IGF-1 concentration that stimulated HeLa cell migration for our purposes. After 20 hours of treatment, we determined that 50nM IGF-1 resulted in marked wound closure without obfuscating the perimeter of the wound (data not shown). Next, we confirmed that the wound closure induced by this concentration of IGF-1 can be suppressed utilising the reversible IGF-1R receptor tyrosine kinase activity inhibitor BMS-754807 (10nM). Treatment of HeLa cells with BMS-754807 resulted in a significant (approximately 1.2 fold change) suppression of IGF-1 induced cell migration, thus validating that our assay is functional in terms of migration activation and suppression (Figure 9). Following assay validation, we investigated whether treatment with the gamma-secretase inhibitor DAPT would reduce IGF-1 induced migration. Cells were first serum starved for 4 hours, in the presence of DAPT (1µM) to attenuate gamma-secretase activity. After serum starvation, DAPT (1µM) was administered alone or alongside IGF-1 (50nM) for 20 hours. Following quantification of wound closure and statistical analysis, it was revealed that DAPT alone did not suppress migration (Figure 10). Next, a similar assay was performed with Pitstop (30µM) in place of DAPT. Pitstop was administered alone or in combination with IGF-1 (50nM) and analysis was performed as outlined previously. Again, no significant reduction in HeLa cell migration was observed (Figure 11). Hence, we decided to perform a combinatorial Pitstop/DAPT treatment in the presence of IGF-1 (50nM). Following co-administration of Pitstop/DAPT in the presence or absence of IGF-1, there was a significant amount of HeLa cell detachment from the wells, indicative of cell death (Figure 12). To try and remedy this, a concentration gradient of Pitstop was performed alongside a constant concentration of DAPT (1µM). Three concentrations of Pitstop were selected however no combination of Pitstop/DAPT was found to ameliorate cell detachment (Figure 12). Unfortunately, due to the majority of cells in each well detaching, we determined that the contemporaneous inhibition of gamma-secretase and clathrin-mediated endocytosis is cytotoxic and thus this dual

treatment approach is likely unsuitable. The final pharmacological agent we administered was the broad-spectrum metalloprotease inhibitor batimistat. Batimistat (20μM) was administered alone or in conjunction with IGF-1 (50nM). Interestingly, batimistat resulted in a significant suppression of wound closure in the presence of IGF-1 (Figure 13). This result indicates two potential reasons for such an outcome. Firstly, ectodomain shedding of IGF-1R likely occurs through ADAM family protein members, similar to other receptor tyrosine kinases as discussed previously. Secondly, the dynamic turnover and dissolution of focal adhesion complexes containing IGF-1R is required for cell migration in response to IGF-1. It is plausible that ectodomain shedding of IGF-1R may contribute to the dissolution of such focal adhesion complexes, potentially through disrupting IGF-1R/integrin association.

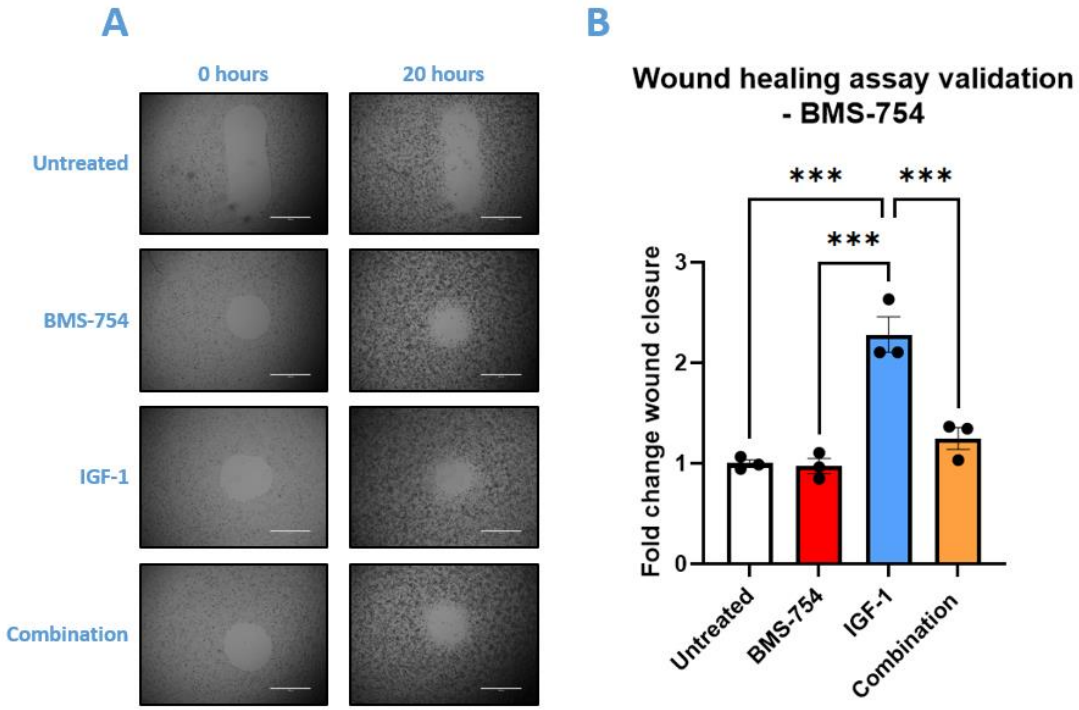

Figure 9: Validation of wound healing assay utilising BMS-754087 (reversible IGF-1R inhibitor)

HeLa cells were seeded ~24 hours prior to wound being inflicted. 3 wounds were created per well, and the degree of wound closure was calculated based off the aggregate percentage closure of the wounds. ***A)*** *Throughout the 20-hour time course, cells were either untreated (serum free DMEM only), treated with BMS-754087 (10nM), stimulated with IGF-1 (50nM), or a combination of BMS-754087 and IGF-1 was administered.* ***B)*** *Anova analysis of the degree of wound closure between treatment types. Wound closure values were obtained as a percentage which were then converted into relative fold change in wound closure.*

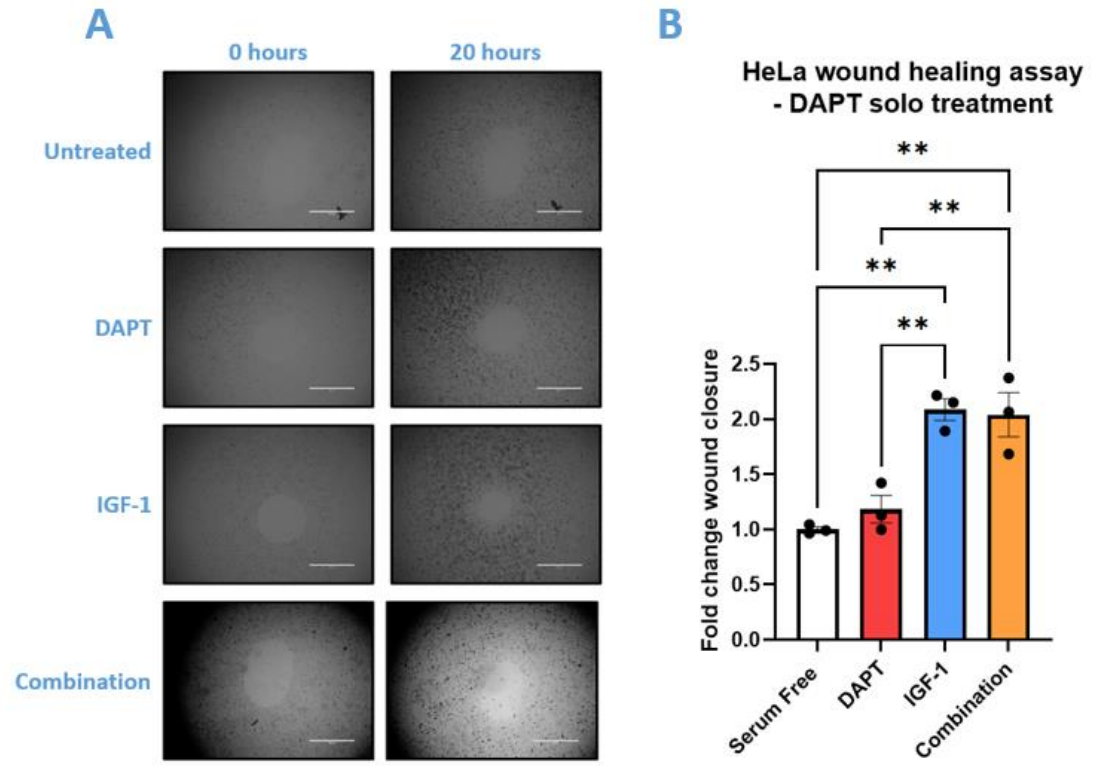

Figure 10: Inhibition of gamma-secretase does not suppress IGF-1 induced migration

HeLa cells were seeded as before, and the degree of wound closure was quantified in the same manner as previously described. ***A)*** *Throughout the 20-hour time course, cells were either left untreated (serum free DMEM only), treated with DAPT (1µM), stimulated with IGF-1 (50nM), or treated with DAPT and IGF-1 in combination.* ***B)*** *Anova analysis of the degree of wound closure between different treatment conditions. Comparison of wound closure between treatments was quantified as before.*

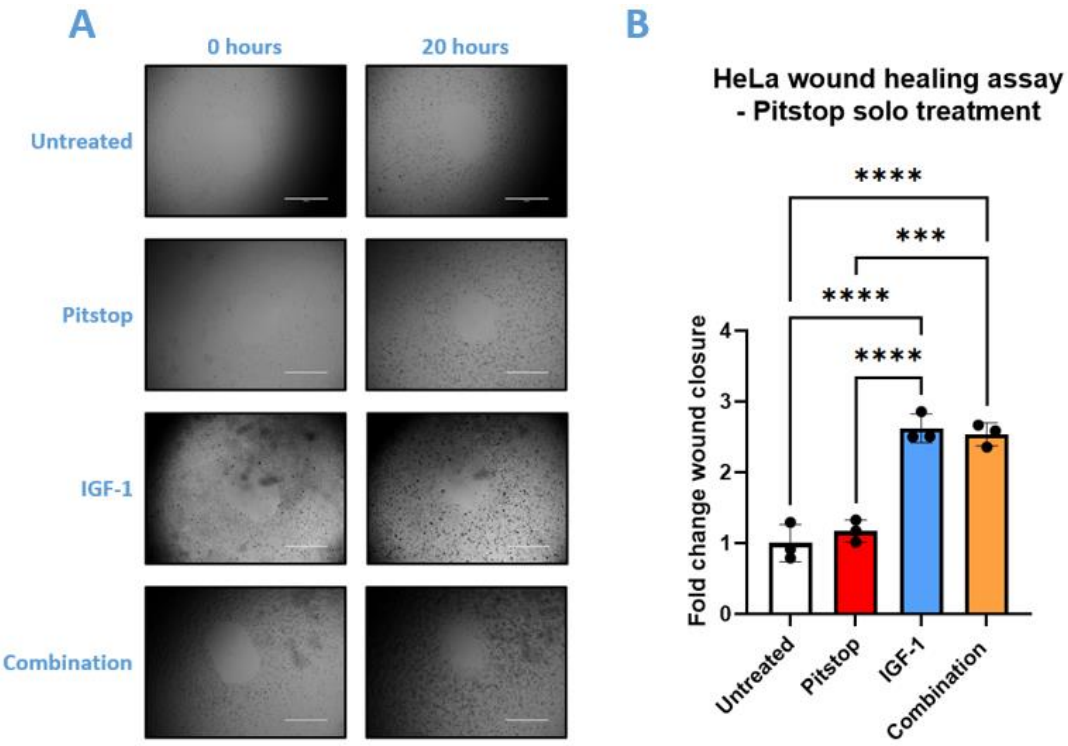

Figure 11: Inhibition of clathrin-mediated endocytosis does not suppress IGF-1 induced migration

HeLa cells were seeded as before, and the degree of wound closure was quantified in the same manner as previously described. ***A)*** *Over the course of 20-hours, cells were either untreated (serum free DMEM only), treated with Pitstop (30µM), stimulated with IGF-1 (50nM), or subjected to a combination of IGF-1 and Pitstop.* ***B)*** *Anova analysis of the degree of wound closure between the different conditions utilised. Comparison of wound closure between treatments was quantified as before.*

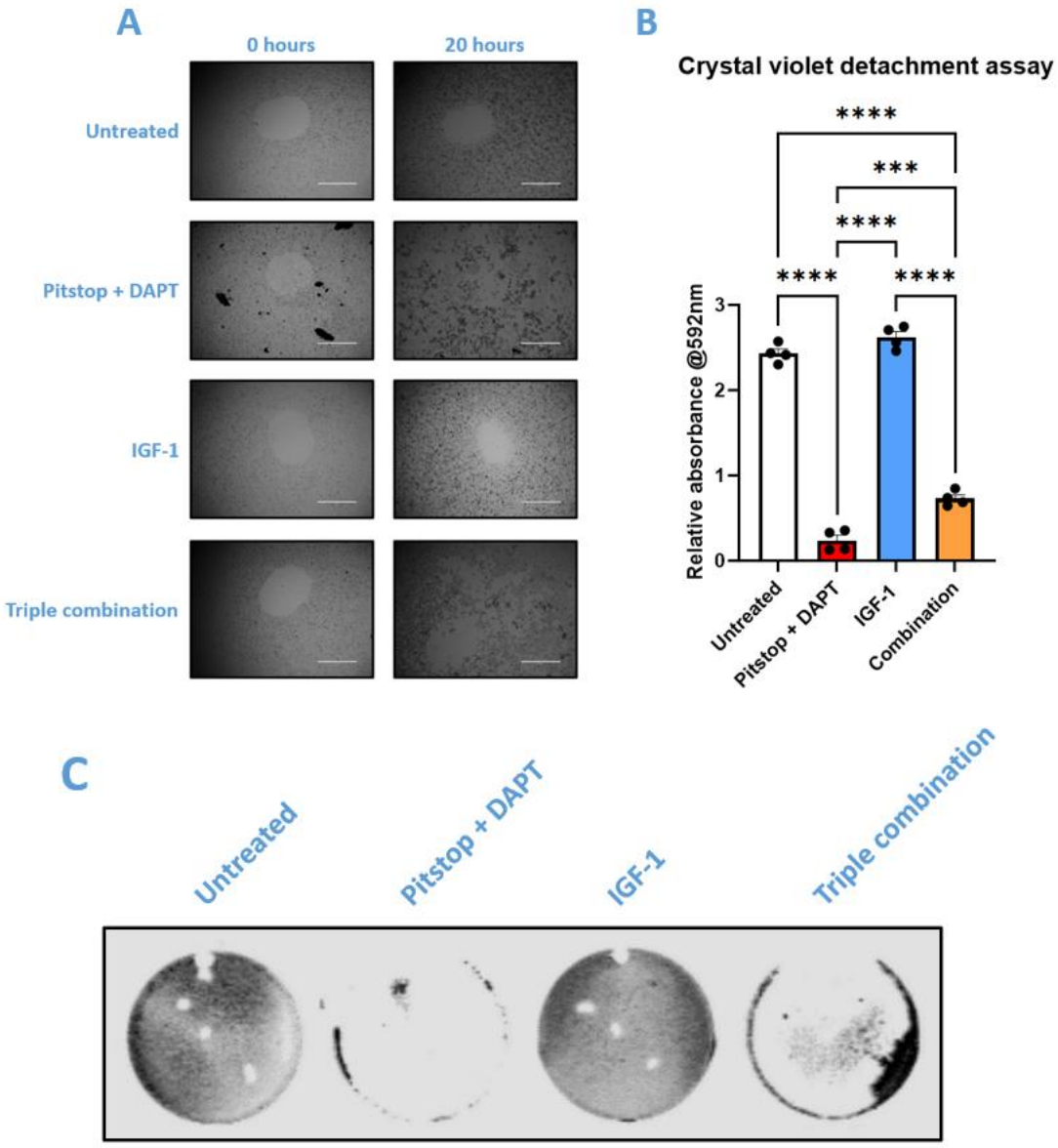
A
0 hours
20 hours
Untreated
Pitstop + DAPT
IGF-1
Triple combination
B
Crystal violet detachment assay
****
***
****
****
****
Relative absorbance @592nm
3
2
1
0
Untreated
Pitstop + DAPT
IGF-1
Combination
C
Untreated
Pitstop + DAPT
IGF-1
Triple combination

Figure 12: Long-term treatment with DAPT and Pitstop leads to HeLa cell cytotoxicity

HeLa cells were seeded as before and treated with DAPT, Pitstop and IGF-1 in a similar fashion as previously outlined. ***A)*** *Cells were left untreated (serum free DMEM only), treated with a combination of DAPT (1µM) and Pitstop (30µM) in the absence or presence of IGF-1 (50nM). Images were captured at 0-hours and 20-hours.* ***B)*** *Anova analysis (n=2) of crystal violet absorbance readings obtained following a crystal violet cell detachment assay and subsequent crystal violet solubilisation. Crystal violet solutions were loaded in duplicate for each sample.* ***C)*** *Visualisation of cells which remained attached, stained with crystal violet. Well images were captured using the LiCOR Odyssey system.*

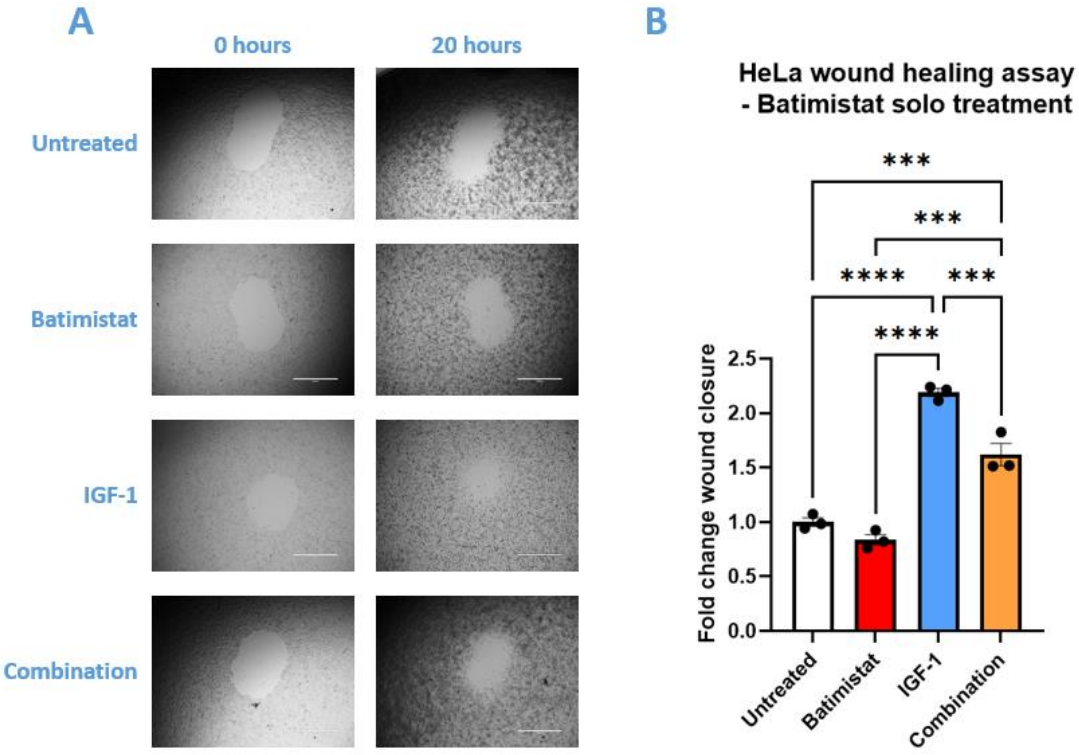

Figure 13: Inhibition of ectodomain shedding suppresses IGF-1 induced cell migration

HeLa cells were seeded as before, and the degree of wound closure was quantified in the same manner as previously described. ***A)*** *Over the course of 20-hours, cells were either untreated (serum free DMEM only), treated with Batimistat (20μM), stimulated with IGF-1 (50nM), or subjected to a combination of IGF-1 and Batimistat.* ***B)*** *Anova analysis of the degree of wound closure between the different conditions utilised. Comparison of wound closure between treatments was quantified as before. Data indicative of replicated experiments (n=3).*

Chapter 4:
Discussion

4.1 Discussion

Various receptor tyrosine kinases undergo regulated intramembrane proteolysis (RIP). Classically, this was regarded as a means of ending receptor signalling. It has now become apparent that the soluble ICDs generated by gamma-secretase during this proteolytic cascade retain signalling activity and, in some instances, acquire atypical signalling activities (Chen and Hung, 2015). RIP begins with ectodomain shedding, catalysed by sheddases (proteases which cleave receptors in the extracellular juxtamembrane region), which generates a membrane anchored C-terminal fragment (CTF) which is subsequently cleaved by gamma-secretase (Hayashida *et al.*, 2010a; Lichtenthaler, Haass and Steiner, 2011; Miller, Sullivan and Lauffenburger, 2017). Gamma-secretase activity generates soluble intracellular domains (ICD) by cleaving CTFs in the plane of the plasma membrane. ICDs are rather labile and are predominantly degraded via the proteasomal system as evidenced by the accumulation of ICDs following administration of MG132/Epoxymycin (proteasomal inhibitors) (Öberg *et al.*, 2001; McElroy, Powell and McCarthy, 2007; Watanabe and Nakamura, 2012).

In this study, initially, a kinase dead mutant of the IGF-1R was created using a site-directed mutagenesis approach. This was accomplished via the conversion of lysine 1003 to arginine. Sanger sequencing determined the successful generation of our desired point mutant. Receptor inactivation was validated via western blot analysis of phospho-ERK1/2 levels. ERK1/2 phosphorylation was only enhanced in HEK293T cells transiently transfected with the wild-type form of the receptor. Levels of phospho-ERK1/2 in cells expressing the kinase dead mutant were similar to that of untransfected cells and IGF-1R-GFP wild-type expressing cells which were not stimulated with IGF-1. The combination of nucleic acid sequence analysis and western blotting proved that our site-directed mutagenesis approach was successful in generating our target kinase dead mutant.

Having created our mutant, we next sought to validate the proteolysis of IGF-1R as reported previously (McElroy, Powell and McCarthy, 2007). This was accomplished via the treatment of cells with PMA (a phorbol ester activator of PKC) and DAPT (a gamma-secretase inhibitor). Indeed, the combination of PMA and DAPT lead to an increase in CTF accumulation in cells expressing both the IGF-1R-GFP wild-type and IGF-1R K1003R-GFP mutant constructs. This consolidated the mechanism described by McElroy et al 2007 while also confirming that the kinase dead mutant construct undergoes ectodomain shedding and gamma-secretase processing much the same as the wild-type. Having validated the cleavage of both IGF-1R constructs, we next interrogated the effect of ligand stimulation with respect to IGF-1R CTF accumulation. HKE293T cells transiently overexpressing IGF-1R-GFP wild-type and IGF-1R K1003R-GFP constructs were treated with the gamma-secretase inhibitor DAPT, however IGF-1 was administered in place of PMA to induce receptor activation. Unlike with PMA treatment, significant accumulation of IGF-1R CTF-GFP was only observed in cells expressing the IGF-1R-GFP wild-type construct. Cells expressing the IGF-1R K1003R-GFP construct displayed no significant variation in IGF-1R CTF-GFP levels. The minute increase in IGF-1R CTF accumulation in the presence of DAPT in cells expressing the IGF-1R K1003-GFP construct is likely due to the intrinsic basal turnover of the receptor by gamma-secretase irrespective of receptor activity. Together, this data indicates that stimulation of IGF-1R with its physiological ligand seems to catalyse regulated intramembrane proteolysis of IGF-1R, culminating in increased IGF-1R CTF accumulation in the presence of DAPT.

Building upon existing research outlining IGF-1R internalisation and nuclear translocation, we wanted to interrogate whether receptor internalisation modulated receptor cleavage and subcellular translocation of the proteolytic fragments, namely the CTF. To accomplish this, cells were treated with clathrin-mediated endocytosis and caveolin-mediated endocytosis (CavME) inhibitors in combination with IGF-1 and DAPT. Inhibition of clathrin-mediated endocytosis appeared to reduce CTF accumulation whereas inhibition of CavME did not suppress CTF accumulation. This data buttresses current research which indicates that clathrin-mediated endocytosis

is the predominant mode of IGF-1R internalisation, and that CavME functions as somewhat of an "overflow pathway" to support clathrin-mediated endocytosis in the event of clathrin-mediated endocytosis saturation (Goh and Sorkin, 2013; Davis *et al.*, 2018a; Rieger and O'Connor, 2021). Utilising a cellular fractionation approach, our data suggests that clathrin-mediated endocytosis may be required for nuclear translocation of CTF-GFP, consistent with contemporary findings which report clathrin-mediated endocytosis as an essential step for nuclear translocation of the full-form receptor. In the presence of Pitstop, cells stimulated with IGF-1 and DAPT displayed less CTF accumulation in the nucleus when compared with cells treated with only IGF-1 and DAPT. Although our data does indicate a potential need for clathrin-mediated endocytosis with respect to CTF nuclear translocation, the REAP fractionation protocol has some inherent limitations. The main limitation is the fact that cellular lysates across different samples can't be normalised by means of a colorimetric assay. Soluble protein is only released from the "whole cell" and "nuclear" fractions following addition of laemmli buffer therefore no assay can subsequently be performed to quantify the protein concentration isolated from each different fraction. Secondly, different fractions display differential protein enrichment. We attempted to account for this by loading the different fractions at different ratios however, again, this is performed using protein lysates which have not been normalised. Based on the levels of Histone H3 detected in the "whole cell" and "nuclear" fractions of our assay, it is evident that there was uneven protein concentrations across sample types. Cells treated with the combination of IGF-1, Pitstop and DAPT displayed much lower protein levels when compared with the other two treatment conditions. Taking these limitations into account, our fractionation data suggests that Pitstop may well have suppress nuclear accumulation of the IGF-1R CTF-GFP however we can't definitively determine that it is an essential regulatory step.

Having identified potential regulatory steps of IGF-1R regulated intramembrane proteolysis utilising a western blotting-based approach, we sought to elucidate a cellular function for IGF-1R regulated intramembrane proteolysis. Contemporary

data regarding IGF-1R translocation to subcellular organelles, and its functions therein, seem to converge on cell migration, chemoresistance and metastasis. Current data insinuates that IGF-1R subcellular translocation contributes to emergence of a more malignant and metastatic phenotype across a slew of cancers. With this in mind, we decided to investigate the effects of our arsenal of pharmacological agents on IGF-1-induced cell migration using a HeLa cell model. Utilising a customised puncture wound healing assay protocol we examined the effects of our pharmacological agents individually and in combination to determine if they were capable of suppressing IGF-1-induced cell migration in our HeLa cancer cell model. The administration of DAPT and Pitstop individually was incapable of suppressing IGF-1 induced cell migration, however, HeLa cell treatment with batimistat alone was able to significantly suppress IGF-1-induced cell migration. With DAPT and Pitstop having failed in individual treatments we hypothesised that perhaps a combination of the two was required to suppress migration. Unfortunately, the combination of DAPT and Pitstop over the course of 20 hours lead to significant cell detachment during crystal violet staining. Detachment indicates cell death in this instance, and a robust level of cell detachment was observed across a range of Pitstop concentrations. As a result of this cell detachment, we deemed the combination of DAPT and Pitstop unsuitable for our analysis. It is likely that the combination of gamma-secretase inhibition coupled with suppression of endocytosis over a protracted period exerts excessive stress on cells leading to apoptosis.

4.2 Future perspectives

Data gathered using our kinase-dead mutant indicates that IGF-1 induced receptor activation catalyses receptor proteolysis. However, when this hypothesis was further examined with an assay which made use of BMS-754807, a potent reversible inhibitor of the IGF-1R/insulin receptor family kinases, there was no significant suppression of CTF accumulation across samples. It would likely be more optimal to perform these assays in a cancer cell line with high levels of endogenous IGF-1R expression such as MCF-7 cells. The overexpression of the receptor may impinge upon the activity of BMS-754807 and may hamper its ability to suppress IGF-1-mediated receptor activation. While our data indicates that metalloproteases are likely the sheddases which catalyse IGF-1R ectodomain shedding, replicating our western blot-based batimistat ectodomain shedding assay with a broad-spectrum serine protease inhibitor (such as camostat) would further clarify the mediators of IGF-1R ectodomain shedding. Furthermore, in place of a broad-spectrum metalloprotease inhibitor (batimistat), it could be worthwhile using specific inhibitors of ADAM family proteins and/or inhibitors of matrix metalloproteases to further validate IGF-1R ectodomain shedding. Importantly, cell lysis, and subsequent western blot analysis of intracellular CTF accumulation, is only one means by which IGF-1R ectodomain shedding could be investigated. Shedding of the IGF-1R α-chain into the extracellular space could be examined as another measure of the degree of ectodomain shedding in the presence of various pharmacological agents. Hypothetically, cells could be treated with sheddase inhibitors and the expended cell culture media could be collected and processed via TCA precipitation. The isolated precipitate could then be assayed, by ELISA and/or western blotting, using an antibody specific to an epitope present in the IGF-1R α-chain. Any difference in α-chain accumulation in this context could be compared to CTF accumulation under the same conditions. A molecular approach to the same query could be to generate ADAM/MMP knock-out cell lines and perform such assays in this cell system. With regards to our internalisation assays, using both endocytic inhibitors and a gamma-secretase inhibitor, it does seem as though clathrin-mediated endocytosis is required for the processing of IGF-1R by gamma-secretase. Our data subtly suggests that gamma-secretase cleavage of IGF-1R is primarily mediated by presenilin-2 however

our data alone does not definitively conclude whether such processing is augmented by different permutations of gamma-secretase complexes. To parse apart to role of different gamma-secretase complexes in IGF-1R cleavage, our internalisation assay could be performed in knock-out cell lines of either presenilin-1 or 2. This would provide more compelling evidence as to which presenilin isoform is required for IGF-1R processing. In the context of subcellular translocation, there is much analysis still required. We interrogated nuclear translocation of the CTF only using Pitstop, therefore it is advisable to perform REAP subcellular fractionation with other inhibitors such as Dynole and methyl-β-cyclodextrin. This would further support our current hypothesis that CTF nuclear translocation necessitates clathrin-mediated endocytosis, consistent with the full-form receptor.

To interrogate the proteolytic processing of the receptor under pseudo-physiological conditions, cleavage analysis assays using our menagerie of pharmacological agents could be performed in a cancer cell model with robust endogenous IGF-1R expression, such as MCF-7 cells. These cells respond well to IGF-1 stimulation and highly express IGF-1R endogenously. The use of overexpression, as we have done, is useful for proof-of-concept based analysis however the translatability and relevance of such work is obfuscated by the synthetic creation of ideal conditions for CTF accumulation. In the case of our wound healing assays, more combinations of our pharmacological agents could be performed to reveal potential synergistic effects across our range of inhibitors. IGF-1-induced cell migration could be further interrogated with a more diverse range of pharmacological agents such as CavME inhibitors and serine protease inhibitors. A means by which our hypothesis that IGF-1R ectodomain shedding contributes to the dissolution of focal adhesions and, by extension, potentiates cell migration in response to IGF-1 could be examined is co-immunoprecipitation (co-IP). IGF-1R co-IP alongside β1-integrin (common IGF-1R interacting partner in focal adhesion complexes) +/- batimistat could reveal whether our hypothesis is correct. Hypothetically, we would anticipate that administration of batimistat would maintain IGF-1R association with β1-integrin. This could be validated through western blot analysis.

4.3 Conclusion

From our western blot analysis across various assays, we propose a framework for RIP of IGF-1R. Ligand-binding induces ectodomain shedding, likely catalysed by metalloproteases, which generates a membrane anchored IGF-1R CTF. This CTF is subsequently internalised in a clathrin-mediated endocytosis-dependent fashion after which it undergoes proteolytic processing by gamma-secretase (likely complexes containing presenilin-2 which are the prominent complex type within endocytic compartments) (Meckler and Checler, 2016). This processing by gamma-secretase then produces a soluble intracellular IGF-1R ICD of ~50kDa as reported by McElroy et al 2007. The production of the IGF-1R CTF, and by extension the ICD, is likely catalysed by ligand-mediated activation of receptor activity. Furthermore, the IGF-1R CTF (and likely the ICD) can undergo nuclear translocation however, it remains unclear whether nuclear translocation of the IGF-1R ICD is clathrin-mediated endocytosis-dependent whereas our current data seems to indicate that clathrin-mediated endocytosis modulates CTF nuclear translocation. Based on data generated from our wound healing assays, it appears that IGF-1R ectodomain shedding, catalysed by metalloproteases, may be involved in IGF-1-mediated cell migration. Ectodomain shedding of IGF-1R may disrupt its localisation within focal adhesion complexes thus promoting dissolution of such complexes, and enhanced cell motility as a result. Prevention of ectodomain shedding in this context may retain IGF-1R in these complexes thus retarding the dispersion of focal adhesions and impeding cell migration. Importantly, a constraint of this conclusion is the fact that batimistat displays a non-specific broad-spectrum inhibition of metalloproteases. This behaviour is pertinent in the context of cell migration due to the inhibition of matrix metalloproteases (MMPs). Many cancers increase their expression of MMPs to enhance their migratory capacity through remodelling of the extracellular matrix. Matrix remodelling is intimately linked to the migration and extravasation of tumour cells therefore it is plausible that the suppression of IGF-1 induced migration by batimistat occurs, in part, due to inhibition of MMP activity. Regardless, there is potentially a rationale for targeting RIP of IGF-1R as a means of attenuating IGF-1 induced cell migration.

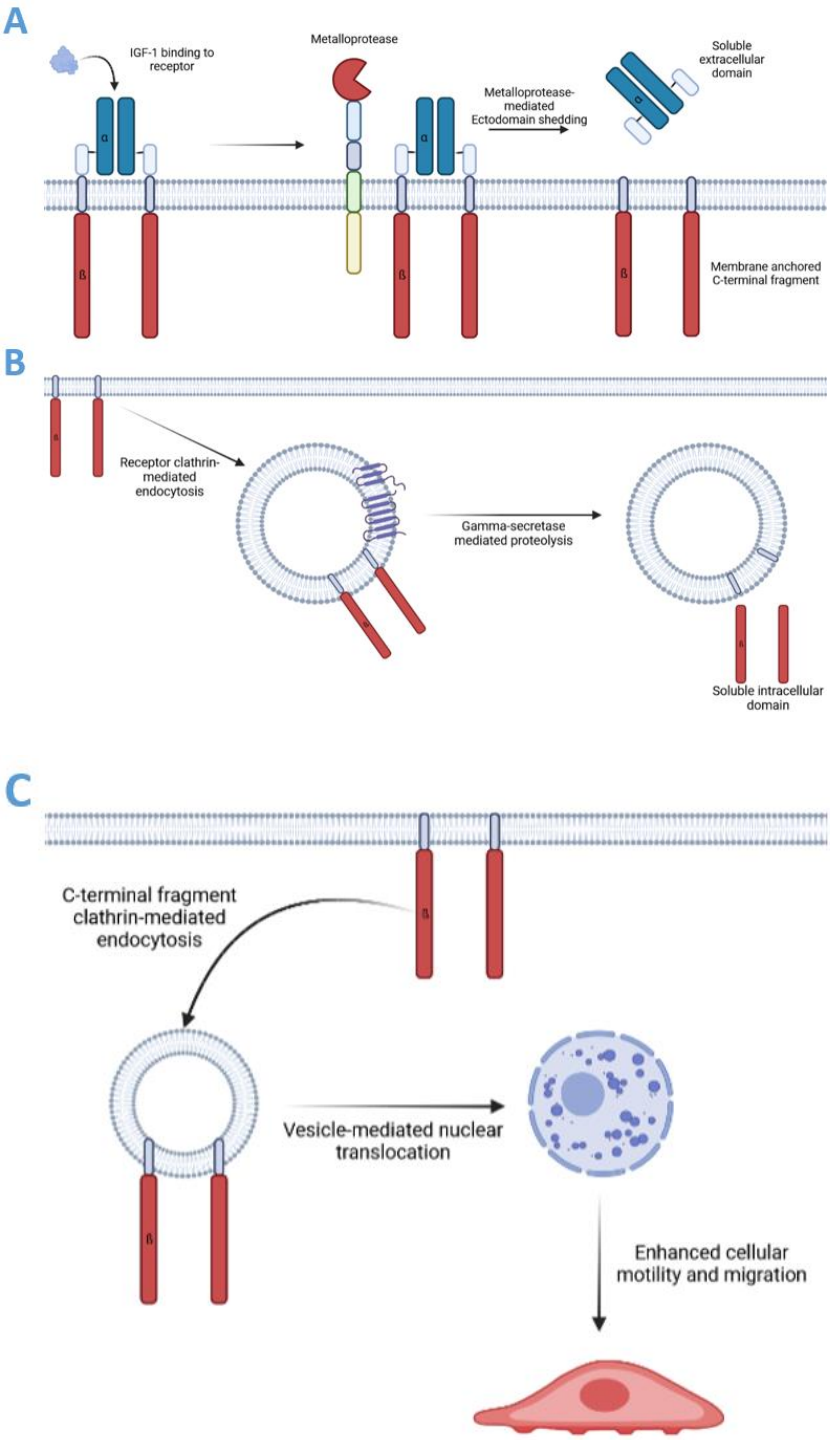
A
IGF-1 binding to receptor
Metalloprotease
Metalloprotease-mediated Ectodomain shedding
Soluble extracellular domain
α
ß
Membrane anchored C-terminal fragment
B
Receptor clathrin-mediated endocytosis
Gamma-secretase mediated proteolysis
Soluble intracellular domain
C
C-terminal fragment clathrin-mediated endocytosis
Vesicle-mediated nuclear translocation
Enhanced cellular motility and migration

Figure 14: Diagrammatic overview of our proposed framework for IGF-1R RIP and CTF localisation

A) *Ligand binding induces metalloprotease-mediated ectodomain shedding thus producing a membrane anchored CTF which serves as a substrate for gamma-secretase mediated proteolysis.* ***B)*** *CTF undergoes clathrin-mediated endocytosis after which IGF-1R is cleaved by gamma-secretase complexes.* ***C)*** *IGF-1R CTF appears to undergo nuclear translocation alongside the full-form IGF-1R. Once in the nucleus, IGF-1R modulates the expression of cell migration associated genes.*

Acknowledgements

First and foremost, I would like to thank Professor Justin McCarthy as my primary supervisor for his support and assistance over the last 2 years. Justin accepted me into is lab during the height of the SARS-CoV-2 pandemic after I (bluntly) approached him at the end of my BSc Biochemistry 4th year research project. Justin granting me this opportunity, and subsequently enabling me to work alongside the fantastic staff of the biochemistry department and my postgraduate peers, has enabled me to secure an excellent PhD researcher position. Despite the odd butting of heads, Justin provided me with excellent mentorship, advice and guidance in developing both as a researcher and a professional. I would also like to thank Professor Rosemary O'Connor as my secondary supervisor for her pertinent insight and advice throughout my project. I owe a massive thanks to my peers and dear friends in the department, particularly the members of the WGB 3.36 lab group. Their support (both scientific and emotional) helped me immensely in all aspects of my masters! James, my lab member, deserves a huge amount of praise. James went above and beyond to help me at all points in my project and aided immensely in my training. James is an excellent mentor, pro-bono lab therapist and editor (among many other unofficial titles). I would have been lost without him and I am forever grateful to him for all his help.

Lastly, I want to extend thanks to my friends and family outside of UCC. Firstly, I want to thank my beloved friends, especially my sister (though not by blood) Alissa for her support and capacity to tolerate my complaints about research without smacking me. Alissa has supported me endlessly and I love her with all my heart. My friend Ben has also been hugely supportive in my journey and has always offered a fresh perspective on my academic work. My wonderful boyfriend Alan also deserves immense thanks for his support! If anyone has helped me with my post-lab meltdowns, it is him. Alan developed a great support system for me after the stress of the lab, namely ordering me pizza when I got home from college and giving me a big hug.

Finally, I want to extend a huge thank you to my mother Kerrie and my grandmother Helen. They have always been immeasurably supportive of me in all that I pursue and have always pushed me to achieve my potential. Though they are not scientists, they are incredibly interested and enthusiastic about my work. The love they have given me has been my driving force. I could not ask for a more supportive duo and I love them from the absolute bottom of my heart.

While this thesis is my work, my loved ones and peers have contributed equally as much to my growth as a scientist and without them I would not be where I am now. This is certainly not an exhaustive list of people I would like to thank but to everyone who has helped me, **go raibh míle maith agat.**

Bibliography

Abd, S., Ibrahim, E.-F., Abudu, A., Jonhson, E., Aftab, N., Conrad, S. and Fluck, M. (no date) *The role of AP-1 in self-sufficient proliferation and migration of cancer cells and its potential impact on an autocrine/paracrine loop*. Available at: www.oncotarget.com.

Adhikary, S. and Eilers, M. (2005) 'Transcriptional regulation and transformation by Myc proteins', *Nature Reviews Molecular Cell Biology*, pp. 635–645. Available at: https://doi.org/10.1038/nrm1703.

Aleksic, T., Chitnis, M.M., Perestenko, O. V., Gao, S., Thomas, P.H., Turner, G.D., Protheroe, A.S., Howarth, M. and Macaulay, V.M. (2010a) 'Type 1 insulin-like growth factor receptor translocates to the nucleus of human tumor cells', *Cancer Research*, 70(16), pp. 6412–6419. Available at: https://doi.org/10.1158/0008-5472.CAN-10-0052.

Aleksic, T., Chitnis, M.M., Perestenko, O. V., Gao, S., Thomas, P.H., Turner, G.D., Protheroe, A.S., Howarth, M. and Macaulay, V.M. (2010b) 'Type 1 insulin-like growth factor receptor translocates to the nucleus of human tumor cells', *Cancer Research*, 70(16), pp. 6412–6419. Available at: https://doi.org/10.1158/0008-5472.CAN-10-0052.

Aleksic, T., Gray, N., Wu, X., Rieunier, G., Osher, E., Mills, J., Verrill, C., Bryant, R.J., Han, C., Hutchinson, K., Lambert, A.G., Kumar, R., Hamdy, F.C., Weyer-Czernilofsky, U., Sanderson, M.P., Bogenrieder, T., Taylor, S. and Macaulay, V.M. (2018) 'Nuclear IGF1R interacts with regulatory regions of chromatin to promote RNA polymerase II recruitment and gene expression associated with advanced tumor stage', *Cancer Research*, 78(13), pp. 3497–3509. Available at: https://doi.org/10.1158/0008-5472.CAN-17-3498.

Alves, C.L., Elias, D., Lyng, M.B., Bak, M. and Ditzel, H.J. (2018) 'SNAI2 upregulation is associated with an aggressive phenotype in fulvestrant-resistant breast cancer cells and is an indicator of poor response to endocrine therapy in estrogen receptor-positive metastatic breast cancer', *Breast Cancer Research*, 20(1). Available at: https://doi.org/10.1186/s13058-018-0988-9.

Andersen, P.L., Xu, F. and Xiao, W. (2008) 'Eukaryotic DNA damage tolerance and translesion synthesis through covalent modifications of PCNA', *Cell Research*, pp. 162–173. Available at: https://doi.org/10.1038/cr.2007.114.

Bammens, L., Chávez-Gutiérrez, L., Tolia, A., Zwijsen, A. and De Strooper, B. (2011) 'Functional and topological analysis of pen-2, the fourth subunit of the γ-secretase complex', *Journal of Biological Chemistry*, 286(14), pp. 12271–12282. Available at: https://doi.org/10.1074/jbc.M110.216978.

Bandaru, P., Kondo, Y. and Kuriyan, J. (2019) 'The interdependent activation of son-of-sevenless and ras', *Cold Spring Harbor Perspectives in Medicine*, 9(2). Available at: https://doi.org/10.1101/cshperspect.a031534.

Bergmans, B.A. and De Strooper, B. (2010) 'γ-secretases: from cell biology to therapeutic strategies', *The Lancet Neurology*, pp. 215–226. Available at: https://doi.org/10.1016/S1474-4422(09)70332-1.

Bi, X. (2015) 'Mechanism of DNA damage tolerance', *World Journal of Biological Chemistry*, 6(3), p. 48. Available at: https://doi.org/10.4331/wjbc.v6.i3.48.

Bjorge, J.D., Jakymiw, A. and Fujita, D.J. (no date) *Selected glimpses into the activation and function of Src kinase*. Available at: www.nature.com/onc.

Brami-Cherrier, K., Gervasi, N., Arsenieva, D., Walkiewicz, K., Boutterin, M.C., Ortega, A., Leonard, P.G., Seantier, B., Gasmi, L., Bouceba, T., Kadaré, G., Girault, J.A. and Arold, S.T. (2014) 'FAK dimerization controls its kinase-dependent functions at focal adhesions', *EMBO Journal*, 33(4), pp. 356–370. Available at: https://doi.org/10.1002/embj.201386399.

Brown, M.S., Ye, J., Rawson, R.B. and Goldstein, J.L. (2000) *Regulated Intramembrane Proteolysis: Review A Control Mechanism Conserved from Bacteria to Humans includes the SREBPs (sterol regulatory element-binding proteins), transmembrane proteins of the ER whose cy-tosolic transcription factor domains are liberated when cells are deprived of sterols, thereby activating genes controlling lipid synthesis and uptake (Brown and Gold*, *Cell*.

Carpenter, G. and Liao, H.J. (2013a) 'Receptor tyrosine kinases in the nucleus', *Cold Spring Harbor Perspectives in Biology*. Available at: https://doi.org/10.1101/cshperspect.a008979.

Carpenter, G. and Liao, H.J. (2013b) 'Receptor tyrosine kinases in the nucleus', *Cold Spring Harbor Perspectives in Biology*. Available at: https://doi.org/10.1101/cshperspect.a008979.

Chambard, J.C., Lefloch, R., Pouysségur, J. and Lenormand, P. (2007) 'ERK implication in cell cycle regulation', *Biochimica et Biophysica Acta - Molecular Cell Research*, pp. 1299–1310. Available at: https://doi.org/10.1016/j.bbamcr.2006.11.010.

Chen, H.X. and Sharon, E. (2013) 'IGF-1R as an anti-cancer target—trials and tribulations'. Available at: https://doi.org/10.5732/cjc.012.10圆.

Chen, M.K. and Hung, M.C. (2015) 'Proteolytic cleavage, trafficking, and functions of nuclear receptor tyrosine kinases', *FEBS Journal*. Blackwell Publishing Ltd, pp. 3693–3721. Available at: https://doi.org/10.1111/febs.13342.

Chen, Q., Zhou, Z., Shan, L., Zeng, H., Hua, Y. and Cai, Z. (2015) 'The importance of Src signaling in sarcoma (review)', *Oncology Letters*, 10(1), pp. 17–22. Available at: https://doi.org/10.3892/ol.2015.3184.

Chuang, C.-F. and Ng, S.-Y. (1994) *divergence of the MAP kinase pathway ERK1 and ERK2 activate specific transcription factors*, *FEBS Letters*.

Chuang, H.H., Zhen, Y.Y., Tsai, Y.C., Chuang, C.H., Hsiao, M., Huang, M.S. and Yang, C.J. (2022) 'FAK in Cancer: From Mechanisms to Therapeutic Strategies', *International Journal of Molecular Sciences*. MDPI. Available at: https://doi.org/10.3390/ijms23031726.

Costa, M.M., Violato, N.M., Taboga, S.R., Góes, R.M. and Bosqueiro, J.R. (2012) 'Reduction of insulin signalling pathway IRS-1/IRS-2/AKT/mTOR and decrease of epithelial cell proliferation in the prostate of glucocorticoid-treated rats', *International Journal of Experimental Pathology*, 93(3), pp. 188–195. Available at: https://doi.org/10.1111/j.1365-2613.2012.00817.x.

Cox, O.T., O'Shea, S., Tresse, E., Bustamante-Garrido, M., Kiran-Deevi, R. and O'Connor, R. (2015) 'IGF-1 receptor and adhesion signaling: An important axis in determining cancer cell phenotype and therapy resistance', *Frontiers in Endocrinology*, 6(JUL). Available at: https://doi.org/10.3389/fendo.2015.00106.

Cullen, P.J. and Steinberg, F. (2018) 'To degrade or not to degrade: mechanisms and significance of endocytic recycling', *Nature Reviews Molecular Cell Biology*. Nature Publishing Group, pp. 679–696. Available at: https://doi.org/10.1038/s41580-018-0053-7.

D. Sarbassov and et al (2005) 'Phosphorylation and Regulation of Akt/PKB by the Rictor-mTOR complex', *Science*, 307(5712), pp. 1095–1098. Available at: https://doi.org/10.1126/science.1108061.

Datta, S.R., Katsov, A., Hu, L., Petros, A., Fesik, S.W., Yaffe, M.B. and Greenberg, M.E. (2000) *14-3-3 Proteins and Survival Kinases Cooperate to Inactivate BAD by BH3 Domain Phosphorylation apoptotic Bcl-2 family members from interacting with and inactivating prosurvival Bcl-2 family members*, *Molecular Cell*.

Davis, R.J., Yoneyama, Y., Lanzerstorfer, P., Niwa, H., Umehara, T., Shibano, T., Yokoyama, S., Chida, K., Weghuber, J., Hakuno, F. and Takahashi, S.-I. (2018a) 'IRS-1 acts as an endocytic regulator of IGF-I receptor to facilitate sustained IGF signaling'. Available at: https://doi.org/10.7554/eLife.32893.001.

Davis, R.J., Yoneyama, Y., Lanzerstorfer, P., Niwa, H., Umehara, T., Shibano, T., Yokoyama, S., Chida, K., Weghuber, J., Hakuno, F. and Takahashi, S.-I. (2018b) 'IRS-1 acts as an endocytic regulator of IGF-I receptor to facilitate sustained IGF signaling'. Available at: https://doi.org/10.7554/eLife.32893.001.

Elkin, S.R., Lakoduk, A.M. and Schmid, S.L. (2016) 'Endocytic pathways and endosomal trafficking: a primer', *Wiener Medizinische Wochenschrift*. Springer-Verlag Wien, pp. 196–204. Available at: https://doi.org/10.1007/s10354-016-0432-7.

Favelyukis, S., Till, J.H., Hubbard, S.R. and Miller, W.T. (2001) 'Structure and autoregulation of the insulin-like growth factor 1 receptor kinase', *Nature Structural Biology*, 8(12), pp. 1058–1063. Available at: https://doi.org/10.1038/nsb721.

Feng, J., Wang, J., Liu, Q., Li, J., Zhang, Q., Zhuang, Z., Yao, X., Liu, C., Li, Y., Cao, L., Li, C., Gong, L., Li, D., Zhang, Y. and Gao, H. (2019) 'DAPT, a γ-secretase inhibitor, suppresses tumorigenesis, and progression of growth hormone-producing adenomas by targeting notch signaling', *Frontiers in Oncology*, 9(AUG). Available at: https://doi.org/10.3389/fonc.2019.00809.

Fujita, M., Ieguchi, K., Davari, P., Yamaji, S., Taniguchi, Y., Sekiguchi, K., Takada, Y.K. and Takada, Y. (2012) 'Cross-talk between integrin α6β4 and Insulin-like Growth Factor-1 Receptor (IGF1R) through direct α6β4 binding to IGF1 and subsequent α6β4-IGF1-IGF1R ternary complex formation in anchorage-independent conditions', *Journal of Biological Chemistry*, 287(15), pp. 12491–12500. Available at: https://doi.org/10.1074/jbc.M111.304170.

García-Gutiérrez, L., Bretones, G., Molina, E., Arechaga, I., Symonds, C., Acosta, J.C., Blanco, R., Fernández, A., Alonso, L., Sicinski, P., Barbacid, M., Santamaría, D. and León, J. (2019) 'Myc stimulates cell cycle progression through the activation of Cdk1 and phosphorylation of p27', *Scientific Reports*, 9(1). Available at: https://doi.org/10.1038/s41598-019-54917-1.

Gertsik, N., Chiu, D. and Li, Y.M. (2015) 'Complex regulation of γ-secretase: From obligatory to modulatory subunits', *Frontiers in Aging Neuroscience*. Frontiers Media S.A., p. 342. Available at: https://doi.org/10.3389/fnagi.2014.00342.

Girnita, L., Worrall, C., Takahashi, S.I., Seregard, S. and Girnita, A. (2014) 'Something old, something new and something borrowed: Emerging paradigm of insulin-like growth factor type 1 receptor (IGF-1R) signaling regulation', *Cellular and Molecular Life Sciences*. Birkhauser Verlag AG, pp. 2403–2427. Available at: https://doi.org/10.1007/s00018-013-1514-y.

Goh, L.K. and Sorkin, A. (2013) 'Endocytosis of receptor tyrosine kinases', *Cold Spring Harbor Perspectives in Biology*, 5(5). Available at: https://doi.org/10.1101/cshperspect.a017459.

Gomez, T.S. and Billadeau, D.D. (2009) 'A FAM21-Containing WASH Complex Regulates Retromer-Dependent Sorting', *Developmental Cell*, 17(5), pp. 699–711. Available at: https://doi.org/10.1016/j.devcel.2009.09.009.

Goñi, G.M., Epifano, C., Boskovic, J., Camacho-Artacho, M., Zhou, J., Bronowska, A., Martín, M.T., Eck, M.J., Kremer, L., Gräter, F., Gervasio, F.L., Perez-Moreno, M. and Lietha, D. (2014) 'Phosphatidylinositol 4,5-bisphosphate triggers activation of focal adhesion kinase by inducing clustering and conformational changes', *Proceedings of the National Academy of Sciences of the United States of America*, 111(31). Available at: https://doi.org/10.1073/pnas.1317022111.

Guo, Y., Pan, W., Liu, S., Shen, Z., Xu, Y. and Hu, L. (2020) 'ERK/MAPK signalling pathway and tumorigenesis (Review)', *Experimental and Therapeutic Medicine* [Preprint]. Available at: https://doi.org/10.3892/etm.2020.8454.

Hanks, S.K., Marie Quinn, A. and Hunter, T. (1985) *The Protein Kinase Family: Conserved Features and Deduced Phylogeny of the Catalytic Domains*, *Faraday Discuss. Chem. Soc*. Oxford Univ. Press. Available at: http://science.sciencemag.org/.

Hayashida, K., Bartlett, A.H., Chen, Y. and Park, P.W. (2010a) 'Molecular and cellular mechanisms of ectodomain shedding', *Anatomical Record*, pp. 925–937. Available at: https://doi.org/10.1002/ar.20757.

Hayashida, K., Bartlett, A.H., Chen, Y. and Park, P.W. (2010b) 'Molecular and cellular mechanisms of ectodomain shedding', *Anatomical Record*, pp. 925–937. Available at: https://doi.org/10.1002/ar.20757.

Henley, J.R., Krueger, E.W.A., Oswald, B.J. and Mcniven, M.A. (1998) *Dynamin-mediated Internalization of Caveolae*, *The Journal of Cell Biology*. Available at: http://www.jcb.org.

Hoa, N., Tsui, S., Afifiyan, N.F., Hikim, A., Li, B., Douglas, R.S. and Smith, T.J. (2012) 'Nuclear targeting of IGF-1 receptor in orbital fibroblasts from Graves' disease: Apparent role of ADAM17', *PLoS ONE*, 7(4). Available at: https://doi.org/10.1371/journal.pone.0034173.

Hua, H., Kong, Q., Yin, J., Zhang, J. and Jiang, Y. (2020a) 'Insulin-like growth factor receptor signaling in tumorigenesis and drug resistance: A challenge for cancer therapy', *Journal of Hematology and Oncology*. BioMed Central Ltd. Available at: https://doi.org/10.1186/s13045-020-00904-3.

Hua, H., Kong, Q., Yin, J., Zhang, J. and Jiang, Y. (2020b) 'Insulin-like growth factor receptor signaling in tumorigenesis and drug resistance: A challenge for cancer therapy', *Journal of Hematology and Oncology*. BioMed Central Ltd. Available at: https://doi.org/10.1186/s13045-020-00904-3.

Jiang, Y. and Fleet, J.C. (2012) 'Effect of phorbol 12-myristate 13-acetate activated signaling pathways on 1α, 25 dihydroxyvitamin D 3 Regulated Human 25-hydroxyvitamin D 3 24-hydroxylase Gene Expression in Differentiated Caco-2 Cells', *Journal of Cellular Biochemistry*, 113(5), pp. 1599–1607. Available at: https://doi.org/10.1002/jcb.24028.

Katzmann, D.J., Babst, M. and Emr, S.D. (2001) 'Ubiquitin-dependent sorting into the multivesicular body pathway requires the function of a conserved endosomal protein sorting complex, ESCRT-I', *Cell*, 106(2), pp. 145–155. Available at: https://doi.org/10.1016/S0092-8674(01)00434-2.

Kavran, J.M., McCabe, J.M., Byrne, P.O., Connacher, M.K., Wang, Z., Ramek, A., Sarabipour, S., Shan, Y., Shaw, D.E., Hristova, K., Cole, P.A. and Leahy, D.J. (2014) 'How IGF-1 activates its receptor', *eLife*, 3. Available at: https://doi.org/10.7554/eLife.03772.

Kiely, P.A., Leahy, M., O'Gorman, D. and O'Connor, R. (2005) 'RACK1-mediated integration of adhesion and insulin-like growth factor I (IGF-I) signaling and cell migration are defective in cells expressing an IGF-I receptor mutated at tyrosines 1250 and 1251', *Journal of Biological Chemistry*, 280(9), pp. 7624–7633. Available at: https://doi.org/10.1074/jbc.M412889200.

Kim, E.K. and Choi, E.J. (2010) 'Pathological roles of MAPK signaling pathways in human diseases', *Biochimica et Biophysica Acta - Molecular Basis of Disease*, pp. 396–405. Available at: https://doi.org/10.1016/j.bbadis.2009.12.009.

Kirchhausen, T., Macia, E. and Pelish, H.E. (2008) 'Use of Dynasore, the Small Molecule Inhibitor of Dynamin, in the Regulation of Endocytosis', *Methods in Enzymology*, pp. 77–93. Available at: https://doi.org/10.1016/S0076-6879(07)38006-3.

Kiss, A.L. and Botos, E. (2009) 'Endocytosis via caveolae: Alternative pathway with distinct cellular compartments to avoid lysosomal degradation?', *Journal of Cellular and Molecular Medicine*, 13(7), pp. 1228–1237. Available at: https://doi.org/10.1111/j.1582-4934.2009.00754.x.

Kooijman, R. (2006) 'Regulation of apoptosis by insulin-like growth factor (IGF)-I', *Cytokine and Growth Factor Reviews*, pp. 305–323. Available at: https://doi.org/10.1016/j.cytogfr.2006.02.002.

Kucab, J.E. and Dunn, S.E. (2003) *Role of IGF-1R in Mediating Breast Cancer Invasion and Metastasis*, *Breast Disease*. IOS Press.

Kumari, S., Mg, S. and Mayor, S. (2010) 'Endocytosis unplugged: Multiple ways to enter the cell', *Cell Research*, pp. 256–275. Available at: https://doi.org/10.1038/cr.2010.19.

Lal, M. and Caplan, M. (2011) 'Regulated intramembrane proteolysis: Signaling pathways and biological functions', *Physiology*, pp. 34–44. Available at: https://doi.org/10.1152/physiol.00028.2010.

LaVoie, M.J., Fraering, P.C., Ostaszewski, B.L., Ye, W., Kimberly, W.T., Wolfe, M.S. and Selkoe, D.J. (2003) 'Assembly of the γ-secretase complex involves early formation of an intermediate subcomplex of Aph-1 and nicastrin', *Journal of Biological Chemistry*, 278(39), pp. 37213–37222. Available at: https://doi.org/10.1074/jbc.M303941200.

Lee, S.F., Shah, S., Yu, C., Wigley, W.C., Li, H., Lim, M., Pedersen, K., Han, W., Thomas, P., Lundkvist, J., Hao, Y.H. and Yu, G. (2004) 'A Conserved GXXXG Motif in APH-1 Is Critical for Assembly and Activity of the γ-Secretase Complex', *Journal of Biological Chemistry*, 279(6), pp. 4144–4152. Available at: https://doi.org/10.1074/jbc.M309745200.

LeRoith, D., Holly, J.M.P. and Forbes, B.E. (2021) 'Insulin-like growth factors: Ligands, binding proteins, and receptors', *Molecular Metabolism*. Elsevier GmbH. Available at: https://doi.org/10.1016/j.molmet.2021.101245.

Leung, W., Baxley, R.M., Moldovan, G.L. and Bielinsky, A.K. (2019) 'Mechanisms of DNA damage tolerance: post-translational regulation of PCNA', *Genes*. MDPI AG. Available at: https://doi.org/10.3390/genes10010010.

Li, H., Batth, I.S., Qu, X., Xu, L., Song, N., Wang, R. and Liu, Y. (2017) 'IGF-IR signaling in epithelial to mesenchymal transition and targeting IGF-IR therapy: Overview and new insights', *Molecular Cancer*. BioMed Central Ltd. Available at: https://doi.org/10.1186/s12943-016-0576-5.

Li, J., Choi, E., Yu, H. and Bai, X. chen (2019) 'Structural basis of the activation of type 1 insulin-like growth factor receptor', *Nature Communications*, 10(1). Available at: https://doi.org/10.1038/s41467-019-12564-0.

Li, R., Pourpak, A. and Morris, S.W. (2009) 'Inhibition of the insulin-like growth factor-1 receptor (IGF1R) tyrosine kinase as a novel cancer therapy approach', *Journal of Medicinal Chemistry*, pp. 4981–5004. Available at: https://doi.org/10.1021/jm9002395.

Lichtenthaler, S.F., Haass, C. and Steiner, H. (2011) 'Regulated intramembrane proteolysis - Lessons from amyloid precursor protein processing', *Journal of Neurochemistry*. Blackwell Publishing Ltd, pp. 779–796. Available at: https://doi.org/10.1111/j.1471-4159.2011.07248.x.

Lietha, D., Cai, X., Ceccarelli, D.F.J., Li, Y., Schaller, M.D. and Eck, M.J. (2007) 'Structural Basis for the Autoinhibition of Focal Adhesion Kinase', *Cell*, 129(6), pp. 1177–1187. Available at: https://doi.org/10.1016/j.cell.2007.05.041.

Lim, S.-T., Chen, X.L., Lim, Y., Hanson, D.A., Vo, T.-T., Howerton, K., Larocque, N., Fisher, S.J., Schlaepfer, D.D. and Ilic, D. (no date) *Nuclear FAK promotes cell proliferation and survival through FERM-enhanced p53 degradation*.

Lin, Y., Liu, H., Waraky, A., Haglund, F., Agarwal, P., Jernberg-Wiklund, H., Warsito, D. and Larsson, O. (2017) 'SUMO-modified insulin-like growth factor 1 receptor (IGF-1R) increases cell cycle progression and cell proliferation', *Journal of Cellular Physiology*, 232(10), pp. 2722–2730. Available at: https://doi.org/10.1002/jcp.25818.

Liu, X., Xu, Y., Zhou, Q., Chen, M., Zhang, Y., Liang, H., Zhao, J., Zhong, W. and Wang, M. (2018) 'PI3K in cancer: Its structure, activation modes and role in shaping tumor microenvironment', *Future Oncology*. Future Medicine Ltd., pp. 665–674. Available at: https://doi.org/10.2217/fon-2017-0588.

Lu, S., Simin, K., Khan, A. and Mercurio, A.M. (2008) 'Analysis of integrin β4 expression in human breast cancer: Association with basal-like tumors and prognostic significance', *Clinical Cancer Research*, 14(4), pp. 1050–1058. Available at: https://doi.org/10.1158/1078-0432.CCR-07-4116.

Luo, J., Zou, H., Guo, Y., Tong, T., Ye, L., Zhu, C., Deng, L., Wang, B., Pan, Y. and Li, P. (2022) 'SRC kinase-mediated signaling pathways and targeted therapies in breast cancer', *Breast Cancer Research*. BioMed Central Ltd. Available at: https://doi.org/10.1186/s13058-022-01596-y.

Mahammad, S. and Parmryd, I. (2008) 'Cholesterol homeostasis in T cells. Methyl-β-cyclodextrin treatment results in equal loss of cholesterol from Triton X-100 soluble and insoluble fractions', *Biochimica et Biophysica Acta - Biomembranes*, 1778(5), pp. 1251–1258. Available at: https://doi.org/10.1016/j.bbamem.2008.02.010.

Maik-Rachline, G., Hacohen-Lev-Ran, A. and Seger, R. (2019) 'Nuclear erk: Mechanism of translocation, substrates, and role in cancer', *International Journal of Molecular Sciences*. MDPI AG. Available at: https://doi.org/10.3390/ijms20051194.

Manning, B.D. and Cantley, L.C. (2007) 'AKT/PKB Signaling: Navigating Downstream', *Cell*, pp. 1261–1274. Available at: https://doi.org/10.1016/j.cell.2007.06.009.

Mao, Y., Shang, Y., Pham, V.C., Ernst, J.A., Lill, J.R., Scales, S.J. and Zha, J. (2011) 'Polyubiquitination of insulin-like growth factor I receptor (IGF-IR) activation loop promotes antibody-induced receptor internalization and down-regulation', *Journal of Biological Chemistry*, 286(48), pp. 41852–41861. Available at: https://doi.org/10.1074/jbc.M111.288514.

Mardilovich, K., Pankratz, S.L. and Shaw, L.M. (2009) 'Expression and function of the insulin receptor substrate proteins in cancer', *Cell Communication and Signaling*, 7. Available at: https://doi.org/10.1186/1478-811X-7-14.

Martin, A., Fernandez, M.C., Cattaneo, E.R., Schuster, C.D., Venara, M., Clément, F., Berenstein, A., Lombardi, M.G., Bergadá, I., Gutierrez, M., Martí, M.A., Gonzalez-Baro, M.R. and Pennisi, P.A. (2022a) 'Type 1 Insulin-Like Growth Factor Receptor Nuclear Localization in High-Grade Glioma Cells Enhances Motility, Metabolism, and In Vivo Tumorigenesis', *Frontiers in Endocrinology*, 13. Available at: https://doi.org/10.3389/fendo.2022.849279.

Martin, A., Fernandez, M.C., Cattaneo, E.R., Schuster, C.D., Venara, M., Clément, F., Berenstein, A., Lombardi, M.G., Bergadá, I., Gutierrez, M., Martí, M.A., Gonzalez-Baro, M.R. and Pennisi, P.A. (2022b) 'Type 1 Insulin-Like Growth Factor Receptor Nuclear Localization in High-Grade Glioma Cells Enhances Motility, Metabolism, and In Vivo Tumorigenesis', *Frontiers in Endocrinology*, 13. Available at: https://doi.org/10.3389/fendo.2022.849279.

Martínez, P.T., Navajas, P.L. and Lietha, D. (2020) 'FAK structure and regulation by membrane interactions and force in focal adhesions', *Biomolecules*. MDPI. Available at: https://doi.org/10.3390/biom10020179.

Martins, A.S., Ordóñez, J.L., Amaral, A.T., Prins, F., Floris, G., Debiec-Rychter, M., Hogendoorn, P.C.W. and de Alava, E. (2011) 'IGF1R signaling in Ewing Sarcoma is shaped by clathrin-/caveolin-dependent endocytosis', *PLoS ONE*, 6(5). Available at: https://doi.org/10.1371/journal.pone.0019846.

Mayer, B.J. and Yu, J. (2018) 'Protein Clusters in Phosphotyrosine Signal Transduction', *Journal of Molecular Biology*. Academic Press, pp. 4547–4556. Available at: https://doi.org/10.1016/j.jmb.2018.05.040.

Mayo, L.D. and Donner, D.B. (no date) *A phosphatidylinositol 3-kinase/Akt pathway promotes translocation of Mdm2 from the cytoplasm to the nucleus*. Available at: www.pnas.orgcgidoi10.1073pnas.181181198.

McElroy, B., Powell, J.C. and McCarthy, J. V. (2007) 'The insulin-like growth factor 1 (IGF-1) receptor is a substrate for γ-secretase-mediated intramembrane proteolysis', *Biochemical and Biophysical Research Communications*, 358(4), pp. 1136–1141. Available at: https://doi.org/10.1016/j.bbrc.2007.05.062.

Meckler, X. and Checler, F. (2016) 'Presenilin 1 and presenilin 2 target γ-secretase complexes to distinct cellular compartments', *Journal of Biological Chemistry*, 291(24), pp. 12821–12837. Available at: https://doi.org/10.1074/jbc.M115.708297.

Mercurio, A.M. and Rabinovitz, I. (2001) 'Towards a mechanistic understanding of tumor invasion - Lessons from the α6β4 integrin', *Seminars in Cancer Biology*, 11(2), pp. 129–141. Available at: https://doi.org/10.1006/scbi.2000.0364.

Mettlen, M., Chen, P.H., Srinivasan, S., Danuser, G. and Schmid, S.L. (2018) 'Regulation of Clathrin-Mediated Endocytosis', *Annual Review of Biochemistry*. Annual Reviews Inc., pp. 871–896. Available at: https://doi.org/10.1146/annurev-biochem-062917-012644.

Meyer Natalie and Penn, L.Z. (no date) 'Reflecting on 25 years with MYC'.

Michael S. Wolfe*, W.X.B.L.O.S.D.W.T.K.D.J.S. (1999) 'Two transmembrane aspartates in presenilin-1 required for presenilin endoproteolysis and γ-secretase activity', *Nature* [Preprint].

Miller, M.A., Oudin, M.J., Sullivan, R.J., Wang, S.J., Meyer, A.S., Im, H., Frederick, D.T., Tadros, J., Griffith, L.G., Lee, H., Weissleder, R., Flaherty, K.T., Gertler, F.B. and Lauffenburger, D.A. (2016) 'Reduced proteolytic shedding of receptor tyrosine kinases is a post-translational mechanism of kinase inhibitor resistance', *Cancer Discovery*, 6(4), pp. 383–399. Available at: https://doi.org/10.1158/2159-8290.CD-15-0933.

Miller, M.A., Sullivan, R.J. and Lauffenburger, D.A. (2017) 'Molecular pathways: Receptor ectodomain shedding in treatment, resistance, and monitoring of cancer', *Clinical Cancer Research*, 23(3), pp. 623–629. Available at: https://doi.org/10.1158/1078-0432.CCR-16-0869.

Mills, J. V., Osher, E., Rieunier, G., Mills, I.G. and Macaulay, V.M. (2021) 'IGF-1R nuclear import and recruitment to chromatin involves both alpha and beta subunits', *Discover Oncology*, 12(1). Available at: https://doi.org/10.1007/s12672-021-00407-8.

Min, H.Y., Yun, J.H., Lee, J.S., Lee, H.J., Cho, J., Jang, H.J., Park, S.H., Liu, D., Oh, S.H., Lee, J.S.H., Wistuba, I.I. and Lee, H.Y. (2015) 'Targeting the insulin-like growth factor receptor and Src signaling network for the treatment of non-small cell lung cancer', *Molecular Cancer*, 14(1). Available at: https://doi.org/10.1186/s12943-015-0392-3.

Mittal, V. (2017) 'Epithelial Mesenchymal Transition in Tumor Metastasis'. Available at: https://doi.org/10.1146/annurev-pathol-020117.

Mochizuki, S. and Okada, Y. (2007) 'ADAMs in cancer cell proliferation and progression', *Cancer Science*, pp. 621–628. Available at: https://doi.org/10.1111/j.1349-7006.2007.00434.x.

Molina, E.R., Chim, L.K., Lamhamedi-Cherradi, S.-E., Mohiuddin, S., Mccall, D., Cuglievan, B., Krishnan, S., Porter, R.W., Ingram, D.R., Wang, W.-L., Lazar, A.J., Scott, D.W., Truong, D.D., Daw, N.C., Ludwig, J.A. and Mikos, A.G. (2022) *Correlation of nuclear pIGF-1R/IGF-1R and YAP/TAZ in a tissue microarray with outcomes in osteosarcoma patients*, *Oncotarget*. Available at: www.oncotarget.com.

Monje, P., Hernández-Losa, J., Lyons, R.J., Castellone, M.D. and Gutkind, J.S. (2005) 'Regulation of the transcriptional activity of c-Fos by ERK: A novel role for the prolyl isomerase Pin1', *Journal of Biological Chemistry*, 280(42), pp. 35081–35084. Available at: https://doi.org/10.1074/jbc.C500353200.

Mundi, P.S., Sachdev, J., McCourt, C. and Kalinsky, K. (2016) 'AKT in cancer: new molecular insights and advances in drug development', *British Journal of Clinical Pharmacology*. Blackwell Publishing Ltd, pp. 943–956. Available at: https://doi.org/10.1111/bcp.13021.

Nassar, Z.D. and Parat, M.O. (2015) 'Cavin Family: New Players in the Biology of Caveolae', *International Review of Cell and Molecular Biology*, 320, pp. 235–305. Available at: https://doi.org/10.1016/bs.ircmb.2015.07.009.

Öberg, C., Li, J., Pauley, A., Wolf, E., Gurney, M. and Lendahl, U. (2001) 'The Notch Intracellular Domain is Ubiquitinated and Negatively Regulated by the Mammalian Sel-10 Homolog', *Journal of Biological Chemistry*, 276(38), pp. 35847–35853. Available at: https://doi.org/10.1074/jbc.M103992200.

Obr, A.E., Bulatowicz, J.J., Chang, Y.J., Ciliento, V., Lemenze, A., Maingrette, K., Shang, Q., Gallagher, E.J., LeRoith, D. and Wood, T.L. (2022) 'Breast tumor IGF1R regulates cell adhesion and metastasis: alignment of mouse single cell and human breast cancer transcriptomics', *Frontiers in Oncology*, 12. Available at: https://doi.org/10.3389/fonc.2022.990398.

P Rodriguez-Viciana, P H Warne, R Dhand, B Vanhaesebroeck, I Gout, M J Fry, M D Waterfield and J Downward (1994) 'Phosphatidylinositol-3-OH kinase as a direct target of Ras', *Nature* [Preprint].

Packham, S., Warsito, D., Lin, Y., Sadi, S., Karlsson, R., Sehat, B. and Larsson, O. (2015a) 'Nuclear translocation of IGF-1R via p150Glued and an importin-β/RanBP2-dependent pathway in cancer cells', *Oncogene*, 34(17), pp. 2227–2238. Available at: https://doi.org/10.1038/onc.2014.165.

Packham, S., Warsito, D., Lin, Y., Sadi, S., Karlsson, R., Sehat, B. and Larsson, O. (2015b) 'Nuclear translocation of IGF-1R via p150Glued and an importin-β/RanBP2-dependent pathway in cancer cells', *Oncogene*, 34(17), pp. 2227–2238. Available at: https://doi.org/10.1038/onc.2014.165.

Pamrén, A., Wanngren, J., Tjernberg, L.O., Winblad, B., Bhat, R., Näslund, J. and Karlström, H. (2011) 'Mutations in nicastrin protein differentially affect amyloid β-peptide production and notch protein processing', *Journal of Biological Chemistry*, 286(36), pp. 31153–31158. Available at: https://doi.org/10.1074/jbc.C111.235267.

Park, S., Chapuis, N., Tamburini, J., Bardet, V., Cornillet-Lefebvre, P., Willems, L., Green, A., Mayeux, P., Lacombe, C. and Bouscary, D. (2010) 'Role of the PI3K/AKT and mTOR signaling

pathways in acute myeloid leukemia', *Haematologica*, 95(5), pp. 819–828. Available at: https://doi.org/10.3324/haematol.2009.013797.

Parton, R.G. and Del Pozo, M.A. (2013) 'Caveolae as plasma membrane sensors, protectors and organizers', *Nature Reviews Molecular Cell Biology*, 14(2), pp. 98–112. Available at: https://doi.org/10.1038/nrm3512.

Phillips, R. (2014) 'Prostate cancer: TMPRSS2 promotes metastasis through proteolysis', *Nature Reviews Urology*. Nature Publishing Group, p. 546. Available at: https://doi.org/10.1038/nrurol.2014.238.

Placanica, L., Tarassishin, L., Yang, G., Peethumnongsin, E., Kim, S.H., Zheng, H., Sisodia, S.S. and Li, Y.M. (2009) 'Pen2 and presenilin-1 modulate the dynamic equilibrium of presenilin-1 and presenilin-2 γ-secretase complexes', *Journal of Biological Chemistry*, 284(5), pp. 2967–2977. Available at: https://doi.org/10.1074/jbc.M807269200.

Poreba, E. and Durzynska, J. (2020) 'Nuclear localization and actions of the insulin-like growth factor 1 (IGF-1) system components: Transcriptional regulation and DNA damage response', *Mutation Research - Reviews in Mutation Research*. Elsevier B.V. Available at: https://doi.org/10.1016/j.mrrev.2020.108307.

Qiao, M., Sheng, S. and Pardee, A.B. (2008) 'Metastasis and AKT activation', *Cell Cycle*. Taylor and Francis Inc., pp. 2991–2996. Available at: https://doi.org/10.4161/cc.7.19.6784.

Rasmussen, H.S. and Mccann, P.P. (1997) *Matrix Metalloproteinase Inhibition as a Novel Anticancer Strategy: A Review with Special Focus on Batimastat and Marimastat*, *Pharmacol. Ther*.

Ratovitski, T., Slunt, H.H., Thinakaran, G., Price, D.L., Sisodia, S.S. and Borchelt, D.R. (1997) 'Endoproteolytic processing and stabilization of wild-type and mutant presenilin', *Journal of Biological Chemistry*, 272(39), pp. 24536–24541. Available at: https://doi.org/10.1074/jbc.272.39.24536.

Reiss, K. and Bhakdi, S. (2017) 'The plasma membrane: Penultimate regulator of ADAM sheddase function', *Biochimica et Biophysica Acta - Molecular Cell Research*. Elsevier B.V., pp. 2082–2087. Available at: https://doi.org/10.1016/j.bbamcr.2017.06.006.

Reunanen N, K.V. (2013) 'Matrix Metalloproteinases in Cancer Cell Invasion', in *Madame Curie Bioscience Database*.

Hynes, R.O. (2002) 'Integrins: Bidirectional, Allosteric Signaling Machines', pp. 673–687.

Rieger, L. and O'Connor, R. (2021) 'Controlled Signaling—Insulin-Like Growth Factor Receptor Endocytosis and Presence at Intracellular Compartments', *Frontiers in Endocrinology*. Frontiers Media S.A. Available at: https://doi.org/10.3389/fendo.2020.620013.

Rieger, L., O'shea, S., Godsmark, G., Stanicka, J., Kelly, G. and O'connor, R. (2020) *IGF-1 receptor activity in the Golgi of migratory cancer cells depends on adhesion-dependent phosphorylation of Tyr 1250 and Tyr 1251*, *Sci. Signal*. Available at: http://stke.sciencemag.org/.

Rigiracciolo, D.C., Nohata, N., Lappano, R., Cirillo, F., Talia, M., Scordamaglia, D., Gutkind, J.S. and Maggiolini, M. (2020) 'IGF-1/IGF-1R/FAK/YAP Transduction Signaling Prompts

Growth Effects in Triple-Negative Breast Cancer (TNBC) Cells', *Cells*, 9(4). Available at: https://doi.org/10.3390/cells9041010.

Roskoski, R. (2015) 'Src protein-tyrosine kinase structure, mechanism, and small molecule inhibitors This paper is dedicated to the memory of Prof. Donald F. Steiner (1930-2014) - Advisor, mentor, and discoverer of proinsulin.', *Pharmacological Research*. Academic Press, pp. 9–25. Available at: https://doi.org/10.1016/j.phrs.2015.01.003.

Rukhlenko, O.S., Khorsand, F., Krstic, A., Rozanc, J., Alexopoulos, L.G., Rauch, N., Erickson, K.E., Hlavacek, W.S., Posner, R.G., Gómez-Coca, S., Rosta, E., Fitzgibbon, C., Matallanas, D., Rauch, J., Kolch, W. and Kholodenko, B.N. (2018) 'Dissecting RAF Inhibitor Resistance by Structure-based Modeling Reveals Ways to Overcome Oncogenic RAS Signaling', *Cell Systems*, 7(2), pp. 161-179.e14. Available at: https://doi.org/10.1016/j.cels.2018.06.002.

Kleiner, D.E. and Stetler-Stevenson, W.G. (1999) 'Matrix metalloproteinases and metastasis', *Cancer Chemotherapy Pharmacology*, pp. 42–51.

Samani, A.A., Yakar, S., LeRoith, D. and Brodt, P. (2007) 'The role of the IGF system in cancer growth and metastasis: Overview and recent insights', *Endocrine Reviews*, pp. 20–47. Available at: https://doi.org/10.1210/er.2006-0001.

Santamaría, D., Barrière, C., Cerqueira, A., Hunt, S., Tardy, C., Newton, K., Cáceres, J.F., Dubus, P., Malumbres, M. and Barbacid, M. (2007) 'Cdk1 is sufficient to drive the mammalian cell cycle', *Nature*, 448(7155), pp. 811–815. Available at: https://doi.org/10.1038/nature06046.

Sarfstein, R., Pasmanik-Chor, M., Yeheskel, A., Edry, L., Shomron, N., Warman, N., Wertheimer, E., Maor, S., Shochat, L. and Werner, H. (2012) 'Insulin-like Growth Factor-I Receptor (IGF-IR) translocates to nucleus and autoregulates IGF-IR gene expression in breast cancer cells', *Journal of Biological Chemistry*, 287(4), pp. 2766–2776. Available at: https://doi.org/10.1074/jbc.M111.281782.

Sato, T., Diehl, T.S., Narayanan, S., Funamoto, S., Ihara, Y., De Strooper, B., Steiner, H., Haass, C. and Wolfe, M.S. (2007) 'Active γ-secretase complexes contain only one of each component', *Journal of Biological Chemistry*, 282(47), pp. 33985–33993. Available at: https://doi.org/10.1074/jbc.M705248200.

Schmid, S.L. and Frolov, V.A. (2011) 'Dynamin: Functional design of a membrane fission catalyst', *Annual Review of Cell and Developmental Biology*, 27, pp. 79–105. Available at: https://doi.org/10.1146/annurev-cellbio-100109-104016.

Sears, R., Nuckolls, F., Haura, E., Taya, Y., Tamai, K. and Nevins, J.R. (2000) 'Multiple Ras-dependent phosphorylation pathways regulate Myc protein stability', *Genes and Development*, 14(19), pp. 2501–2514. Available at: https://doi.org/10.1101/gad.836800.

Sehat, B., Tofigh, A., Lin, Y., Trocmé, E., Liljedahl, U., Lagergren, J. and Larsson, O. (2010) 'SUMOylation mediates the nuclear translocation and signaling of the IGF-1 receptor', *Science Signaling*, 3(108). Available at: https://doi.org/10.1126/scisignal.2000628.

Serneels, L., Van Biervliet, J., Craessaerts, K., Dejaegere, T., Horré, K., Houtvin, T. Van, Esselmann, H., Paul, S., Schäfer, M.K., Berezovska, O., Hyman, B.T., Sprangers, B., Sciot, R., Moons, L., Jucker, M., Yang, Z., May, P.C., Karran, E., Wiltfang, J., Hooge, R.D.' and De

Strooper, B. (2019) *g-Secretase Heterogeneity in the Aph1 Subunit: Relevance for Alzheimer's Disease*. Available at: https://www.science.org.

Shah, S., Lee, S.F., Tabuchi, K., Hao, Y.H., Yu, C., LaPlant, Q., Ball, H., Dann, C.E., Südhof, T. and Yu, G. (2005) 'Nicastrin functions as a γ-secretase-substrate receptor', *Cell*, 122(3), pp. 435–447. Available at: https://doi.org/10.1016/j.cell.2005.05.022.

Shen, Y. and White, E. (2001) *p53-Dependent Apoptosis Pathways*.

Shirotani, K., Edbauer, D., Prokop, S., Haass, C. and Steiner, H. (2004) 'Identification of distinct γ-secretase complexes with different APH-1 variants', *Journal of Biological Chemistry*, 279(40), pp. 41340–41345. Available at: https://doi.org/10.1074/jbc.M405768200.

Simanshu, D.K., Nissley, D. V. and McCormick, F. (2017) 'RAS Proteins and Their Regulators in Human Disease', *Cell*. Cell Press, pp. 17–33. Available at: https://doi.org/10.1016/j.cell.2017.06.009.

Smith, S.J., Gu, L., Phipps, E.A., Dobrolecki, L.E., Mabrey, K.S., Gulley, P., Dillehay, K.L., Dong, Z., Fields, G.B., Chen, Y.R., Ann, D., Hickey, R.J. and Malkas, L.H. (2015) 'A peptide mimicking a region in proliferating cell nuclear antigen specific to key protein interactions is cytotoxic to breast cancer', *Molecular Pharmacology*, 87(2), pp. 263–276. Available at: https://doi.org/10.1124/mol.114.093211.

Solomon-Zemler, R., Sarfstein, R. and Werner, H. (2017) 'Nuclear insulin-like growth factor-1 receptor (IGF1R) displays proliferative and regulatory activities in non-malignant cells', *PLoS ONE*, 12(9). Available at: https://doi.org/10.1371/journal.pone.0185164.

Song, R.X., Barnes, C.J., Zhang, Z., Bao, Y., Kumar, R. and Santen, R.J. (2004) *The role of Shc and insulin-like growth factor 1 receptor in mediating the translocation of estrogen receptor to the plasma membrane*. Available at: www.pnas.orgcgidoi10.1073pnas.0308334100.

Song, S., Rosen, K.M. and Corfas, G. (2013) 'Biological function of nuclear receptor tyrosine kinase action', *Cold Spring Harbor Perspectives in Biology*, 5(7). Available at: https://doi.org/10.1101/cshperspect.a009001.

Sonoda, Y., Matsumoto, Y., Funakoshi, M., Yamamoto, D., Hanks, S.K. and Kasahara, T. (2000) *Anti-apoptotic Role of Focal Adhesion Kinase (FAK) INDUCTION OF INHIBITOR-OF-APOPTOSIS PROTEINS AND APOPTOSIS SUPPRESSION BY THE OVEREXPRESSION OF FAK IN A HUMAN LEUKEMIC CELL LINE, HL-60**. Available at: http://www.jbc.org.

Stanicka, J., Rieger, L., O'Shea, S., Cox, O., Coleman, M., O'Flanagan, C., Addario, B., McCabe, N., Kennedy, R. and O'Connor, R. (2018) 'FES-related tyrosine kinase activates the insulin-like growth factor-1 receptor at sites of cell adhesion', *Oncogene*, 37(23), pp. 3131–3150. Available at: https://doi.org/10.1038/s41388-017-0113-z.

Steiner, H., Fluhrer, R. and Haass, C. (2008) 'Intramembrane proteolysis by γ-secretase', *Journal of Biological Chemistry*, pp. 29627–29631. Available at: https://doi.org/10.1074/jbc.R800010200.

Strooper, B. De (2003) 'Aph-1, Pen-2, and Nicastrinwith Presenilin Generate an Active gamma-Secretase Complex'.

De Strooper, B. and Annaert, W. (2010) ‘Novel research horizons for presenilins and γ-secretases in cell biology and disease’, *Annual Review of Cell and Developmental Biology*, pp. 235–260. Available at: https://doi.org/10.1146/annurev-cellbio-100109-104117.

SUN, W.-Y., YUN, H.-Y., SONG, Y.-J., KIM, H., LEE, O.-J., NAM, S.-J. and KOO, J.-S. (2015) ‘Insulin-like growth factor 1 receptor expression in breast cancer tissue and mammographic density’, *Molecular and Clinical Oncology*, 3(3), pp. 572–580. Available at: https://doi.org/10.3892/mco.2015.497.

Sun, Y., Sun, X. and Shen, B. (2017) ‘Molecular Imaging of IGF-1R in Cancer’, *Molecular Imaging*. SAGE Publications Inc. Available at: https://doi.org/10.1177/1536012117736648.

Suzuki, K., Bose, P., Leong-Quong, R.Y., Fujita, D.J. and Riabowol, K. (2010a) ‘REAP: A two minute cell fractionation method’, *BMC Research Notes*, 3. Available at: https://doi.org/10.1186/1756-0500-3-294.

Suzuki, K., Bose, P., Leong-Quong, R.Y., Fujita, D.J. and Riabowol, K. (2010b) ‘REAP: A two minute cell fractionation method’, *BMC Research Notes*, 3. Available at: https://doi.org/10.1186/1756-0500-3-294.

Svalina, M.N., Kikuchi, K., Abraham, J., Lal, S., Davare, M.A., Settelmeyer, T.P., Young, M.C., Peckham, J.L., Cho, Y.J., Michalek, J.E., Hernandez, B.S., Berlow, N.E., Jackson, M., Guillaume, D.J., Selden, N.R., Bigner, D.D., Nazemi, K.J., Green, S.C., Corless, C.L., Gultekin, S., Mansoor, A., Rubin, B.P., Woltjer, R. and Keller, C. (2016) ‘IGF1R as a Key Target in High Risk, Metastatic Medulloblastoma’, *Scientific Reports*, 6. Available at: https://doi.org/10.1038/srep27012.

Tahara, E., Kadara, H., Lacroix, L., Lotan, D. and Lotan, R. (2009) ‘Activation of protein kinase C by phorbol 12-myristate 13-acetate suppresses the growth of lung cancer cells through KLF6 induction’, *Cancer Biology and Therapy*, 8(9), pp. 801–807. Available at: https://doi.org/10.4161/cbt.8.9.8186.

Takada, Y., Takada, Y.K. and Fujita, M. (2017) ‘Crosstalk between insulin-like growth factor (IGF) receptor and integrins through direct integrin binding to IGF1’, *Cytokine and Growth Factor Reviews*. Elsevier Ltd, pp. 67–72. Available at: https://doi.org/10.1016/j.cytogfr.2017.01.003.

Takasugi, N., Tomita, T., Hayashi, I., Tsuruoka, M., Niimura, M., Takahashi, Y., Thinakaran, G. and Iwatsubo, T. (2003) ‘The role of presenilin cofactors in the γ-secratase complex’, *Nature*, 422(6930), pp. 438–441. Available at: https://doi.org/10.1038/nature01506.

Terrell, E.M. and Morrison, D.K. (2019) ‘Ras-mediated activation of the Raf family kinases’, *Cold Spring Harbor Perspectives in Medicine*, 9(1). Available at: https://doi.org/10.1101/cshperspect.a033746.

Trojan, J., Cloix, J.F., Ardourel, M.Y., Chatel, M. and Anthony, D.D. (2007) ‘Insulin-like growth factor type I biology and targeting in malignant gliomas’, *Neuroscience*, pp. 795–811. Available at: https://doi.org/10.1016/j.neuroscience.2007.01.021.

Truebestein, L., Hornegger, H., Anrather, D., Hartl C , M., Fleming, K.D., Stariha, J.T.B., Pardon, E., Steyaert, J., Burke, J.E. and Leonard, T.A. (2021) ‘Structure of autoinhibited Akt1 reveals mechanism of PIP 3-mediated activation’, 118. Available at: https://doi.org/10.1073/pnas.2101496118/-/DCSupplemental.

Vivanco, I. and Sawyers, C.L. (2002) 'The phosphatidylinositol 3-kinase-AKT pathway in human cancer', *Nature Reviews Cancer*, 2(7), pp. 489–501. Available at: https://doi.org/10.1038/nrc839.

Walker EH, Perisic O, Ried C, Stephens L and Williams RL (1999) 'Structural insights into phosphoinositide 3-kinase catalysis and signalling', *Nature* [Preprint].

Wang, P., Mak, V.C. and Cheung, L.W. (2023) 'Drugging IGF-1R in cancer: New insights and emerging opportunities', *Genes and Diseases*, Chongqing University. Available at: https://doi.org/10.1016/j.gendis.2022.03.002.

Wang, Qiaozhen, Liu, H., Wang, Qing, Zhou, F., Liu, Y., Zhang, Y., Ding, H., Yuan, M., Li, F. and Chen, Y. (2017) 'Involvement of c-Fos in cell proliferation, migration, and invasion in osteosarcoma cells accompanied by altered expression of Wnt2 and Fzd9', *PLoS ONE*, 12(6). Available at: https://doi.org/10.1371/journal.pone.0180558.

Waraky, A., Lin, Y., Warsito, D., Haglund, F., Aleem, E., Larsson, O. and Wang, X.F. (2017) 'Nuclear insulin-like growth factor 1 receptor phosphorylates proliferating cell nuclear antigen and rescues stalled replication forks after DNA damage', *Journal of Biological Chemistry*, 292(44), pp. 18227–18239. Available at: https://doi.org/10.1074/jbc.M117.781492.

Watanabe, Y. and Nakamura, H. (2012) 'Nuclear translocation of intracellular domain of Protogenin by proteolytic cleavage', *Development Growth and Differentiation*, 54(2), pp. 167–176. Available at: https://doi.org/10.1111/j.1440-169X.2011.01315.x.

Willox, A.K., Sahraoui, Y.M.E. and Royle, S.J. (2014) 'Non-specificity of Pitstop 2 in clathrin-mediated endocytosis', *Biology Open*, 3(5), pp. 326–331. Available at: https://doi.org/10.1242/bio.20147955.

Wu, Z., Nicoll, M. and Ingham, R.J. (2021) 'AP-1 family transcription factors: a diverse family of proteins that regulate varied cellular activities in classical hodgkin lymphoma and ALK+ ALCL', *Experimental Hematology and Oncology*. BioMed Central Ltd. Available at: https://doi.org/10.1186/s40164-020-00197-9.

Xu, Y., Kong, G.K.W., Menting, J.G., Margetts, M.B., Delaine, C.A., Jenkin, L.M., Kiselyov, V. V., De Meyts, P., Forbes, B.E. and Lawrence, M.C. (2018) 'How ligand binds to the type 1 insulin-like growth factor receptor', *Nature Communications*, 9(1). Available at: https://doi.org/10.1038/s41467-018-03219-7.

Ye, X., Ling, B., Xu, H., Li, G., Zhao, X., Xu, J., Liu, J. and Liu, L. (2020) 'Clinical significance of high expression of proliferating cell nuclear antigen in non-small cell lung cancer', *Medicine*, 99(16), p. e19755. Available at: https://doi.org/10.1097/MD.0000000000019755.

Yeo, C.D., Park, K.H., Park, C.K., Lee, S.H., Kim, S.J., Yoon, H.K., Lee, Y.S., Lee, E.J., Lee, K.Y. and Kim, T.J. (2015) 'Expression of insulin-like growth factor 1 receptor (IGF-1R) predicts poor responses to epidermal growth factor receptor (EGFR) tyrosine kinase inhibitors in non-small cell lung cancer patients harboring activating EGFR mutations', *Lung Cancer*, 87(3), pp. 311–317. Available at: https://doi.org/10.1016/j.lungcan.2015.01.004.

Yuan, J., Yin, Z., Tao, K., Wang, G. and Gao, J. (2018) 'Function of insulin-like growth factor 1 receptor in cancer resistance to chemotherapy', *Oncology Letters*. Spandidos Publications, pp. 41–47. Available at: https://doi.org/10.3892/ol.2017.7276.

Zech T, C.S.C.P.S.H.C.M.I.R.N.J.M.L. (2011) 'The Arp2/3 activator WASH regulates α5β1-integrin-mediated invasive migration', *Journal of Cell Science* [Preprint].

Zhan, T., Rindtorff, N. and Boutros, M. (2017) 'Wnt signaling in cancer', *Oncogene*. Nature Publishing Group, pp. 1461–1473. Available at: https://doi.org/10.1038/onc.2016.304.

Zhang, W., Zong, C.S., Hermanto, U., Lopez-Bergami, P., Ronai, Z. and Wang, L.-H. (2006) 'RACK1 Recruits STAT3 Specifically to Insulin and Insulin-Like Growth Factor 1 Receptors for Activation, Which Is Important for Regulating Anchorage-Independent Growth', *Molecular and Cellular Biology*, 26(2), pp. 413–424. Available at: https://doi.org/10.1128/mcb.26.2.413-424.2006.

Zhang, X., Li, Y., Xu, H. and Zhang, Y.W. (2014) 'The γ-secretase complex: From structure to function', *Frontiers in Cellular Neuroscience*. Frontiers Media S.A. Available at: https://doi.org/10.3389/fncel.2014.00427.

Zhao, J., Pestell, R. and Guan, J.-L. (2001) *Transcriptional Activation of Cyclin D1 Promoter by FAK Contributes to Cell Cycle Progression*, *Molecular Biology of the Cell*.

Zhao, L. and Vogt, P.K. (2008) 'Class I PI3K in oncogenic cellular transformation', *Oncogene*, pp. 5486–5496. Available at: https://doi.org/10.1038/onc.2008.244.

Zhou, B.P., Liao, Y., Xia, W., Zou, Y., Spohn, B. and Hung, M.-C. (2001) *HER-2/neu induces p53 ubiquitination via Akt-mediated MDM2 phosphorylation*, *NATURE CELL BIOLOGY*. Available at: http://cellbio.nature.com.